Online ISSN : 2249-4626
Print ISSN : 0975-5896
DOI : 10.17406/GJSFR

Global Journal

of Science Frontier Research: A

Physics and Space Science



Dynamics of the Cosmic Dark

Description of Galaxy Rotation

Highlights

New Functional and Structural

Dose Rate Levels in Poultry Feeds

Discovering Thoughts, Inventing Future

VOLUME 18 ISSUE 4 VERSION 1.0

© 2001-2018 by Global Journal of Science Frontier Research, USA

Volume 18 Issue 19 was originally issued as A4

Global Journal of Science Frontier Research: A
Physics & Space Science

Volume 18 Issue 19
Originally issued as A4

Global Journal of Science Frontier Research: A
Physics & Space Science

Volume 18 Issue 4 (Ver. 1.0)

Open Association of Research Society

© Global Journal of Science Frontier Research. 2018.

All rights reserved.

This is a special issue published in version 1.0 of "Global Journal of Science Frontier Research." By Global Journals Inc.

All articles are open access articles distributed under "Global Journal of Science Frontier Research"

Reading License, which permits restricted use. Entire contents are copyright by of "Global Journal of Science Frontier Research" unless otherwise noted on specific articles.

No part of this publication may be reproduced or transmitted in any form or by any means, electronic or mechanical, including photocopy, recording, or any information storage and retrieval system, without written permission.

The opinions and statements made in this book are those of the authors concerned. Ultraculture has not verified and neither confirms nor denies any of the foregoing and no warranty or fitness is implied.

Engage with the contents herein at your own risk.

The use of this journal, and the terms and conditions for our providing information, is governed by our Disclaimer, Terms and Conditions and Privacy Policy given on our website http://globaljournals.us/terms-and-condition/menu-id-1463/

By referring / using / reading / any type of association / referencing this journal, this signifies and you acknowledge that you have read them and that you accept and will be bound by the terms thereof.

All information, journals, this journal, activities undertaken, materials, services and our website, terms and conditions, privacy policy, and this journal is subject to change anytime without any prior notice.

Incorporation No.: 0423089
License No.: 42125/022010/1186
Registration No.: 430374
Import-Export Code: 1109007027
Employer Identification Number (EIN):
USA Tax ID: 98-0673427

Global Journals Inc.

*(A Delaware USA Incorporation with "Good Standing"; **Reg. Number: 0423089**)*

Sponsors: Open Association of Research Society
Open Scientific Standards

Publisher's Headquarters office

Global Journals® Headquarters
945th Concord Streets,
Framingham Massachusetts Pin: 01701,
United States of America
USA Toll Free: +001-888-839-7392
USA Toll Free Fax: +001-888-839-7392

Offset Typesetting

Global Journals Incorporated
2nd, Lansdowne, Lansdowne Rd., Croydon-Surrey,
Pin: CR9 2ER, United Kingdom

Packaging & Continental Dispatching

Global Journals Pvt Ltd
E-3130 Sudama Nagar, Near Gopur Square,
Indore, M.P., Pin:452009, India

Find a correspondence nodal officer near you

To find nodal officer of your country, please email us at *local@globaljournals.org*

eContacts

Press Inquiries: *press@globaljournals.org*
Investor Inquiries: *investors@globaljournals.org*
Technical Support: *technology@globaljournals.org*
Media & Releases: *media@globaljournals.org*

Pricing (Excluding Air Parcel Charges):

Yearly Subscription (Personal & Institutional)
250 USD (B/W) & 350 USD (Color)

Editorial Board

Global Journal of Science Frontier Research

Dr. John Korstad

Ph.D., M.S. at California State University
Professor of Biology
Department of Biology Oral Roberts University

Dr. Rafael Gutiérrez Aguilar

Ph.D., M.Sc., B.Sc., Psychology (Physiological). National Autonomous University of Mexico.

Andreas Maletzky

Zoologist, University of Salzburg, Department of Ecology and Evolution Hellbrunnerstraße, Salzburg Austria, Universitat Salzburg, Austria

Tuncel M. Yegulalp

Professor of Mining, Emeritus
Earth & Environmental Engineering
Henry Krumb School of Mines, Columbia University
Director, New York Mining and Mineral
Resources Research Institute, USA

Nora Fung-yee TAM

DPhil
University of York, UK
Department of Biology and Chemistry
MPhil (Chinese University of Hong Kong)

Prof. Philippe Dubois

Ph.D. in Sciences
Scientific director of NCC-L, Luxembourg
Full professor,
University of Mons UMONS, Belgium

Dr. Mazeyar Parvinzadeh Gashti

Ph.D, M.Sc., B.Sc. Science and Research Branch of Islamic Azad University, Tehran, Iran
Department of Chemistry & Biochemistry
University of Bern, Bern, Switzerland

Dr. Eugene A. Permyakov

Institute for Biological Instrumentation
Russian Academy of Sciences, Director, Pushchino State Institute of Natural Science, Department of Biomedical Engineering, Ph.D., in Biophysics
Moscow Institute of Physics and Technology, Russia

Prof. Dr. Zhang Lifei

Dean, School of Earth and Space Sciences
Ph.D., Peking University
Beijing, China

Prof. Jordi Sort

ICREA Researcher Professor
Faculty, School or Institute of Sciences
Ph.D., in Materials Science, Autonomous University of Barcelona, Spain

Dr. Matheos Santamouris

Prof. Department of Physics
Ph.D., on Energy Physics
Physics Department
University of Patras, Greece

Dr. Bingsuo Zou

Ph.D. in Photochemistry and Photophysics of Condensed Matter
Department of Chemistry, Jilin University,
Director of Micro- and Nano- technology Center

Dr. Gayle Calverley

Ph.D. in Applied Physics University of Loughborough, UK

Dr. Linda Gao

Ph.D. in Analytical Chemistry,
Texas Tech University, Lubbock,
Associate Professor of Chemistry,
University of Mary Hardin-Baylor

Dr. Richard B Coffin

Ph.D., in Chemical Oceanography
Department of Physical and Environmental
Texas A&M University, USA

Dr. Indranil Sen Gupta

Ph.D., Mathematics, Texas A & M University
Department of Mathematics, North Dakota State University, North Dakota, USA

Prof. Ulrich A. Glasmacher

Institute of Earth Sciences, University Heidelberg, Germany, Director of the Steinbeis Transfer Center, TERRA-Explore

Dr. Alicia Esther Ares

Ph.D. in Science and Technology,
University of General San Martin, Argentina
State University of Misiones, US

Dr. Fabiana Barbi

B.Sc., M.Sc., Ph.D., Environment, and Society,
State University of Campinas, Brazil
Center for Environmental Studies and Research
State University of Campinas, Brazil

Dr. Lev V. Eppelbaum

Ph.D. Institute of Geophysics,
Georgian Academy of Sciences, Tbilisi
Assistant Professor Dept Geophys & Planetary Science,
Tel Aviv University Israel

Dr. Yiping Li

Ph.D. in Molecular Genetics,
Shanghai Institute of Biochemistry,
The Academy of Sciences of China, Senior Vice Director,
UAB Center for Metabolic Bone Disease

Dr. A. Heidari

Ph.D., D.Sc
Faculty of Chemistry
California South University (CSU), United States

Dr. Maria Gullo

Ph.D., Food Science, and Technology
University of Catania
Department of Agricultural and Food Sciences
University of Modena and Reggio Emilia, Italy

Dr. Qiang Wu

Ph.D. University of Technology, Sydney
Department of Machematics, Physics and Electrical Engineering
Northumbria University

Dr. Bingyun Li

Ph.D. Fellow, IAES
Guest Researcher, NIOSH, CDC, Morgantown, WV
Institute of Nano and Biotechnologies
West Virginia University, US

Dr. Giuseppe A Provenzano

Irrigation and Water Management, Soil Science, Water Science Hydraulic Engineering
Dept. of Agricultural and Forest Sciences
Universita di Palermo, Italy

Dr. Sahraoui Chaieb

Ph.D. Physics and Chemical Physics
M.S. Theoretical Physics
B.S. Physics, École Normale Supérieure, Paris
Associate Professor, Bioscience
King Abdullah University of Science and Technology

Dr. Arshak Poghossian

Ph.D. Solid-State Physics
Leningrad Electrotechnical Institute, Russia
Institute of Nano and Biotechnologies
Aachen University of Applied Sciences, Germany

Dr. Lucian Baia

Ph.D. Julius-Maximilians University Würzburg, Germany
Associate professor
Department of Condensed Matter Physics and Advanced Technologies Babes-Bolyai University, Romania

Dr. T. David A. Forbes

Associate Professor and Range Nutritionist
Ph.D. Edinburgh University - Animal Nutrition
M.S. Aberdeen University - Animal Nutrition
B.A. University of Dublin- Zoology.

Dr. Mauro Lenzi

Ph.D.
Biological Science,
Pisa University, Italy
Lagoon Ecology and Aquaculture Laboratory
Orbetello Pesca Lagunare Company

Dr. Fotini Labropulu

Mathematics - Luther College
University of Regina, Ph.D., M.Sc. in Mathematics
B.A. (Honours) in Mathematics
University of Windsor
Web: luthercollege.edu/Default.aspx

Dr. Mihaly Mezei

Associate Professor
Department of Structural and Chemical Biology
Mount Sinai School of Medical Center
Ph.D., Etvs Lornd University, New York University, United State

Dr. Miguel Angel Ariño

Professor of Decision Sciences
IESE Business School
Barcelona, Spain (Universidad de Navarra)
Ph.D. in Mathematics, University of Barcelona, Spain

Dr. Wen-Yih Sun

Professor of Earth and Atmospheric Sciences
Purdue University, Director, National Center for Typhoon and Flooding, United State

Dr. Della Ata

BS in Biological Sciences
MA in Regional Economics, Hospital Pharmacy
Pharmacy Technician Educator

Dr. Shengbing Deng

Departamento de Ingeniería Matemática,
Universidad de Chile.
Facultad de Ciencias Físicas y Matemáticas.
Blanco Encalada 2120, piso 4.
Casilla 170-3. Correo 3. - Santiago, Chile

Dr. Claudio Cuevas

Department of Mathematics
Universidade Federal de Pernambuco
Recife PE
Brazil

Dr. Yap Yee Jiun

B.Sc.(Manchester), Ph.D.(Brunel), M.Inst.P.(UK)
Institute of Mathematical Sciences,
University of Malaya,
Kuala Lumpur, Malaysia

Dr. Latifa Oubedda

National School of Applied Sciences,
University Ibn Zohr, Agadir, Morocco
Lotissement Elkhier N°66, Bettana Salé Maroc

Dr. Hai-Linh Tran

Ph.D. in Biological Engineering
Department of Biological Engineering
College of Engineering, Inha University, Incheon, Korea

Angelo Basile

Professor
Institute of Membrane Technology (ITM)
Italian National, Research Council (CNR), Italy

Dr. Yaping Ren

School of Statistics and Mathematics
Yunnan University of Finance and Economics
Kunming 650221, China

Dr. Gerard G. Dumancas

Postdoctoral Research Fellow,
Arthritis and Clinical Immunology Research Program,
Oklahoma Medical Research Foundation
Oklahoma City, OK, United States

Dr. Bondage Devanand Dhondiram

Ph.D.
No. 8, Alley 2, Lane 9, Hongdao station,
Xizhi district, New Taipei city 221, Taiwan (ROC)

Dr. Eman M. Gouda

Biochemistry Department,
Faculty of Veterinary Medicine,
Cairo University,
Giza, Egypt

Dr. Bing-Fang Hwang

Ph.D., in Environmental and Occupational Epidemiology,
Professor, Department of Occupational Safety
and Health, China Medical University, Taiwan

Dr. Baziotis Ioannis

Ph.D. in Petrology-Geochemistry-Mineralogy
Lipson, Athens, Greece

Dr. Vishnu Narayan Mishra

B.Sc.(Gold Medalist), M.Sc. (Double Gold Medalist), Ph.D.
(I.I.T. Roorkee)

Dr. Xianghong Qi

University of Tennessee
Oak Ridge National Laboratory
Center for Molecular Biophysics
Oak Ridge National Laboratory
Knoxville, TN 37922, United States

Dr. Vladimir Burtman

Research Scientist
The University of Utah, Geophysics, Frederick Albert
Sutton Building, 115 S 1460 E Room 383
Salt Lake City, UT 84112, US

Dr. Yaping Ren

School of Statistics and Mathematics
Yunnan University of Finance and Economics
Kunming 650221, China

Contents of the Issue

i. Copyright Notice
ii. Editorial Board Members
iii. Chief Author and Dean
iv. Contents of the Issue

1. Dark Matter May be a Possible Amplifier of Black Hole Formation in the Context of New Functional and Structural Dynamics of the Cosmic Dark Matter Fractal Field Theory(CDMFFT). *1-5*
2. New Methods for Solving the Problem of Radiation and Propagation of Electromagnetic Waves. *7-24*
3. Origin of Gravitation and Description of Galaxy Rotation in a Fundamental Bound State Approach. *25-37*
4. Current Self- Induction and Potential Well on the Superconductive Rings. *39-45*
5. Variations in the Aerosol Optical Depth above the European Russia Territory from the Data Obtained at the Russian Actinometric Network in 1976–2016 Years. *47-51*
6. Activity Concentrations and Gamma Dose Rate Levels in Poultry Feeds and Manure used in Ibadan, Nigeria. *53-66*
7. Hexamethylenetetramine Assisted Wet Chemical Route to Synthesize Nanostructured Cadmium Sulfide Thin Film. *67-72*
8. External and Internal Radiation Doses from Chemical Fertilizers used in Ibadan, Oyo State, Nigeria. *73-81*

v. Fellows
vi. Auxiliary Memberships
vii. Preferred Author Guidelines
viii. Index

Global Journal of Science Frontier Research: a
Physics and Space Science
Volume 18 Issue 4 Version 1.0 Year 2018
Type: Double Blind Peer Reviewed International Research Journal
Publisher: Global Journals
Online ISSN: 2249-4626 & Print ISSN: 0975-5896

Dark Matter May be a Possible Amplifier of Black Hole Formation in the Context of New Functional and Structural Dynamics of the Cosmic Dark Matter Fractal Field Theory (CDMFFT)

By T. Fulton Johns DDS

Abstract- It is possible that as the dominate component of our cosmos, dark matter/dark energy, could be a driving force behind black hole(BH) formation at all scales in our universe. There is reason to believe that the extreme density of baryonic matter/gravity that produces stellar formation throughout our universe and its end of life transition explosion seen in supernova produces enough outward pressure it pulls in dark matter/dark energy (DM/DE) into the stellar core. This extreme event seen throughout our universe could conceivably produce enough negative pressure at its core to "suck-in" DM/DE from the other side of the baryonic matter/cosmic dark matter fractal field/interface(BM/CDMFF/I); creating a super massive injection of dark matter derived gravity within the collapsing star core fueling the extreme gravity conditions and the resulting implosion believed to occur in black hole (BH) formation of massive Chandra limit stars of all types. The Cosmic Dark Matter Fractal Field theory as described in the book "The Great Cosmic Sea of Reality" has given science a new paradigm to consider when examining our reality in a very different way.

GJSFR-A Classification: *FOR Code: 020199p*

DARKMATTERMAYBEAPOSSIBLEAMPLIFIEROFBLACKHOLEFORMATIONINTHECONTEXTOFNEWFUNCTIONALANDSTRUCTURALDYNAMICSOFTHECOSMICDARKMATTERFRACTALFIELDTHEORYCDMFFT

Strictly as per the compliance and regulations of:

© 2018. T. Fulton Johns DDS. This is a research/review paper, distributed under the terms of the Creative Commons Attribution-Noncommercial 3.0 Unported License http://creativecommons.org/licenses/by-nc/3.0/), permitting all non commercial use, distribution, and reproduction in any medium, provided the original work is properly cited.

Dark Matter May be a Possible Amplifier of Black Hole Formation in the Context of New Functional and Structural Dynamics of the Cosmic Dark Matter Fractal Field Theory (CDMFFT)

T. Fulton Johns DDS

Abstract- It is possible that as the dominate component of our cosmos, dark matter/dark energy, could be a driving force behind black hole(BH) formation at all scales in our universe. There is reason to believe that the extreme density of baryonic matter/gravity that produces stellar formation throughout our universe and its end of life transition explosion seen in supernova produces enough outward pressure it pulls in dark matter/dark energy (DM/DE) into the stellar core. This extreme event seen throughout our universe could conceivably produce enough negative pressure at its core to "suck-in" DM/DE from the other side of the baryonic matter/cosmic dark matter fractal field/interface(BM/CDMFF/I); creating a super massive injection of dark matter derived gravity within the collapsing star core fueling the extreme gravity conditions and the resulting implosion believed to occur in black hole (BH) formation of massive Chandra limit stars of all types. The Cosmic Dark Matter Fractal Field theory as described in the book "The Great Cosmic Sea of Reality" has given science a new paradigm to consider when examining our reality in a very different way. Such a shift in understanding our cosmos should lead us to question many conventional theories and so called "natural laws" that fit well in the Newtonian worldview but like many other scientist the advent of quantum field theory has required that we rethink some of these still closely held explanations of how our cosmos is structured and functions at all scales.

I. Introduction

Our reality is indeed illusory when taken into full context as a part of an expanse that sits almost exactly in the middle of a scalar continuum from the Planck scale to the vast visible universe and the super-massive objects known to exist there. Even more illusory when we consider that all of the matter that we can perceive through scientific inspection and even our individual sensory perceptions make up only 4% of our entire cosmos. The presence of dark matter and dark energy accounting for the other 96% leaves quite a void in our pretense to understand the cosmos. However, there are significant clues that lead to clarity when the body of scientific research is considered across multiple disciplines. That is what I have done for most of my professional years as a perpetual student of the sciences and have discovered a common thread that encompasses all forces of nature including the neglected life force. So it is not as an authority on any one subject that I bring this theory forward for your consideration but as a student who has uncovered a concept that keeps answering questions I have pondered for decades.

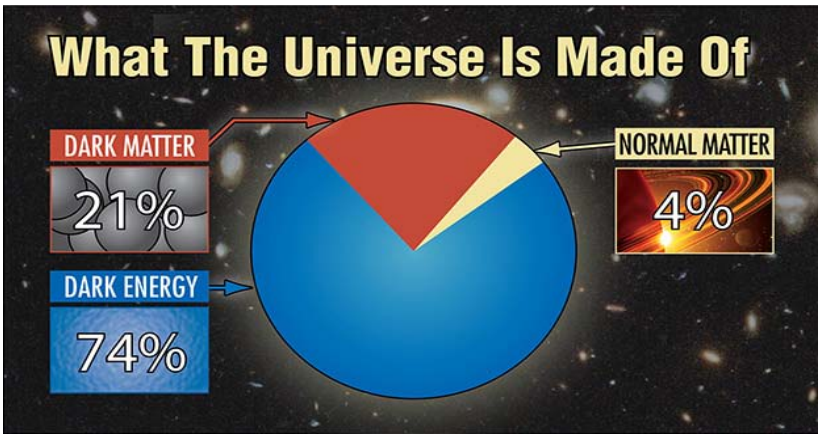


Figure 1

Author: *e-mail: tfjohns@gmail.com*

© 2018 Global Journals

II. Black Hole Dynamics

This is a quote from an article from Space.com "Astronomers know of two "flavors" of black holes: "stellar-mass," which are up to a few dozen times the mass of Earth's sun, and "massive," which can be billions of times the sun's mass — nearly the mass of all the stars in the entire Milky Way galaxy. Stellar-mass black holes are known to be the remains of dead stars, but it remains a mystery how the far-more-massive black holes formed. [Photos: Black Holes of the Universe].

There is a relatively new focus in astrophysics and astronomy using the vast array of both land based, space based telescopes and gravity wave detectors in a collaborative network to study BH dynamics in deep space. This announcement from Space.com concerning the detection of gravity waves from the Light Interferometer Gravity Observatory (LIGO) "On Sept. 14, 2015, LIGO made the first-ever direct detection of gravitational waves, more than 100 years after Einstein first predicted them. (The detection was announced in February 2016.) The space-time ripples were coming from two black holes that had been orbiting each other, growing gradually closer and closer together until they finally collided. All five of the black-hole merger events detected by LIGO have involved so-called stellar-mass black holes, which have masses of between about five and 100 times that of Earth's sun." This event gives evidence that the fabric of space-time model given to us by Albert Einstein and the "wave like" bending of space-time action predicted by his theory of General Relativity (GR) has been verified with this new type of cosmic detector/observatory instrument. There are now three of these LIGO installation locations across the globe separated by thousands of miles and on two continents. The two LIGO locations in the United States and the VIRGO installation in Italy act as comparison confirmation of observed data to these cosmic events, as well as, triangulation locators of the event for cosmic navigational positioning of BH's and other supermassive collisions which produce a now measurable splash in what I call "The Great Cosmic Sea of Reality".

Black holes (BH) appear to be the incinerator of baryonic matter (BM) as they sit at the center of all galaxies and exist elsewhere at different scales known as rogue solo black holes (RSBH). The black hole at the center of our galaxy is estimated to be 3 billion solar masses. Our Milky Way galactic center is not the largest of the BH family in our universe any two colliding BH's seem to always produce a larger one. However, there are limits to stellar derived BH's and it is the influx of DM/DE into this process that could solve the mystery as to the massive and supermassive BH's common to galactic centers. This produces extreme density of mass/gravity and larger and larger BH's, therefore producing ever growing extreme gravity along with what is known as an event horizon also known as the Schwarzschild radius. The Schwarzschild radius is a zone around the BH that is the point of no return once BM crosses this theorized line. The BM will be consumed within the core space-time singularity and according to the CDMFF theory changed to something else that conserves and carries the information contained within into this great vortex of immense energetic gravity and recycled as the memory of morphic fields at the Planck scale at the BM/CDMFF/I of all BH's.

However, the real source of this gravity injection would theoretically be white holes(WH). It is very possible that (WH)'s exist there at the BM/CDMFF/I as well, both are predicted to exist from Einstein's General Relativity Theory (GR). "The possibility of the existence of white holes was put forward by Russian cosmologist Igor Novikov in 1964. White holes are predicted as part of a solution to the Einstein field equations known as the maximally extended version of the Schwarzschild metric" according to Wikipedia. Working in a quantum field dynamic of Planck-foam interconnected black hole/wormholes, these enigmatic (GR) derived organs of Planckian origin, could conceivably create the cyclical flux of the energy/information of baryonic matter (BM) across the baryonic matter/dark matter membrane barrier of two different worlds; while possibly creating the virtual particles required for organic as well as inorganic reality.

See Possible Origin of Virtual Particles:-

https://globaljournals.org/GJSFR_Volume17/1-Possible-Origins-of-Virtual.pdf.

This highly energetic thermodynamic zone seems to exhibit reverse entropy as Planck Virtual Black Holes (PVBH) produce cyclical energy/information as BM is consumed, conserved, and recycled through WH dynamics creating a memory of nature through a feedback loop process I call biomorphic transradiation.

https://globaljournals.org/GJSFR_Volume18/1-Entropy-is-Not-a-One.pdf

The White Hole or Interface?

The CDMFFT predicts that white holes are more like an interface (WH/I) with wormhole dynamics within the foam-like Planck interface as described by the late Prof. Steven Hawking in his work on (BH) dynamics at the Planck scale (October 6, 1994 paper entitled 'Virtual Black Holes').

"It seems that topological fluctuations on the Planck scale should give space-time a foam-like structure. The wormhole scenario and the quantum bubbles picture are two forms this foam might take. They are characterized by very large values of the first and second Betti numbers respectively. I argued that the wormhole picture didn't really fit with what we know

© 2018 Global Journals

of black holes. On the other hand, pair creation of black holes in a magnetic field or in cosmology is described by instantons with topology S2 ×S2. This shows that one can interpret S2×S2 topological fluctuations as closed loops of virtual black holes".

More recently this Black Hole/White Hole /Wormhole model has been given more plausibility from such evidence as seen in this paper:

Hal M. Haggard∗ and Carlo Rovelli† Aix-Marseille Universit´e and Universit´e de Toulon, CPT-CNRS, Luminy, F-13288 Marseille (Dated: Fourth of July, 2014)

"We show that there is a classical metric satisfying the Einstein equations outside a finite space-time region where matter collapses into a black hole and then emerges from a white hole. We compute this metric explicitly. We show how quantum theory determines the (long) time for the process to happen.

A black hole can thus quantum-tunnel into a white hole. For this to happen, quantum gravity should affect the metric also in a small region outside the horizon: we show that contrary to what is commonly assumed, this is not forbidden by causality or by the semi-classical approximation, because quantum effects can pile up over a long time. This scenario alters radically the discussion on the black hole information puzzle."

They further state this:

"Surprisingly, we find that such a metric exists: it is an exact solution of the Einstein equations everywhere, including inside the Schwarzschild radius, except for a finite—small, as we shall see—region, surrounding the points where the classical Einstein equations are likely to fail. It describes in-falling and then out-coming matter."

This seems to be describing a Planck singularity within PVBH's. The zone where classical general relativity and Einstein equations break down and a reverse singularity emerges as does reverse entropy. Furthermore, this is evidence that a cosmic scale BH singularity is the same as a Planck level PVBH singularity. Which makes perfect sense because even the largest object in the universe has a Planck scale. They conclude:

III. Relation With a Full Quantum Gravity Theory

We have constructed the metric of a black hole tunneling into a white hole by using the classical equations outside the quantum region, an order of magnitude estimate for the onset of quantum gravitational phenomena, and some indirect indications on the effects of quantum gravity. This, of course, is not a first principle derivation. For a first principle derivation a full theory of quantum gravity is needed. However, the metric we have presented poses the problem neatly for a quantum gravity calculation. The problem now can be restricted to the calculation of a quantum transition in a finite portion of space-time. The quantum region that we have determined is bounded by a well defined classical geometry. Given the classical boundary geometry, can we compute the corresponding quantum transition amplitude? Since there is no classical solution that matches the in and out geometries of this region, the calculation is conceptually a rather standard tunneling calculation in quantum mechanics. Indeed, this is precisely the form of the problem that is adapted for a calculation in a theory like covariant loop quantum gravity [26, 27]. The spin-foam formalism is designed for this. Notice that the process to be considered is a process that takes a short time and is bounded in space".

"Loop quantum gravity (LQG) is a theory of quantum gravity, merging quantum mechanics and general relativity. Its goal unifies gravity in a common theoretical framework with the other three fundamental forces of nature, beginning with relativity and adding quantum features. It competes with string theory that begins with quantum field theory and adds gravity" Also this "In 2014 Carlo Rovelli and Francesca Vidotto proposed that there is a Planck star inside a black hole.[19] This theory, if correct, would resolve the black hole firewall and black hole information paradox. This idea is based on loop quantum gravity" this definition according to Wikipedia.

It is conceivable from the model of the baryonic matter/cosmic dark matter fractal field/interface that the sudden instantaneous implosion followed by an explosion of a star, when the gravity dynamics produce supernova that a substantial gravity shift might occur. This gigantic energy producing display may internally produce large fluid dynamic motion through this BM/DM zone injecting this mysterious dark matter into the core of the newly formed BH.

© 2018 Global Journals

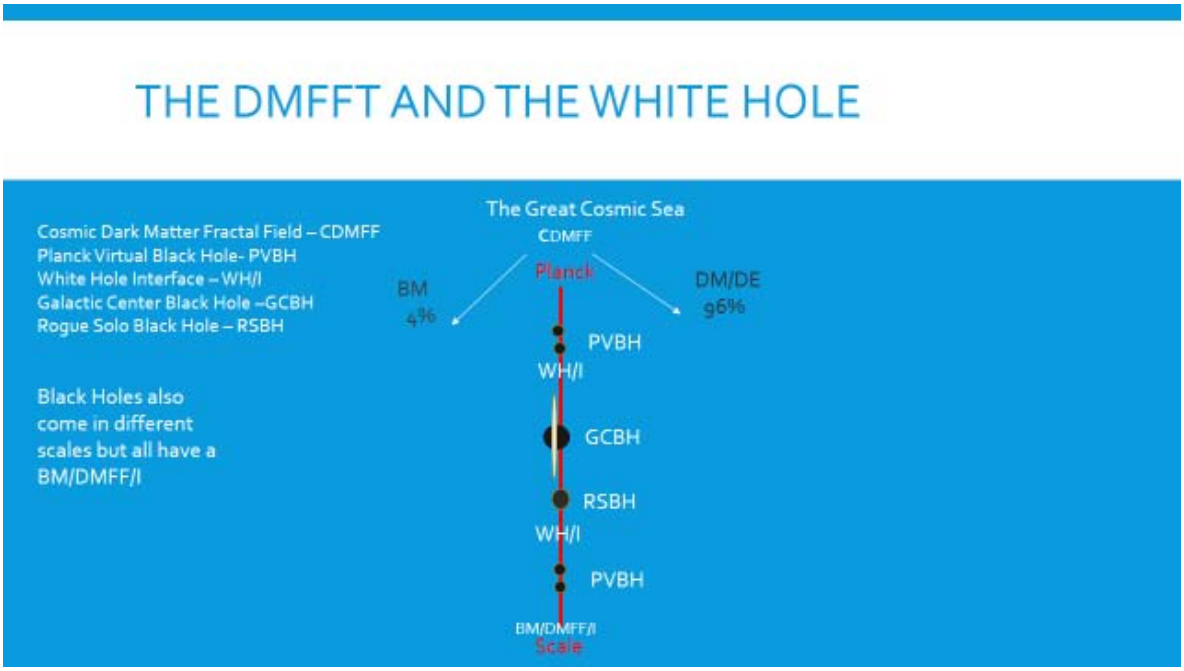


Figure 2

IV. Conclusions

There is a prediction of the Cosmic Dark Matter Fractal Field theory that is easily missed. This model of our reality predicts that all animate and inanimate objects are held in formation by morphic resonate coherent domains, which is the vast majority, have a Baryonic Matter/Cosmic Dark Matter Fractal Field/ Interface. (Fig2) This interface is likely to be a zone of very high energy production due to the dynamo-like action that occurs there secondary to the high velocity and constant motion of our planet moving through space-time engulfed in the Great Cosmic Sea. The best way to envision how this new concept of black hole birth occurs is to see this dynamic occurring at that membrane of baryonic matter/dark matter/dark energy within the dying star, merging Neutron stars or merging black holes called kilonova. This new model of black hole creation can now explain the almost limitless source of high energy activity/mega-gravity events observed in and around all black holes especially and including colliding neutron stars with black holes and supper massive black hole (SMBH) galaxy collisions as well as PVBH/wormhole dynamics at work at the Planck scale throughout The Great Cosmic Sea.

There is now much scientific attention and investigation occurring throughout high energy astrophysics and astronomy concerning these illusive gravitational giants and the energy dynamics at work in our cosmos. The level of black hole/white hole functional dynamics seem to be much more at work according to CDMFF theory in the Planck scale than first thought and now with the advances made in multiple electromagnetic frequency detection across the visual and nonvisual spectrum as well as gravity wave detection much more will be learned at a faster pace to discover the mysteries of the black hole dynamics.

See this report of the October 2017 KIlovova event:

https://www.space.com/38471-gravitational-waves-neutron-star-crashes-discovery-explained.html

The recent collaborative efforts by astronomers of all persuasions called multi-messenger detection which has been greatly enhanced by the more recent LIGO/VIRGO gravity wave detectors has led our new ability of multiple observational study and verification of the massive energy/mega-gravitational events occurring in our cosmos using data collected in the visual land-based telescopes, radio telescopes, as well as, space-based satellite telescopes of all spectrums of the electromagnetic spectrum have confirmed such collisions and greatly increased the knowledge of BH mega-energy dynamics.

Space-time is neither smooth nor-homogeneous; it is highly energetic and dynamical in ways we have not yet even considered. We should explore our reality not just by its pieces and parts but as a holographic fractal whole. You cannot understand the complex life of a butterfly by only looking at the cocoon from which it emerged an atom at a time. Therefore, with this in mind my experience tells me that the cosmos makes more sense in the context of a fractal derived model as described in the cosmic dark matter fractal field theory. The injecting of multiple zones of high energy focal points in space-time, we call black holes, with dark matter/dark energy has amazing implications and gives science a new context to explore the

© 2018 Global Journals

functional and structural nature of these ubiquitous massive and super massive objects.

The link below takes you to a documentary that you will see more information on mulit-messenger detection of the October 2017 Kilonova event!

https://www.amazon.com/Star-Crash-Explosion-Transformed Astronomy/dp/B078YHMMZ7/ref=sr_1_2_?ie=UTF8&qid=15-20705270&sr=8-2&keywords=Star+crash

© 2018 Global Journals

This page is intentionally left blank

© 2018 Global Journals

Global Journal of Science Frontier Research: a
Physics and Space Science
Volume 18 Issue 4 Version 1.0 Year 2018
Type: Double Blind Peer Reviewed International Research Journal
Publisher: Global Journals
Online ISSN: 2249-4626 & Print ISSN: 0975-5896

New Methods for Solving the Problem of Radiation and Propagation of Electromagnetic Waves

By F. F. Mende

Abstract- The history of the establishment of the laws of electrodynamics counts already more than 200 years, but, in spite of this, physics of the emission of electromagnetic waves up to now so is not explained and there are only phenomenological laws, which they use, until now. As the basis of such laws is assumed the concept of the vector potential of magnetic field, which follows from the phenomenological Ampere law, which is established on the basis empirical laws about power interaction of the current carrying systems. In the article it is shown that physical nature of electromagnetic waves is obliged to the dependence of scalar potential on the speed. This approach gives the possibility to introduce into the electrodynamics new concept–the scalar-vector potential of the moving charge, which determines all dynamic laws of electrodynamics.

Keywords: magnetic field, vector potential, electromagnetic wave, the laws of self-induction, wave equation, telegraphic equations, scalar-vector potential.

GJSFR-A Classification: FOR Code: 260203



Strictly as per the compliance and regulations of:

© 2018. F. F. Mende. This is a research/review paper, distributed under the terms of the Creative Commons Attribution-Noncommercial 3.0 Unported License http://creativecommons.org/licenses/by-nc/3.0/), permitting all non commercial use, distribution, and reproduction in any medium, provided the original work is properly cited.

New Methods for Solving the Problem of Radiation and Propagation of Electromagnetic Waves

F. F. Mende

Abstract- The history of the establishment of the laws of electrodynamics counts already more than 200 years, but, in spite of this, physics of the emission of electromagnetic waves up to now so is not explained and there are only phenomenological laws, which they use, until now. As the basis of such laws is assumed the concept of the vector potential of magnetic field, which follows from the phenomenological Ampere law, which is established on the basis empirical laws about power interaction of the current carrying systems. In the article it is shown that physical nature of electromagnetic waves is obliged to the dependence of scalar potential on the speed. This approach gives the possibility to introduce into the electrodynamics new concept – the scalar- vector potential of the moving charge, which determines all dynamic laws of electrodynamics.

Keywords: magnetic field, vector potential, electromagnetic wave, the laws of self-induction, wave equation, telegraphic equations, scalar- vector potential.

I. Concept of Emission in the Classical Electrodynamics

Any field is this field, which can be revealed with the aid of the meters. If there is a charged parallel-plate capacitor (Fig. 1), consisting of two flat plates, the electric field between them it is easy to reveal, introducing between these plates trial charge. By the force, which acts on this charge, and is revealed the electric field? By the characteristic property of this field is the fact that it presents the continuous homogeneous medium, which possesses specific energy, proportional to the square of electric field. Of this easily it will be convinced with the aid of the simple experiment. If we begin to separate the plates of capacitor, then in this case it will be necessarily spend the specific work.

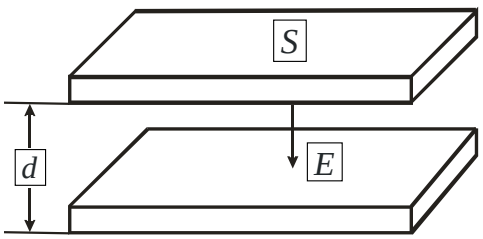


Fig. 1: Capacitor, which consists of the plane-parallel charged plates

Author: Kharkov, Ukraine. e-mail: fedormende@gmail.com

If the surface density of charges on its plates is equal σ, that the tension of the electric field between its plates is equal

$$E=\frac{\sigma}{2\varepsilon_0}.$$

Without taking into account edge effects the electric force, which acts on the plates of capacitor is determined by the relationship

$$F=\frac{1}{2}\varepsilon_0 E^2 S.$$

If in this case plates are moved apart up to the distance d, that in this case the mechanical work will be perfected

$$W=\frac{1}{2}\varepsilon_0 E^2 Sd.$$

But energy of electrical pour on also it will be equal to the same value. But if plates converge, then, on the contrary, electrical energy will be converted into the mechanical. These examples show, as mechanical energy it can be converted into the electrical and vice versa.

It is well known that near the wires, along which flows alternating electric current, are formed the electrical induction fields, which can be connected with the alternating magnetic field. Magnetic field was introduced by ampere by phenomenological way on the basis of the observation of power interaction between the conductors, along which flows the current.

The Ampere law, expressed in the vector form, determines magnetic field at the point [1]:

$$\vec{H}=\frac{1}{4\pi}\int\frac{I\left[d\vec{l}\ \vec{r}\right]}{r^3},$$

where I - current in the element $d\vec{l}$, $\vec{r}$ - vector, directed from $d\vec{l}$ to the viewpoint (Fig. 2).
It is possible to show that

$$\frac{[d\vec{l}\vec{r}]}{r^3}=\left[grad\left(\frac{1}{r}\right)d\vec{l}\right]$$

© 2018 Global Journals

And, besides the fact that

$$\left[grad\left(\frac{1}{r}\right)d\vec{l} \right]=rot\left(\frac{d\vec{l}}{r}\right)-\frac{1}{r}rotd\vec{l} .$$

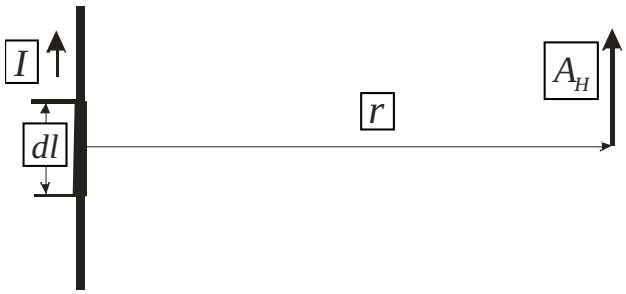


Fig. 2: The formation of vector potential by the element of the conductor dl, along which flows the current I

But the rotor of $d\vec{l}$ is equal to zero and therefore is final

$$\vec{H} = rot\int I\left(\frac{d\vec{l}}{4\pi r}\right) = rot\ \vec{A}_H ,$$

where

$$\vec{A}_H=\int I\left(\frac{d\vec{l}}{4\pi r}\right) . \qquad (1.1)$$

The remarkable property of this expression is the fact that the dependence of vector potential is inversely proportional to distance to the observation point, which is characteristic for the emission laws. Specifically, this property makes it possible to obtain emission laws.

Since $I=gv$, where g the quantity of charges, which falls per unit of the length of conductor, from (1.1) we obtain:

$$\vec{A}_H=\int\frac{gv\ d\vec{l}}{4\pi r} .$$

If the size of element $d\vec{l}$, along which flows current, it is considerably less than distance to the observation point, then this relationship takes the form:

$$\vec{A}_H=\frac{gv\ d\vec{l}}{4\pi r} .$$

From this relationship follows interesting fact. Even on the direct current the dependence of vector potential on the distance corresponds to emission laws. And, it would seem, that, changing by jumps current in the short section of wire, and measuring the vector potential at the remote point, it is possible to transfer information into this point by the emission laws. But this interferes with the circumstance that the direct-current circuit is always locked to the local power source and therefore always there is both straight and return conductor. This special feature leads to the fact that in this situation the vector potential in the distant zone occurs inversely it is proportional to the square of distance to the observed point. This is easy to show based on the example of two parallel elements of conductor, located at a distance d (Fig. 3), in which flow the opposite currents.

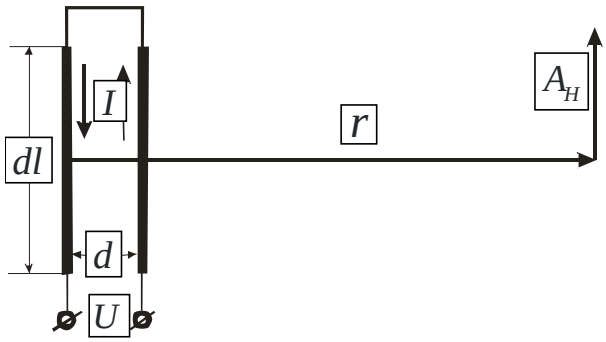


Fig. 3: Two conductors with the opposite currents

In this case vector potential in the remote zone is defined as the sum of the vector potentials, created in the distant zone individually by each current element. When considerably more than we obtain:

$$\vec{A}_H=\frac{gv\ d\vec{l}}{4\pi r}-\frac{gv\ d\vec{l}}{4\pi(r+d)}\cong\frac{gv\ d\vec{l}\ d}{4\pi r^2} .$$

To avoid these difficulties is possible by the way of using alternating currents. Since the electric field and vector potential in the free space are connected with the relationship

$$\vec{E}=-\mu_0\frac{\partial\vec{A}}{\partial t} ,$$

where μ_0 - magnetic permeability of vacuum, the electric field, created in the distant zone by current element $gvd\vec{l}$, will depend on the acceleration of charges in this element

$$\vec{E}=-\frac{\mu_0 ga\ d\vec{l}}{4\pi r} , \qquad (1.2)$$

where $a=\frac{dv}{dt}$ - acceleration of charge. It is known from Maxwell's equations that the electric fields are extended in the free space with the speed

$$c=\frac{1}{\sqrt{\varepsilon_0\mu_0}} , \qquad (1.3)$$

where ε_0 - the dielectric constant of vacuum.

© 2018 Global Journals

Therefore, if the current elements are arranged at a distance equal to half the wavelength and create multidirectional currents in them, then in the far zone, due to the delay, the electric fields from the individual current elements will add up and the total electric field will be doubled:

$$\vec{E}_{\Sigma}=-\frac{\mu_0 ga\ d\vec{l}}{2\pi r}.$$

If we in the relationship (1.2) consider that the fields are extended with the final speed and to consider delay $\left(t-\frac{r}{c}\right)$, that we will obtain taking into account (1.3) relationship:

$$\vec{E}=-\int\frac{ga(t-\frac{r}{c})\ d\vec{l}}{4\pi\varepsilon_0 c^2 r} \qquad .(1.4)$$

When the acceleration of charges changes according to the harmonic law $a=a_0\sin\omega\left(t-\frac{r}{c}\right)$ Relationship (1.4) takes the form

$$\vec{E}=-\int\frac{ga_0\sin\omega\left(t-\frac{r}{c}\right)\ d\vec{l}}{4\pi\varepsilon_0 c^2 r}. \qquad (1.5)$$

In the case, when the size of current element is considerably lower than the distance to the observation point, we obtain:

$$\vec{E}=-\frac{ga_0\sin\omega\left(t-\frac{r}{c}\right)\ d\vec{l}}{4\pi\varepsilon_0 c^2 r}. \qquad (1.6)$$

Relationships (1.4-1.6) it shows that the electric fields in the distant zone for the case examined depend on the acceleration of charges. Examining the electric fields of parallel-plate capacitor, we saw that such fields possess the specific energy, which they will transfer with their propagation.

But in this examination metal of the place for the magnetic field, which is located in the electromagnetic wave. This field can be introduced as purely mathematical concept from the second equation of Maxwell

$$rot\vec{H}=\varepsilon_0\frac{\partial\vec{E}}{\partial t}.$$

We have for the case of the smallness of current element in comparing with the distance to the observation point:

$$rot\vec{H}=-\frac{\omega ga_0\cos\omega\left(t-\frac{r}{c}\right)\ d\vec{l}}{4\pi c^2 r}. \qquad (1.7)$$

From these relationships it follows that the magnetic field is the gradient of electric field.

If there is a single charge e, that relationship (1.6), (1.7) they will be rewritten as follows:

$$\vec{E}=-\frac{ea_0\sin\omega\left(t-\frac{r}{c}\right)\ \vec{k}}{4\pi\varepsilon_0 c^2 r}, \qquad (1.8)$$

$$rot\vec{H}=-\frac{\omega ea_0\cos\omega\left(t-\frac{r}{c}\right)\ \vec{k}}{4\pi c^2 r}, \qquad (1.9)$$

where $\vec{k}$ - unit vector in the direction of the motion of charge.

Let us write down these relationships in the Cartesian coordinate system, by considering that direction of propagation is the axis y, and vector $\vec{E}$ it is directed along the axis z (Fig. 4).



Fig. 4: Diagram of shaping of magnetic field

From relationship (18.2) we obtain

$$\frac{\partial H_x}{\partial y}=-\frac{\omega ea_0\cos\omega\left(t-\frac{y}{c}\right)}{4\pi c^2 y}, \qquad (1.10)$$

One should consider with the integration of this relationship that with the wavelength considerably smaller than distance to the observation point, harmonic derivative on the coordinate is considerably more than derivative of the reverse value of coordinate. Therefore coordinate in the numerator of the right side of the relationship (1.10) can be considered constant. We obtain with this condition from (1.10) the relationship

$$H_x=-\frac{ea_0\sin\omega\left(t-\frac{y}{c}\right)}{4\pi cy}. \qquad (1.11)$$

© 2018 Global Journals

This value of magnetic field is obtained with the condition for existence Z of the component of the electric field

$$E_z = -\frac{ea_0 \sin\omega\left(t-\frac{r}{c}\right)}{4\pi\varepsilon_0 c^2 r}. \qquad (1.12)$$

After dividing (1.12) on (1.11) we obtain

$$\frac{E_z}{H_x} = \sqrt{\frac{\mu_0}{\varepsilon_0}} = Z_0,$$

where Z_0 - the wave drag of vacuum.

The carried out examination showed that in the free space can be extended the so-called electromagnetic wave, whose vectors of electrical and magnetic field are cophasal. Let us emphasize again that the introduction of the vector of magnetic field is the purely mathematical formality, which is not the necessary for the construction theory of emission.

Thus, relying on the phenomenological concept of magnetic field, are obtained the laws of the propagation of electromagnetic waves. These laws exclude the need of using Maxwell's equations, since all laws of propagation can be obtained from them, and Maxwell's equations with respect to these equations are the special case, when distance from the emitter to the observation point is great.

There remains only to ask, why electrodynamics is not banal along this way immediately after the introduction of the concept of magnetic field. Answer lies in the fact that then no one knew about existence of electromagnetic waves and only experiences of Hertz confirmed this.

Thus, the physical basis of this approach is not thus far clear, since it is not understandable that the vector potential represents from a physical point of view and why it is connected with the motion of charges. In connection with the incomprehension of these questions, but vector potential is critical not only for the emission, but also for the power of interaction of the current carrying systems, the classical electrodynamics and it is divided up to now into two those not connected with each other of part. Its one parts this of Maxwell's equation, the determining wave processes in the material media. Another part, which determines power interaction of the current carrying systems, is based on the experimental postulate about the Lorentz force.

From the relationships (8) and (11) it is evident that the electrical and magnetic fields of electromagnetic waves in this posing of the question depend only on the second the derivatives of coordinate on the time, and in this case as yet there is no answer apropos of that, can these fields depend on higher derivatives.

This question is examined from a formal phenomenological point of view by the way of the introduction of the concept of magnetic field and vector potential, and the obtained results well correspond with the experiment. However, basic problem today consists in the fact that physical nature of this potential until is known.

Further development of phenomenological approaches to questions of the propagation of electromagnetic waves.

a) Laws of the self-induction

To the laws of self-induction should be carried those laws, which describe the reaction of such elements of radio-technical chains as capacity, inductance and resistance with the galvanic connection to them of the sources of current or voltage [2-4]. These laws are the basis of the theory of electrical chains. The motion of charges in any chain, which force them to change their position, is connected with the energy consumption from the power sources. The processes of interaction of the power sources with such structures are regulated by the laws of self-induction.

To the self-induction let us carry also that case, when its parameters can change with the presence of the connected power source or the energy accumulated in the system. This self-induction we will call parametric. Subsequently we will use these concepts: as current generator and the voltage generator. By ideal voltage generator we will understand such source, which ensures on any load the lumped voltage, internal resistance in this generator equal to zero. By ideal current generator we will understand such source, which ensures in any load the assigned current, internal resistance in this generator equally to infinity. The ideal current generators and voltage in nature there does not exist, since both the current generators and the voltage generators have their internal resistance, which limits their possibilities.

If we to one or the other network element connect the current generator or voltage, then opposition to a change in its initial state is the response reaction of this element and this opposition is always equal to the applied action, which corresponds to third Newton's law.

If the capacity C is charged to a potential difference U, then the charge Q, accumulated in it, is determined by the relationship

$$Q_{C,U} = CU. \qquad (2.1.1)$$

The charge $Q_{C,U}$, depending on the capacitance values of capacitor and from a voltage drop across it, we will call still the flow of electrical self-induction.

© 2018 Global Journals

When speech goes about a change in the charge, determined by relationship (2.1.1), that this value it can change with the method of changing the potential difference with a constant capacity, either with a change in capacity itself with a constant potential difference, or and that and other parameter simultaneously.

If capacitance value or voltage drop across it depend on time, then the current strength is determined by the relationship:

$$I=\frac{dQ_{C,U}}{dt}=C\frac{dU}{dt}+U\frac{dC}{dt}.$$

This expression determines the law of electrical self-induction. Thus, current in the circuit, which contains capacitor, can be obtained by two methods, changing voltage across capacitor with its constant capacity either changing capacity itself with constant voltage across capacitor, or to produce change in both parameters simultaneously.

For the case, when the capacity C_1 is constant, we obtain known expression for the current, which flows through the capacity:

$$I=C_1\frac{dU}{dt}. \qquad (2.1.2)$$

When changes capacity, and at it is supported the constant voltage U_1, we have:

$$I=U_1\frac{dC}{dt}. \qquad (2.1.3)$$

This case to relate to the parametric electrical self-induction, since the presence of current is connected with a change in this parameter as capacity.

Let us examine the consequences, which escape from relationship (1.1.2).

If we to the capacity connect the direct-current generator I_0, then voltage on it will change according to the law:

$$U=\frac{I_0 t}{C_1}. \qquad (2.1.4)$$

Thus, the capacity, connected to the source of direct current, presents for it the effective resistance

$$R=\frac{t}{C_1} \qquad (2.1.5)$$

linearly depending on the time. The it should be noted that obtained result is completely obvious; however, such properties of capacity, which customary to assume by reactive element they were for the first time noted in the work [1].

This is understandable from a physical point of view, since in order to charge capacity, source must expend energy.

The power, output by current source, is determined in this case by the relationship:

$$P(t)=\frac{I_0^2 t}{C_1} \qquad (2.1.6)$$

The energy, accumulated by capacity in the time t we will obtain after integrating relationship (2.1.6) with respect to the time:

$$W_C=\frac{I_0^2 t^2}{2C_1}.$$

Substituting here the value of current from relationship (2.1.4), we obtain the dependence of the value of the accumulated in the capacity energy from the instantaneous value of voltage on it:

$$W_C=\frac{1}{2}C_1U^2.$$

Using for the case examined a concept of the flow of electrical induction, which is the charge, we obtain

$$\Phi_U=C_1U=Q(U) \qquad (2.1.7)$$

and using relationship (2.1.2), let us write down:

$$I_0=\frac{d\Phi_U}{dt}=\frac{dQ(U)}{dt}, \qquad (2.1.8)$$

i.e. if we to a constant capacity connect the source of direct current, then the current strength will be equal to the derivative of the flow of capacitive induction on the time.

Now we will support at the capacity constant voltage U_1, and change capacity itself, then

$$I=U_1\frac{dC}{dt}. \qquad (2.1.9)$$

It is evident that the value

$$R_C=\left(\frac{dC}{dt}\right)^{-1} \qquad (2.1.10)$$

plays the role of the effective resistance. This result is also physically intelligible, since with an increase in the capacitance increases the energy accumulated in it, and thus, capacity extracts in the voltage source energy, presenting for it resistive load. The power, expended in this case by source, is determined by the relationship:

© 2018 Global Journals

$$P(t)=\frac{dC}{dt}U_1^2. \qquad (2.1.11)$$

From relationship (2.1.11) is evident that depending on the sign of derivative the expendable power can have different signs. When the derived positive, expendable power goes for the accomplishment of external work. If derived negative, then external source accomplishes work, charging capacity.

Again, introducing concept the flow of the capacitive induction

$$\Phi_C=CU_1=Q(C),$$

we obtain

$$I=\frac{\partial\Phi_C}{\partial t}. \qquad (2.1.12)$$

Relationships (2.1.8) and (2.1.12) indicate that regardless of the fact, how changes the flow of electrical self-induction (charge), its time derivative is always equal to current.

Let us examine one additional process, which earlier the laws of induction did not include; however, it falls under for our extended determination of this concept. From relationship (2.1.7) it is evident that if the charge, left constant (we will call this regime the regime of the frozen electric flux), and then voltage on the capacity can be changed by its change. In this case the relationship will be carried out:

$$CU=C_0U_0=const,$$

where C, U - instantaneous values, and C_0, U_0 - initial values of these parameters, which occur with turning off from the capacity of the power source.

The voltage on the capacity and the energy, accumulated in it, will be in this case determined by the relationships:

$$U=\frac{C_0U_0}{C}, \qquad (2.1.13)$$

$$W_C=\frac{1}{2}\frac{(C_0U_0)^2}{C}.$$

It is natural that this process of self-induction can be connected only with a change in capacity itself, and therefore it falls under for the determination of parametric self-induction.

Thus, are located three relationships (2.1.8), (2.1.12) and (2.1.13), which determine the processes of electrical self-induction. We will call their rules of capacitive flow. Relationship (2.1.8) determines the electrical self-induction, during which there are no changes in the capacity, and therefore this self-induction can be named simply electrical self-induction. Relationships (2.1.3) and (2.1.9-2.1.11) assume the presence of changes in the capacity; therefore the processes, which correspond by these relationships, we will call electrical parametric self-induction.

Let us now move on to the examination of the processes, proceeding in the inductance. Let us introduce the concept of the flow of the inductive self-induction

$$\Phi_{L,I}=LI.$$

If inductance is shortened outed, and made from the material, which does not have effective resistance, for example from the superconductor, then

$$\Phi_{L,I}=L_1I_1=const,$$

where L_1 and I_1 - initial values of these parameters, which are located at the moment of the short circuit of inductance with the presence in it of current.

This regime we will call the regime of the frozen flow. In this case the relationship is fulfilled:

$$I=\frac{I_1L_1}{L}, \qquad (2.1.14)$$

where I and L - the instantaneous values of the corresponding parameters.

In flow regime examined of current induction remains constant, however, in connection with the fact that current in the inductance it can change with its change, this process falls under for the determination of parametric self-induction. The energy, accumulated in the inductance, in this case will be determined by the relationship

$$W_L=\frac{1}{2}\frac{(L_1I_1)^2}{L}=\frac{1}{2}\frac{(const)^2}{L}.$$

Voltage on the inductance is equal to the derivative of the flow of current induction on the time:

$$U=\frac{d\Phi}{dt}=L\frac{dI}{dt}+I\frac{dL}{dt}.$$

Let us examine the case, when the inductance of is constant

$$U=L_1\frac{dI}{dt} \qquad (2.1.15)$$

designating $\Phi_I=L_1I$, we obtain

$$U=\frac{d\Phi_I}{dt}.$$

After integrating expression (2.1.15) on the time, we will obtain:

© 2018 Global Journals

$$I=\frac{Ut}{L_1} \quad . \tag{2.1.16}$$

Thus, the capacity, connected to the source of direct current, presents for it the effective resistance

$$R=\frac{L_1}{t}, \tag{2.1.17}$$

which decreases inversely proportional to time.

The power, expended in this case by source, is determined by the relationship:

$$P(t)=\frac{U^2t}{L_1} \quad . \tag{2.1.18}$$

This power linearly depends on time. After integrating relationship (2.1.18) on the time, we will obtain the energy, accumulated in the inductance

$$W_L=\frac{1}{2}\frac{U^2t^2}{L_1}. \tag{2.1.19}$$

After substituting into expression (2.1.19) the value of voltage from relationship (2.1.16), we obtain:

$$W_L=\frac{1}{2}L_1I^2.$$

This energy can be returned from the inductance into the external circuit, if we open inductance from the power source and to connect effective resistance to it.

Now let us examine the case, when the current I_1, which flows through the inductance, is constant, and inductance itself can change. In this case we obtain the relationship

$$U=I_1\frac{dL}{dt} \tag{2.1.20}$$

Thus, the value

$$R(t)=\frac{dL}{dt} \tag{2.1.21}$$

plays the role of the effective resistance.

As in the case the electric flux, effective resistance can be (depending on the sign of derivative) both positive and negative. This means that the inductance can how derive energy from without, so also return it into the external circuits.

Introducing the designation $\Phi_L=LI_1$ and, taking into account (2.1.20), we obtain:

$$U=\frac{d\Phi_L}{dt}. \tag{2.1.22}$$

The relationship (2.1.14), (2.1.19) and (2.1.22) we will call the rules of current self-induction, or the flow rules of current self-induction. From relationships (2.1.19) and (2.1.22) it is evident that, as in the case with the electric flux, the method of changing the flow does not influence eventual result, and its time derivative is always equal to the applied potential difference. Relationship (2.1.19) determines the current self-induction, during which there are no changes in the inductance, and therefore it can be named simply current self-induction. Relationships (2.1.20-2.1.21) assume the presence of changes in the inductance; therefore we will call such processes current parametric self-induction.

b) Work presents the new method of obtaining the wave equation for the long lines

The processes, examined in two previous paragraphs, concern chains with the lumped parameters, when the distribution of potential differences and currents in the elements examined can be considered uniform. However, there are chains, for example the long lines, into which potential differences and currents are not three-dimensional uniform. These processes are described by the wave equations, which can be obtained from Maxwell's equations or with the aid of the telegraphic equations, but physics of phenomenon itself in these processes to us is not clear.

We will use the results, obtained in the previous paragraph, for examining the processes, proceeding in the long lines, in which the capacity and inductance are the distributed parameters [5-7]. Let us assume that linear (falling per unit of length) capacity and inductance of this line are equal C_0 and L_0. If we to this line connect the dc power supply U_1, then its front will be extended in the line some by the speed v and the moving coordinate of this front will be determined by the relationship $z=vt$. In this case the total quantity of the charged capacity and the value of the summary inductance, along which it flows current, calculated from the beginning lines to the location of the front of voltage, will change according to the law:

$$C(t)=zC_0=vt\ C_0,$$

$$L(t)=zL_0=vt\ L_0.$$

The source of voltage U_1 will in this case charge the being increased capacity of line, for which from the source to the charged line in accordance with relationship (2.1.9) must leak the current:

$$I_1=U_1\frac{dC(t)}{dt}=vU_1C_0. \tag{2.2.1}$$

This current there will be the leak through the conductors of line that possess inductance. But, since

© 2018 Global Journals

the inductance of line in connection with the motion of the front of voltage, also increases, in accordance with relationship (2.1.20), on it will be observed a voltage drop:

$$U=I_1\frac{dL}{dt}=vI_1L_0=v^2U_1C_0L_0.$$

But a voltage drop across the conductors of line in the absolute value is equal to the voltage, applied to its entrance; therefore in the last expression should be placed $U=U_1$. We immediately find taking this into account that the rate of the motion of the front of voltage with the assigned linear parameters and when, on, the incoming line of constant voltage of U_1 is present, must compose

$$v=\frac{1}{\sqrt{L_0C_0}}. \qquad (2.2.2)$$

This expression corresponds to the signal velocity in line itself. Consequently if we to the infinitely long line connect the voltage source, then in it will occur the expansion of electrical pour on and the currents, which fill line with energy, and the speed of the front of constant voltage and current will be equal to the velocity of propagation of electromagnetic vibrations in this line. This wave we will call electric current wave. It is interesting to note that the obtained result does not depend on the form of the function U, i.e. to the line can be connected both the dc power supply and the source, whose voltage changes according to any law. In all these cases the value of the local value of voltage on incoming line will be extended along it with the speed, which follows from relationship (2.2.2). This result could be, until now, obtained only by the method of solution of wave equation, but in this case he indicates the physical cause for this propagation, and it gives the physical picture of process itself. Examination shows that very process of propagation is connected with the energy processes of the filling of line with electrical and current energy. This process occurs in such a way that the wave front, being extended with the speed v, leaves after itself the line, charged to a potential difference U_1, which corresponds to the filling of line with electrostatic electric field energy. However, in the section of line from the voltage source also to the wave front flows the current I_1, which corresponds to the filling of line in this section with energy, which is connected with the motion of the charges along the conductors of line, which possess inductance.

The current strength in the line can be obtained, after substituting the values of the velocity of propagation of the wave front, determined by relationship (2.2.2), into relationship (2.2.1). After making this substitution, we will obtain

$$I_1=U_1\sqrt{\frac{C_0}{L_0}},$$

where $Z=\sqrt{\frac{L_0}{C_0}}$ - line characteristic.

In this case

$$U_1=I\ \frac{dL}{dt}=\frac{d\Phi_L}{dt}.$$

So accurately

$$I_1=U_1\frac{dC}{dt}=\frac{d\Phi_C}{dt}.$$

It is evident that the flow rules both for the electrical and for the current self-induction are observed also in this case.

Thus, the processes of the propagation of a potential difference along the conductors of long line and current in it are connected and mutually supplementing each other, and to exist without each other they do not can. This process can be called electric current spontaneous parametric self-induction. This name connected with the fact that flow expansion they occur arbitrarily and characterizes the rate of the process of the filling of line with energy. From the aforesaid the connection between the energy processes and the velocity of propagation of the wave fronts in the long lines becomes clear. Since with the emission of electromagnetic waves the free space is also transmission line, similar laws must characterize propagation in this space.

That will be, if we in the considered case as one of the conductors of long line take spiral, or to as is customary call, long solenoid. Obviously, in this case the velocity of propagation of the front of voltage in this line will decrease, since the linear inductance of line will increase. This propagation will accompany the process of the propagation not only of external with respect to the solenoid pour on and currents, but both the process of the propagation of magnetic flux inside the solenoid itself and the velocity of propagation of this flow will be equal to the velocity of propagation of electromagnetic wave in line itself.

Knowing current and voltage in the line, it is possible to calculate the specific energy, concluded in the linear capacity and the inductance of line. These energies will be determined by the relationships:

$$W_C=\frac{1}{2}C_0U_1^2, \qquad (2.2.3)$$

© 2018 Global Journals

$$W_L=\frac{1}{2}L_0I_1^2. \qquad (2.2.4)$$

It is not difficult to see that $W_C=W_L$.

Now let us discuss a question about the duration of the front of electric current wave and about which space will occupy this front in line itself. Answer to the first question is determined by the properties of the very voltage source, since local derivative $\frac{\partial U}{\partial t}$ at incoming line depends on transient processes in the source itself and in that device, with the aid of which this source is connected to the line. If the process of establishing the voltage on incoming line will last some time Δt, then in the line it will engage section with the length $v\Delta t$. If we to the line exert the voltage, which is changed with the time according to the law $U(t)$, then the same value of function will be observed at any point of the line at a distance Z relaunch. Of beginning with the delay $t=\frac{z}{v}$. Thus, the function

$$U(t,z)=U\left(t-\frac{z}{v}\right). \qquad (2.2.5)$$

Can be named propagation function, since it establishes the connection between the local temporary and three-dimensional values of function in the line. Long line is the device, which converts local derivative voltage on the time on incoming line into the gradients in line itself. On the basis propagation function (2.2.5) it is possible to establish the connection between the local and gradients in the long line. It is obvious that

$$\frac{\partial U(z)}{\partial z}=\frac{1}{v}\frac{\partial U(t)}{\partial t}.$$

Is important to note that very process of propagation in this case is obliged to the natural expansion of electric field and current in the line and it is subordinated to the rules of parametric self-induction. In the second place, for solving the wave equations of the long lines

$$\frac{\partial^2 U}{\partial z^2}=\frac{1}{v^2}\frac{\partial^2 U}{\partial t^2}$$

$$\frac{\partial^2 I}{\partial z^2}=\frac{1}{v^2}\frac{\partial^2 I}{\partial t^2} \qquad (2.2.6)$$

Obtained from the telegraphic equations

$$\frac{\partial U}{\partial z}=-L\frac{\partial I}{\partial t}$$

$$\frac{\partial I}{\partial z}=-C\frac{\partial U}{\partial t}$$

the knowledge second derivative voltages and currents are required.

But what is to be done, if to incoming line is supplied voltage, whose second derivative is equal to zero (case, when the voltage of source it does change according to the linear law)? Answer to this question equation (2.2.6) they do not give. The utilized method gives answer also to this question.

With the examination of processes in the long line figured such concepts as linear capacity and inductance, and also currents and voltage in the line. However, in the electrodynamics, based on Maxwell's equations, there are no such concepts as capacity and inductance, and there are concepts of the electrical and magnetic permeability of medium. In the carried out examination such concepts as electrical and magnetic fields also was absent. Let us show how to pass from such categories as linear inductance and capacity, current and voltage in the line to such concepts as dielectric and magnetic constant, and also electrical and magnetic field. For this let us take the simplest construction of line, located in the vacuum, as shown in Fig. 5.

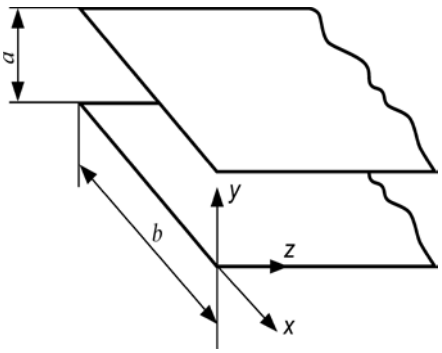


Fig. 5: The two-wire circuit, which consists of two ideally conducting planes

We will consider that $b>>a$ and edge effects it is possible not to consider. Then the following connection will exist between the linear parameters of line and the magnetic and dielectric constants:

$$L_0=\mu_0\frac{a}{b}, \qquad (2.2.7)$$

$$C_0=\varepsilon_0\frac{b}{a} \qquad (2.2.8)$$

where μ_0, ε_0 - dielectric and magnetic constant of vacuum.

© 2018 Global Journals

The phase speed in this line will be determined by the relationship:

$$v=\frac{1}{\sqrt{L_0C_0}}=\frac{1}{\sqrt{\mu_0\varepsilon_0}}=c,$$

where c - velocity of propagation of light in the vacuum. The wave drag of the line examined will be equal

$$Z=\frac{a}{b}\sqrt{\frac{\mu_0}{\varepsilon_0}}=\frac{a}{b}Z_0,$$

where $Z_0=\sqrt{\frac{\mu_0}{\varepsilon_0}}$ - wave drag of free space.

Moreover with the observance of the condition $a=b$ we obtain the equality $L_0=\mu_0$.

This means that magnetic permeability μ_0 plays the role of the longitudinal specific inductance of vacuum. In this case is observed also the equality $C_0=\varepsilon_0$. This means that the dielectric constant ε_0 plays the role of the transverse specific capacity of vacuum. In this interpretation both μ_0 and ε_0 acquire clear physical sense and, just as in the long line, ensure the process of the propagation of electromagnetic wave in the free space.

The examination of electromagnetic wave in the long line can be considered as filling of space, which is been located between its conductors, special form of material, which present the electrical and magnetic fields. Mathematically it is possible to consider that these fields themselves possess specific energy and with their aid it is possible to transfer energy by the transmission lines. But if we examine the processes, which take place with the emission of electromagnetic waves with the aid of any antenna, then it is possible to examine also as the filling of free space with this form of material. However, pour on geometric form and currents in this case it will be more complexly, since they will always be present both transverse and longitudinal component pour on. This approach excludes the need for application, for describing the propagation of electromagnetic waves, this substance as ether.

If we to the examined line of infinite length, or of line of that loaded with wave drag, connect the dc power supply U, and then the field strength in the line will comprise:

$$E_y=\frac{U}{a},$$

and the current, which flows into the line from the power source, will be determined by the relationship:

$$I=\frac{U}{Z}=\frac{aE_y}{Z} \qquad (2.2.9)$$

Magnetic field in the line will be equal to the specific current, flowing in the line

$$H_x=\frac{I}{b}=\frac{aE_y}{bZ}.$$

Substituting here the value Z, we obtain

$$H_x=\frac{E_y}{Z_0}. \qquad (2.2.10)$$

The same connection between the electrical and magnetic field exists also for the case of the transverse electromagnetic waves, which are extended in the free space.

Comparing expressions for the energies, it is easy to see that the specific energy can be expressed through the electrical and magnetic fields

$$\frac{1}{2}\mu_0H_x^2=\frac{1}{2}\varepsilon_0E_y^2. \qquad (2.2.11)$$

This means that the specific energy, accumulated in the magnetic and electric field in this line is identical. If the values of these energies are multiplied by the volumes, occupied by fields, then the obtained values coincide with expressions (2.2.3-2.2.4).

Thus, it is possible to make the conclusion that in the line examined are propagated the same transverse plane waves, as in the free space. Moreover this conclusion is obtained not by the method of solution of Maxwell's equations, but by the way of examining the dynamic processes, which are related to the discharge of parametric self-induction. The special feature of this line will be the fact that in it, in contrast to the free space, the stationary magnetic and electric fields can be extended, but this case cannot be examined by the method of solution of Maxwell's equations.

Cconsequently, conditionally it is possible to consider that the long line is the device, which with the connection to it of dc power supply is filled up with two forms of the energy: electrical and magnetic. The specific densities of these energies are equal, and since and electrical and magnetic energy fill identical volumes, the general energy, accumulated in these fields is identical. The special feature of this line is the fact that with the flow in the line of direct current the distribution of electrical and magnetic pour on in it is uniform. It is not difficult to show that the force, which acts on the conductors of this line, is equal to zero. This follows from relationship (2.2.11), in which its right and leftist of part present the force gradients, applied to the planes of line. But electrical and magnetic forces have different signs; therefore they compensate each other. This

© 2018 Global Journals

conclusion concerns the transmission lines of any other configuration.

If we to the line exert the voltage, which is changed in the course of time according to any law $U(t)=aE_y(t)$, the like of analogy (2.2.5) it is possible to write down

$$E_y(z)=E_y\left(t-\frac{z}{c}\right). \qquad (2.2.12)$$

Analogous relationship will be also pouring on for the magnetic.

Is obvious that the work $I(t)U(t)$ represents the power P, transferred through the cross section of line in the direction z. If in this relationship current and voltage was replaced through the tensions of magnetic and electrical pour on, then we will obtain $P=abE_yH_x$. The work E_yH_x represents the absolute value of Pointing's vector, which represents the specific power, transferred through the cross section of the line of single area. Certainly, all these relationships can be written down also in the vector form.

Thas all conclusions, obtained on the basis of the examination of processes in the long line by two methods, coincide. Therefore subsequently, without risking committing the errors of fundamental nature, it is possible for describing the processes in the long lines successfully to use such parameters as the distributed inductance and capacity. Certainly, in this case one should understand that C_0 and this L_0 some integral characteristics, which do not consider structure, pour on. It should be noted that from a practical point of view, the application of the parameters C_0 and L_0 has important significance, since can be approximately solved the tasks, which with the aid of Maxwell's equations cannot be solved. This, for example, the case, when spirals are the conductors of transmission line.

II. New Approaches to Questions of Emission and Propagation of the Electromagnetic Waves

a) Dynamic potentials and the field of the moving charges

With the propagation of wave in the long line it is filled up with two forms of energy, which can be determined through the currents and the voltages or through the electrical and magnetic fields in the line. And only after wave will fill with electromagnetic energy all space between the generator and the load on it will begin to be separated energy. I.e. the time, by which stays this process, generator expended its power to the filling with energy of the section of line between the generator and the load. But if we begin to move away load from incoming line, then a quantity of energy being inflated on it will decrease, since the part of the energy, expended by source, will leave to the filling with energy of the additional length of line, connected with the motion of load. If load will approach a source, then it will obtain an additional quantity of energy due to the decrease of its length. But if effective resistance is the load of line, then an increase or the decrease of the power expendable in it can be connected only with a change in the voltage on this resistance. Therefore we come to the conclusion that during the motion of the observer of those of relatively already existing in the line pour on must lead to their change.

Being located in assigned inertial frame of reference [IFR], we interest those fields, which are created in it by the fixed and moving charges, and also by the electromagnetic waves, which are generated by the fixed and moving sources of such waves [7-10]. The fields, which are created in this IFR by moving charges and moving sources of electromagnetic waves, we will call dynamic. Can serve as an example of dynamic field the magnetic field, which appears around the moving charges.

As already mentioned, in the classical electrodynamics be absent the rule of the conversion of electrical and magnetic pour on upon transfer of one inertial system to another. This deficiency removes STR, basis of which are the covariant conversions of Lorenz. With the entire mathematical validity of this approach the physical essence of such conversions up to now remains unexplained.

In this division will made attempt find the precisely physically substantiated ways of obtaining the conversions pour on upon transfer of one IFR to another, and to also explain what dynamic potentials and fields can generate the moving charges. Next step, demonstrated in the works [11-15], was made in this direction a way of the introduction of the symmetrical laws of magneto electric and electromagnetic induction. These laws are written as follows:

$$\oint \vec{E}'dl'=-\int\frac{\partial\vec{B}}{\partial t}d\vec{s}+\oint\left[\vec{v}\times\vec{B}\right]dl'$$
$$\oint \vec{H}'dl'=\int\frac{\partial\vec{D}}{\partial t}d\vec{s}-\oint\left[\vec{v}\times\vec{D}\right]dl' \qquad (3.1.1)$$

or

$$rot\vec{E}'=-\frac{\partial\vec{B}}{\partial t}+rot\left[\vec{v}\times\vec{B}\right]$$
$$rot\vec{H}'=\frac{\partial\vec{D}}{dt}-rot\left[\vec{v}\times\vec{D}\right] \qquad (3.1.2)$$

For the constants pour on these relationships they take the form:

© 2018 Global Journals

$$\vec{E}' = \left[\vec{v}\times\vec{B}\right]$$
$$\vec{H}' = -\left[\vec{v}\times\vec{D}\right] \qquad (3.1.3)$$

In relationships (3.1.1-3.1.3), which assume the validity of the conversions of Galilei prime and not prime values present fields and elements in moving and fixed IFR respectively. It must be noted, that conversions (3.1.3) earlier could be obtained only from the conversions of Lorenz.

Of relationships (3.1.1-3.1.3), which present the laws of induction, do not give information about how arose fields in initial fixed IFR. They describe only laws governing the propagation and conversion pour on in the case of motion with respect to the already existing fields.

Of relationship (3.1.3) attest to the fact that in the case of relative motion of frame of references, between the fields of $\vec{E}$ and $\vec{H}$ there is a cross coupling, i.e., motion in the fields of $\vec{H}$ leads to the appearance pour on $\vec{E}$ and vice versa. From these relationships escape the additional consequences, which were for the first time examined in the work [16]. The electric field $E=\frac{g}{2\pi\varepsilon r}$ outside the charged long rod, per unit length of which there is a charge g, decreases according to the law $\frac{1}{r}$, where r is the distance from the central axis of the rod to the observation point.

If we in parallel to the axis of rod in the field of E begin to move with the speed of Δv another IFR, then in it will appear the additional magnetic field $\Delta H = \varepsilon E \Delta v$. If we now with respect to already moving IFR begin to move third frame of reference with the speed Δv, then already due to the motion in the field ΔH will appear additive to the electric field $\Delta E=\mu\varepsilon E(\Delta v)^2$. This process can be continued and further, as a result of which can be obtained the number, which gives the value of the electric field $E'_v(r)$ in moving IFR with reaching of the speed $v=n\Delta v$, when $\Delta v\to 0$, and $n\to\infty$. In the final analysis in moving IFR the value of dynamic electric field will prove to be more than in the initial and to be determined by the relationship:

$$E'(r,v_\perp)=\frac{gch\frac{v_\perp}{c}}{2\pi\varepsilon r}=Ech\frac{v_\perp}{c}.$$

If speech goes about the electric field of the single charge e, then its electric field will be determined by the relationship:

$$E'(r,v_\perp)=\frac{ech\frac{v_\perp}{c}}{4\pi\varepsilon r^2},$$

where $v_\perp$ - normal component of charge rate to the vector, which connects the moving charge and observation point.

Expression for the scalar potential, created by the moving charge, for this case will be written down as follows [1-4]:

$$\varphi'(r,v_\perp)=\frac{ech\frac{v_\perp}{c}}{4\pi\varepsilon r}=\varphi(r)ch\frac{v_\perp}{c} \qquad (3.1.4)$$

where $\varphi(r)$ - scalar potential of fixed charge.

The potential of can be named scalar- vector, since it depends not only on the absolute value of charge, but also on speed and direction of its motion with respect to the observation point. Maximum value this potential has in the direction normal to the motion of charge itself. Moreover, if charge rate changes, which is connected with its acceleration, then can be calculated the electric fields, induced by the accelerated charge.

During the motion in the magnetic field, using the already examined method, we obtain:

$$H'(v_\perp)=Hch\frac{v_\perp}{c},$$

where $v_\perp$ - speed normal to the direction of the magnetic field.

If we apply the obtained results to the electromagnetic wave and to designate components pour on parallel speeds IFR as $E_\uparrow$, $H_\uparrow$, and $E_\perp$, $H_\perp$ as components normal to it, then conversions pour on they will be written down:

$$\vec{E}'_\uparrow = \vec{E}_\uparrow,$$
$$\vec{E}'_\perp = \vec{E}_\perp ch\frac{v}{c} + \frac{Z_0}{v}\left[\vec{v}\times\vec{H}_\perp\right]sh\frac{v}{c},$$
$$\vec{H}'_\uparrow=\vec{H}_\uparrow,$$
$$\vec{H}'_\perp = \vec{H}_\perp ch\frac{v}{c} - \frac{1}{vZ_0}\left[\vec{v}\times\vec{E}_\perp\right]sh\frac{v}{c}, \qquad (3.1.5)$$

where $Z_0=\sqrt{\frac{\mu_0}{\varepsilon_0}}$ - impedance of free space, $c=\sqrt{\frac{1}{\mu_0\varepsilon_0}}$ - speed of light.

© 2018 Global Journals

Conversions pour on (3.1.5) they were for the first time obtained in the work [16-18] they are called Mende conversions.

b) Phase aberration and the transverse Doppler effect

Of the aid of relationships (3.1.5) it is possible to explain the phenomenon of phase aberration, which did not have within the framework existing classical electrodynamics of explanations.

We will consider that there are components of the plane wave H_z and E_x, which is extended in the direction y, and primed system moves in the direction of the axis x with the speed v_x. Then components pour on in the prime coordinate system in accordance with relationships (3.1.5) they will be written down:

$$E'_x = E_x,$$

$$E'_y = H_z sh\frac{v_x}{c},$$

$$H'_z = H_z ch\frac{v_x}{c}.$$

Thas is a heterogeneous wave, which has in the direction of propagation the component E'_v.

Let us write down the summary field E' in moving IFR:

$$E' = \left[\left(E'_x\right)^2 + \left(E'_y\right)^2\right]^{\frac{1}{2}} = E_x ch\frac{v_x}{c}. \qquad (3.2.1)$$

If the vector $\vec{H}'$ is as before orthogonal the axis y, then the vector $\vec{E}'$ is now inclined toward it to the angle α, determined by the relationship:

$$\alpha \cong sh\frac{v}{c} \cong \frac{v}{c} \qquad (3.2.2)$$

This is phase aberration. Specifically, to this angle to be necessary to incline telescope in the direction of the motion of the Earth around the sun in order to observe stars, which are located in the zenith?

The vector of Pointing is now also directed no longer along the axis y, but being located in the plane xy, it is inclined toward the axis y to the angle, determined by relationships (3.2.2). However, the relation of the absolute values of the vectors $\vec{E}'$ and $\vec{H}'$ in both systems they remained identical. However, the absolute value of the very vector of Pointing increased. Thus, even transverse motion of inertial system with respect to the direction of propagation of wave increases its energy in the moving system. This phenomenon is understandable from a physical point of view. It is possible to give an example with the rain drops. When they fall vertically, then is energy in them one. But in the inertial system, which is moved normal to the vector of their of speed, to this speed the velocity vector of inertial system is added. In this case the absolute value of the speed of drops in the inertial system will be equal to square root of the sum of the squares of the speeds indicated. The same result gives to us relationship (3.2.1).

Is not difficult to show that, if we the polarization of electromagnetic wave change ourselves, then result will remain before. Conversions with respect to the vectors $\vec{E}$ and $\vec{H}$ are completely symmetrical, only difference will be the fact that to now come out the wave, which has to appear addition in the direction of propagation in the component H'_v.

Such waves have in the direction of its propagation additional of the vector of electrical or magnetic field, and in this they are similar to E and H of the waves, which are extended in the waveguides. In this case appears the uncommon wave, whose phase front is inclined toward the vector of Pointing to the angle, determined by relationship (3.2.2). In fact obtained wave is the superposition of plane wave with the phase speed $c = \sqrt{\frac{1}{\mu\varepsilon}}$ and additional wave of plane wave with the infinite phase speed orthogonal to the direction of propagation.

The transverse Doppler effect, who long ago is discussed sufficiently, until now, did not find its confident experimental confirmation. For observing the star from moving IFR it is necessary to incline telescope on the motion of motion to the angle, determined by relationship (3.2.2). But in this case the star, observed with the aid of the telescope in the zenith, will be in actuality located several behind the visible position with respect to the direction of motion. Its angular displacement from the visible position in this case will be determined by relationship (3.2.2). But this means that this star with respect to the observer has a radial velocity component, determined by the relationship

$$v_r = v\sin\alpha,$$

since for the low values of the angles $\sin\alpha \cong \alpha$, and $\alpha = \frac{v}{c}$, Doppler frequency shift will compose

$$\omega_{d\perp} = \omega_0 \frac{v^2}{c^2}. \qquad (3.2.3)$$

This result numerically coincides with results special theory of relativity (STR), but it is principally characterized by relaunch. Of results fact that it is considered into STR that the transverse Doppler effect, determined by relationship (3.2.3), there is in actuality, while in this case this only apparent effect. If we

© 2018 Global Journals

compare the results of conversions pour on (3.1.5) with conversions STR, then it is not difficult to see that they coincide with accuracy to the quadratic members of the ratio of the velocity of the motion of charge to the speed of light.

Of conversion STR, although they were based on the postulates, could correctly explain sufficiently accurately many physical phenomena, which before this explanation did not have. With this circumstance is connected this great success of this theory. Conversions (3.1.4) and (3.1.5) are obtained on the physical basis without the use of postulates and they with the high accuracy coincided with STR. Difference is the fact that in conversions (3.1.5) there are no limitations on the speed for the material particles, and also the fact that the charge is not the invariant of speed. The experimental confirmation of the fact indicated can serve as the confirmation of correctness of the proposed conversions.

c) Laws of the electro-electrical induction

Since pour on any process of the propagation of electrical and potentials it is always connected with the delay, let us introduce the being late scalar- vector potential, by considering that the field of this potential is extended in this medium with a speed of light [19-20]:

$$\varphi(r,t)=\frac{g\ ch\dfrac{v_{\perp}\left(t-\dfrac{r}{c}\right)}{c}}{4\pi\ \varepsilon_0 r}, \qquad (3.3.1)$$

where $v_{\perp}\left(t-\frac{r}{c}\right)$ - component of the charge rate g, normal to the vector $\vec{r}$ at the moment of the time $t'=t-\frac{r}{c}$, r-the distance between the charge and the point at which the field is determined at the time t.

But does appear a question, on what bases, if we do not use Maxwell's equation, from whom does follow wave equation, is introduced the being late scalar- vector potential? This question was examined in the thirteenth paragraph, when the velocity of propagation of the front of the wave of the tension of magnetic and electric field in the long line was determined. There, without resorting to Maxwell's equations, it was shown that electrical and magnetic field they are extended with the final speed, which in the vacuum line is equal to the speed of light. Consequently, such fields are late to the period $\frac{r}{c}$. The same delay we introduce in this case and for the scalar-vector potential, which is the carrier of electrical field.

Using relationship $\vec{E}=-grad\ \varphi(r,t)$, let us find field at point 1 (Fig. 6)

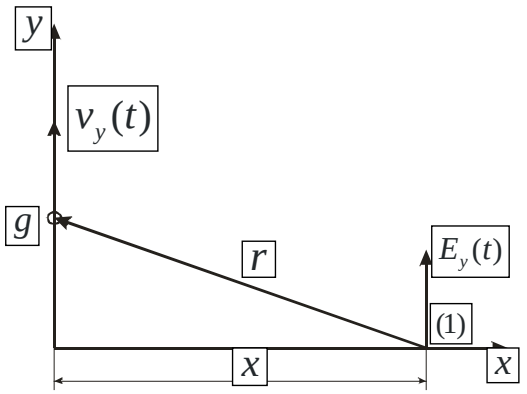


Fig. 6: Diagram of shaping of the induced electric field

The gradient of the numerical value of a radius of the vector of is a scalar function of two points: the initial point of a radius of vector and its end point (in this case this point 1 on the axis of and point 0 at the origin of coordinates). Point 1 is the point of source, while point 0 - by observation point. With the determination of gradient from the function, which contains a radius depending on the conditions of task it is necessary to distinguish two cases:

1) The point of source is fixed and is considered as the function of the position of observation point.
2) Observation point is fixed and $\vec{r}$ is considered as the function of the position of the point of source.

We will consider that the charge e accomplishes fluctuating motion along the axis y, in the environment of point 0, which is observation point, and fixed point 1 is the point of source and $\vec{r}$ is considered as the function of the position of charge. Then we write down the value of electric field at point 1:

$$E_y(1)=-\frac{\partial}{\partial y}\frac{e}{4\pi\varepsilon_0 r(y,t)}\ ch\frac{v_y\left(t-\dfrac{r(y,t)}{c}\right)}{c},$$

when the amplitude of the fluctuations of charge is considerably less than distance to the observation point, it is possible to consider a radius vector constant. We obtain with this condition:

$$E_y(x,t)=-\frac{e}{4\pi\varepsilon_0 cx}\frac{\partial v_y\left(t-\dfrac{x}{c}\right)}{\partial y}sh\frac{v_y\left(t-\dfrac{x}{c}\right)}{c}, \qquad (3.3.2)$$

where x - some fixed point on the axis x.
Taking into account that

$$\frac{\partial v_y\left(t-\frac{x}{c}\right)}{\partial y}=\frac{\partial v_y\left(t-\frac{x}{c}\right)}{\partial t}\frac{\partial t}{\partial y}=\frac{\partial v_y\left(t-\frac{x}{c}\right)}{\partial t}\frac{1}{v_y\left(t-\frac{x}{c}\right)},$$

© 2018 Global Journals

we obtain from (3.3.2):

$$E_y(x,t)=\frac{e}{4\pi\varepsilon_0 cx}\frac{1}{v_y\left(t-\frac{x}{c}\right)}\frac{\partial v_y\left(t-\frac{x}{c}\right)}{\partial t}sh\frac{v_y\left(t-\frac{x}{c}\right)}{c}. \quad (3.3.3)$$

This is a complete emission law of the moving charge.

If we take only first term of the expansion $sh\frac{v_y\left(t-\frac{x}{c}\right)}{c}$, then we will obtain from (3.3.3):

$$E_y(x,t)=-\frac{ea_y\left(t-\frac{x}{c}\right)}{4\pi\varepsilon_0 c^2 x}, \quad (3.3.4)$$

where $a_y\left(t-\frac{x}{c}\right)$ - being late acceleration of charge.

This relationship is wave equation and defines both the amplitude and phase responses of the wave of the electric field, radiated by the moving charge.

If we as the direction of emission take the vector, which lies at the plane xy, and which constitutes with the axis y the angle α, then relationship (3.3.4) takes the form:

$$E_y(x,t,\alpha)=-\frac{ea_y\left(t-\frac{x}{c}\right)\sin\alpha}{4\pi\varepsilon_0 c^2 x}. \quad (3.3.5)$$

Relationship (3.3.5) determines the radiation pattern. Since in this case there is axial symmetry relative to the axis y, it is possible to calculate the complete radiation pattern of this emission. This diagram corresponds to the radiation pattern of dipole emission.

Since

$$\frac{ev_z\left(t-\frac{x}{c}\right)}{4\pi x}=A_H\left(t-\frac{x}{c}\right)$$

there is the being late vector potential, the relationship (3.3.5) can be rewritten

$$E_y(x,t,\alpha)=-\frac{ea_y\left(t-\frac{x}{c}\right)\sin\alpha}{4\pi\varepsilon_0 c^2 x},$$

or

$$E_y(x,t,\alpha)=-\mu_0\frac{\partial A_H\left(t-\frac{x}{c}\right)}{\partial t}.$$

Is again obtained complete agreement with the equations of the being late vector potential, but vector potential is introduced here not by phenomenological method, but with the use of a concept of the being late scalar-vector potential. It is necessary to note one important circumstance: in Maxwell's equations the electric fields, which present wave, vortex. In this case the electric fields bear gradient nature.

Let us demonstrate the still one possibility, which opens relationship (3.3.5). Is known that in the electrodynamics there is this concept, as the electric dipole and the dipole emission, when the charges, which are varied in the electric dipole, emit electromagnetic waves. Two charges with the opposite signs have the dipole moment:

$$\vec{p}=e\vec{d}, \quad (3.3.6)$$

where the vector $\vec{d}$ is directed from the negative charge toward the positive charge. Therefore current can be expressed through the derivative of dipole moment on the time

$$e\vec{v}=e\frac{\partial\vec{d}}{\partial t}=\frac{\partial\vec{p}}{\partial t}.$$

Consequently

$$\vec{v}=\frac{1}{e}\frac{\partial\vec{p}}{\partial t},$$

and

$$\vec{a}=\frac{\partial\vec{v}}{\partial t}=\frac{1}{e}\frac{\partial^2\vec{p}}{\partial t^2}.$$

Substituting this relationship into expression (3.3.5), we obtain the emission law of the being varied dipole.

$$\vec{E}=-\frac{1}{4\pi r\varepsilon_0 c^2}\frac{\partial^2 p(t-\frac{r}{c})}{\partial t^2}. \quad (3.3.7)$$

This is also very well-known relationship [21].

In the process of fluctuating the electric dipole are created the electric fields of two forms. Firs, these are the electrical induction fields of emission, represented by equations (3.3.4), (3.3.5) and (3.3.6), connected with the acceleration of charge. In addition to this, around the being varied dipole are formed the electric fields of static dipole, which change in the time in connection with the fact that the distance between the charges it depends on time. However, the summary value of field, around this dipole defines as the superposition of those obtained pour on.

© 2018 Global Journals

Laws (3.3.4), (3.3.5), (3.3.7) neither are the laws of the direct action, in which already there is neither magnetic pour on nor vector potentials. I.e. those structures, by which there were the magnetic field and magnetic vector potential, are already taken and they no longer were necessary to us.

Using relationship (3.3.5) it is possible to obtain the laws of reflection and scattering both for the single charges and, for any quantity of them. If any charge or group of charges undergo the action of external (strange) electric field, then such charges begin to accomplish a forced motion, and each of them emits electric fields in accordance with relationship (3.3.5). The superposition of electrical pour on, radiated by all charges, it is electrical wave.

If on the charge acts the electric field $E'_y = E'_{y0}\sin\omega t$, then the acceleration of charge is determined by the equation

$$a = -\frac{e}{m}E'_{y0}\sin\omega t .$$

Taking into account this relationship (18.5) assumes the form

$$E_y(x,t,\alpha) = \frac{e^2}{4\pi\varepsilon_0 c^2 m}\frac{\sin\alpha}{x}E'_{y0}\sin\omega\left(t-\frac{x}{c}\right), \quad (3.3.8)$$

where the coefficient

$$K = \frac{e^2}{4\pi\varepsilon_0 c^2 m}\sin\alpha ,$$

where the coefficient of can be named the coefficient of scattering (re-emission) single charge in the assigned direction, since it determines the ability of charge to re-emit the acting on it external electric field.

The current wave of the displacement accompanies the wave of electric field:

$$j_y(x,t) = -\frac{e\sin\alpha}{4\pi c^2 x}\frac{\partial^2 v_y\left(t-\frac{x}{c}\right)}{\partial t^2} .$$

If charge accomplishes its motion under the action of the electric field $E' = E'_0\sin\omega t$, then bias current in the distant zone will be written down as

$$j_y(x,t) = -\frac{e^2\omega}{4\pi c^2 m x}E'_{y0}\cos\omega\left(t-\frac{x}{c}\right). \quad (3.3.9)$$

The sum wave, which presents the propagation of electrical pour on (3.3.8) and bias currents (3.3.9), can be named electric current wave. In this current wave of displacement lags behind the wave of electric field to the angle equal $\frac{\pi}{2}$. For the firth time this term and definition of this wave was used in the works [2,3].

In parallel with the electrical waves it is possible to introduce magnetic waves, if we assume that

$$\vec{j} = \varepsilon_0\frac{\partial\vec{E}}{\partial t} = rot\vec{H} , \quad (3.3.10)$$

$$div\vec{H} = 0 .$$

Introduced thus magnetic field is vortex. Comparing (3.3.9) and (3.3.10) we obtain:

$$\frac{\partial H_z(x,t)}{\partial x} = \frac{e^2\omega}{4\pi c^2 m x}\sin\alpha\, E'_{y0}\cos\omega\left(t-\frac{x}{c}\right).$$

Integrating this relationship on the coordinate, we find the value of the magnetic field

$$H_z(x,t) = \frac{e^2}{4\pi c m x}\sin\alpha\, E'_{y0}\sin\omega\left(t-\frac{x}{c}\right). \quad (3.3.11)$$

Thus, relationship (3.3.8), (3.3.9) and (3.3.11) can be named the laws of electrical induction, since they give the direct coupling between the electric fields, applied to the charge, and by fields and by currents induced by this charge in its environment. Charge itself comes in the role of the transformer, which ensures this reradiation.

The magnetic field, which can be calculated with the aid of relationship (3.3.11), is directed normally both toward the electric field and toward the direction of propagation, and their relation at each point of the space is equal o

$$Z = \frac{E_y}{H_z} = \frac{1}{\varepsilon_0 c} = \left(\frac{\mu_0}{\varepsilon_0}\right)^{\frac{1}{2}},$$

where Z - wave drag of free space.

Wave drag determines the active power of losses on the single area, located normal to the direction of propagation of the wave:

$$P = \frac{1}{2}ZE^2{}_{y0} .$$

Therefore electric current wave, crossing this area, transfers through it the power, determined by the data by relationship, which is located in accordance with by Pointing's theorem about the power flux of electromagnetic wave. Therefore, for finding all parameters, which characterize wave process, it is sufficient examination only of electric current wave and knowledge of the wave drag of space. In this case it is in no way compulsory to introduce this concept as "magnetic field" and its vector potential, although there

© 2018 Global Journals

is nothing illegal in this. In this setting of the relationships, obtained for the electrical and magnetic field, they completely satisfy Helmholtz's theorem. This theorem says, that any single-valued and continuous vectorial field $\vec{F}$, which turns into zero at infinity, can be represented uniquely as the sum of the gradient of a certain scalar function φ and rotor of a certain vector function $\vec{C}$, whose divergence is equal to zero:

$$\vec{F}=grad\varphi+rot\vec{C},$$

$$div\vec{C}=0.$$

C consequently, must exist clear separation pour on to the gradient and the vortex. It is evident that in the expressions, obtained for those induced pour on, this separation is located. Electric fields bear gradient nature, and magnetic - vortex.

Thus, the construction of electrodynamics should have been begun from the acknowledgement of the dependence of scalar potential on the speed. But nature very deeply hides its secrets, and in order to come to this simple conclusion, it was necessary to pass way by length almost into two centuries. The grit, which so harmoniously were erected around the magnet poles, in a straight manner indicated the presence of some power pour on potential nature, but to this they did not turn attention; therefore it turned out that all examined only tip of the iceberg, whose substantial part remained invisible of almost two hundred years.

Taking into account entire aforesaid one should assume that at the basis of the overwhelming majority of static and dynamic phenomena at the electrodynamics only one formula (3.3.1), which assumes the dependence of the scalar potential of charge on the speed, lies. From this formula it follows and static interaction of charges, and laws of power interaction in the case of their mutual motion, and emission laws and scattering. This approach made it possible to explain from the positions of classical electrodynamics such phenomena as phase aberration and the transverse Doppler effect, which within the framework the classical electrodynamics of explanation did not find. After entire aforesaid it is possible to remove construction forests, such as magnetic field and magnetic vector potential, which do not allow here already almost two hundred years to see the building of electrodynamics in entire its sublimity and beauty.

References Références Referencias

1. С. Рамо, Дж. Уиннери. Поля и волны в современной радиотехнике. ОГИЗ: 1948, - 631 с.
2. Ф. Ф. Менде, А. С. Дубровин. Особые свойства реактивных элементов и потоков заряженных частиц. Инженернаяфизика, №11, 2016, с. 13-21.
3. F. F. Mende. Induction and Parametric Properties of Radio-Technical Elements and Lines and Property of Charges and Their Flows, AASCIT Journal of Physics Vol.1 , No. 3, Publication Date: May 21, 2015, Page: 124-134.
4. F. F. Mende. New Properties of Reactive Elements, Lines of Transmission of Energy and the Relaxation Properties of Electronic Fluxes and Conductors, AASCIT Journal of Physics, Vol.1, No. 3, Publication Date: June 12, 2015, Page: 190-200.
5. F. F. Mende, New Properties of Reactive Elements and the Problem of Propagation of Electrical Signals in Long Lines, American Journal of Electrical and Electronic Engineering, Vol. 2, No. 5, (2014), 141-145.
6. F. F. Mende. Nominal and Parametric Self-Induction of Reactive Elements and Long Lines, Engineering and Technology, Vol.2, No. 2, Publication Date: April 3, 2015, Page: 69-73.
7. F. F. Mende, Consideration and the Refinement of Some Laws and Concepts of Classical Electrodynamics and New Ideas in Modern Electrodynamics, International Journal of Physics, 2014, Vol. 2, No. 8, 231-263.
8. F. F. Mende. Dynamic Scalar Potential and the Electrokinetic Electric Field, AASCIT Journal of Physics, Vol.1 , No. 1, Publication Date: March 28, 2015, Page: 53-57.
9. F. F. Mende. Concept of Scalar-Vector Potential and Its Experimental Confirmation. AASCIT Journal of Physics, Vol.1, No. 3, Publication Date: May 21, 2015, Page: 135-148.
10. F. F. Mende. Physics of Magnetic Field and Vector Potential, AASCIT Journal of Physics, Vol.1, No. 1, Publication Date: March 28, 2015, Page: 19-27.
11. Ф. Ф. Менде. Непротиворечивая электродинамика. Харьков, НТМТ, 2008, – 153 с. ISBN 978-966-8603-23-5.
12. Ф. Ф. Менде. Существуют ли ошибки в современной физике. Харьков, Константа, 2003.- 72 с.
13. F. F. Mende. On refinement of certain laws of classical electrodynamics, arXiv, physics/0402084.
14. Ф. Ф. Менде. Великие заблуждения и ошибки физиков XIX-XX столетий. Революция в современной физике. Харьков, НТМТ, 2010, – 176 с. ISBN 978-617-578-010-7.
15. F. F. Mende. Symmetrization and the Modification of the Equations of Induction and Material Equations of Maxwell , AASCIT Journal of Physics, Vol.1 , No. 3, Publication Date: June 3, 2015, Page: 171-179.
16. Ф. Ф. Менде. К вопросу об уточнении уравнений элетромагнитной индукции. - Харьков, депонированав ВИНИТИ, №774-В88 Деп., 1988.-32с.
17. F. F. Mende On refinement of certain laws of classical electrodynamics, arXiv, physics/0402084.

© 2018 Global Journals

18. F. F. Mende. Conception of the scalar-vector potential in contemporary electrodynamics, arXiv.org/abs/physics/0506083.
19. Ф. Ф. Менде, А.С. Дубровин. Альтернативная идеология электродинамики. Монография. М.: Перо, 2016. – 198 с.
20. F. F. Mende, A. S.Dubrovin. Alternative ideology of electrodynamics. Monograph. M.: Перо, 2016. - 216 p.
21. Р. Фейнман, Р. Лейтон , М. Сэндс. Фейнмановские лекции по физике. М: Мир, 1977.

© 2018 Global Journals

Global Journal of Science Frontier Research: a
Physics and Space Science
Volume 18 Issue 4 Version 1.0 Year 2018
Type: Double Blind Peer Reviewed International Research Journal
Publisher: Global Journals
Online ISSN: 2249-4626 & Print ISSN: 0975-5896

Origin of Gravitation and Description of Galaxy Rotation in a Fundamental Bound State Approach

By Hans-Peter Morsch

Abstract- Considering gravitation as magnetic binding of (e-p) pairs, galactic systems are described in a fundamental theory based on a QED like Lagrangian with fermions coupled to boson fields. In this formalism severe boundary conditions have to be fulfilled, related to geometry, momentum and energy-momentum conservation. In this way all needed parameters are determined; thus giving rise to a description based on first principles.

The primary process is magnetic binding of (e-p) pairs, leading to a very small binding energy of about 3 10^{-38} GeV and a first-order equivalent coupling constant, which is in agreement with Newton's gravitational constant G_N.

Keywords: description of gravitational systems as magnetic binding of many (e-p) pairs. quantitative account of the rotation profiles of galaxies, giving rise to masses in agreement with gravitation theory by including the finite size of these systems.

GJSFR-A Classification: FOR Code: 020199



Strictly as per the compliance and regulations of:

© 2018. Hans-Peter Morsch. This is a research/review paper, distributed under the terms of the Creative Commons Attribution-Noncommercial 3.0 Unported License http://creativecommons.org/licenses/by-nc/3.0/), permitting all non commercial use, distribution, and reproduction in any medium, provided the original work is properly cited.

Origin of Gravitation and Description of Galaxy Rotation in a Fundamental Bound State Approach

Hans-Peter Morsch

Abstract- Considering gravitation as magnetic binding of (e-p) pairs, galactic systems are described in a fundamental theory based on a QED like Lagrangian with fermions coupled to boson fields. In this formalism severe boundary conditions have to be fulfilled, related to geometry, momentum and energy-momentum conservation. In this way all needed parameters are determined; thus giving rise to a description based on first principles.

The primary process is magnetic binding of (e-p) pairs, leading to a very small binding energy of about 3 10^{-38} GeV and a first-order equivalent coupling constant, which is in agreement with Newton's gravitational constant G_N.

Systems of magnetic binding of $10^{\sim 100}$ (e-p) pairs (or hydrogen atoms) are related to galaxies. Their rotation velocities are well described, yielding information on the mass, the average particle density and the damping of coherent rotation. Different from the mass estimate $M^{gr} \sim v_{max}^2 R/G_N$ derived from gravitation theory, the deduced galaxy masses show a rapid fall-off to smaller radii, which can be understood by the finiteness of these systems.

No evidence has been found for galactic dark matter contributions.

Keywords: description of gravitational systems as magnetic binding of many (e-p) pairs. quantitative account of the rotation profiles of galaxies, giving rise to masses in agreement with gravitation theory by including the finite size of these systems.

I. Introduction

Elementary bound or stationary states may be considered as the building blocks of nature, since they give rise to stability of matter over long periods of time. These systems require an equilibrium between binding and kinetic energy, governed by the virial theorem. Their description in form of atoms, hadrons, and leptons has been discussed recently [1, 2].

Galactic systems have also the important property of stability over long time scales. However, it appears to be difficult to consider these systems as bound states, since it is known that the universe is not of static structure: starting from a cosmic system, in which all matter had been confined in a small volume of high density, it expands permanently. In addition, for a realistic description of galaxies the origin of gravitation has to be understood.

Gravitation has been mostly described by Newton's gravitation theory, often complemented by Einstein's theory of general relativity [3]. In the latter, gravitation is considered as a deformation of space-time caused by massive objects. However, this theory is not satisfactory from a fundamental point of view: by eliminating gravity by the equivalence principle the real physical origin of the gravitational attraction rests unknown. Differently, in a (first-order) quantum theory similar to those applied to other fundamental forces, the extremely weak interaction has been tentatively interpreted [4] as tensor-exchange of "gravitons", but such spin=2 particles have not been found. Further, serious attempts have been made to describe gravity in high-dimensional string-type models [5], in which the notion of point particles is replaced by one-dimensional strings. However, these models have a very complicated structure with too many parameters to be adjusted. Also it is not clear, whether (and eventually how) curved space-time has to be included in a quantum description of gravity.

Important to note that all known theories applied to fundamental forces have been constructed empirically and need external parameters, which have to be fixed in some way. Also general relativity is an empirical theory, in which space-time parameters related to curvature, expansion, etc. have to be adjusted to astrophysical observations. But this does not allow absolute predictions, which can be tested experimentally. The requirement of an adequate fundamental theory can be expressed by the theorem: If in a theory adjustable parameters are needed, which cannot be determined from basic constraints, a (more) fundamental theory has to exist, in which all parameters can be deduced from first principles.

During the last years, such a self-contained theory has been developed [1, 2], in which atoms, but also hadrons and leptons can be understood without employing external parameters. One can also expect that such a fundamental theory can describe systems bound by gravitation. Indeed, in the study of magnetic bound states, a solution of two hydrogen atoms has been found [2], which has a tiny binding energy and a first order equivalent coupling constant in agreement

Author: H.P.M., HOFF, Brockmüllerstr. 11 D-52428 Jülich, Germany. e-mail: h.p.morsch@gmx.de

© 2018 Global Journals

with Newton's gravitational constant G_N. Therefore, this type of binding could be the origin of gravitation. To test this conjecture, in the present paper this formalism has been applied to the description of galactic systems.

First, we give a brief discussion of the theoretical framework with emphasis on basic boundary conditions. Then, a magnetic bound state composed of (e-p) pairs is discussed in detail, in which the parameter ambiguities could be removed by requiring a consistent account of the rotation velocity. Based on this fundamental system we describe galactic systems by a large number of such (e-p) pairs. In this way a complete and self-consistent description of galaxies is obtained.

II. Theoretical Background and Constraints on Magnetically Bound States

The present description is based on field theory, with a Lagrangian similar to that of quantum electrodynamics (QED), in which the fermions Ψ^+ and Ψ^- are accompanied by boson fields A_μ

$$\mathcal{L} = \frac{1}{\tilde{m}^2}(\bar{\Psi}^- D_\nu)\; i\gamma^\mu D_\mu\; (D^\nu \Psi^+) \;-\; \frac{1}{4} F_{\mu\nu}F^{\mu\nu}\;. \tag{1}$$

The reduced mass $\tilde{m}$ is given by $\tilde{m}=m_1 m_2/(m_1+m_2)$, where m_i are the masses of the participating particles. The vector boson fields A_μ with coupling g to fermions are contained in the covariant derivatives $D_\mu = \partial_\mu - igA_\mu$. Further, the second term of the Lagrangian represents the Maxwell term with Abelian field strength tensors $F^{\mu\nu}$ given by $F^{\mu\nu}=\partial^\mu A^\nu - \partial^\nu A^\mu$, which gives rise to both electric and magnetic coupling (magnetic effects arise from the motion of fermions).

This framework has been discussed in detail in refs. [1, 2]. It leads to a theory of finite structure for radii $r\to 0$ and $r\to\infty$, giving rise to matrix elements, which can be described by fermion and boson wave functions $\psi_{s,v}(r)$ and $w_{s,v}(r)$ (of scalar and vector structure) connected by bosonic interaction potentials. For fermions this results in two matrix elements

$$\mathcal{M}^f_{ng}(r) = \bar{\psi}_{s,v}(r)\; V_{ng}(r)\, \psi_{s,v}(r)\; (v/c)^2\;, \tag{2}$$

with n=2,3 and potentials of the form

$$V_{2g}(r) = \frac{\alpha^2(\hbar c)^2(2s+1)}{8\tilde{m}}\;\Big(\frac{d^2 w_s(r)}{dr^2} + \frac{2}{r}\frac{dw_s(r)}{dr}\Big)\frac{1}{w_s(r)} + E_o \tag{3}$$

with s=0 for scalar and s=1 for vector states, and

$$V_{3g}(r) = \frac{\alpha^3(\hbar c)}{\tilde{m}}\int dr'\; w_{s,v}(r')\; v_v(r-r')\; w_{s,v}(r')\;. \tag{4}$$

The boson matrix element is of the form

$$\mathcal{M}^g(r) = \frac{\alpha^3(\hbar c)}{\tilde{m}}\; w_{s,v}(r)\; v_v(r)\; w_{s,v}(r)\; (v/c)\;. \tag{5}$$

The geometric boundary conditions [1, 2] are satisfied by using $\psi_{s,v}(r) \sim w_{s,v}(r)$, with

$$w_s(r) = w_{s_o}\; exp\{-(r/b)^\kappa\} \tag{6}$$

and

$$w_v(r) = w_{v_o}\; [w_s(r) + \beta R\; \frac{dw_s(r)}{dr}]\;. \tag{7}$$

The normalization of $\psi_{s,v}(r)$ and $w_{s,v}(r)$ is obtained by requiring $4\pi\int r^2 dr\; \psi^{\,2}_{s,v}(r)=1$, $2\pi\int r dr\; w^2_{s,v}(r)=1$ and $\beta R = -\int r^2 dr\, w_s(r)/\int r^2 dr[dw_s(r)/dr]$. Further, $v_v(r)$ is a boson-exchange interaction, which has a radial form similar to $w_v(r)$. In addition, for magnetically bound systems (v/c) is the relative velocity of different fermion and boson components, see the details in ref. [2].

An important point is that a consistent description (in which about 10 constraints have to be fulfilled) can be obtained only [1], if the energy E_o in eq. (3) is set to zero. This indicates a coupling of the theory to the (absolute) vacuum of fluctuating boson fields, which allows creation of massless fermion-antifermion pairs during overlap of boson fields. These particles are immediately bound to form simple $q\bar{q}$ mesons, q indicating massless fermions (quantons).

The binding and kinetic energies have been calculated as given in refs. [1, 2]. The mass is defined by the absolute binding energies $M = |E_{2g}| + |E_{3g}|$, where E_{2g} and E_{3g} are the binding energies in $V_{2g}(r)$ and $V_{3g}(r)$, respectively.

© 2018 Global Journals

In addition to the geometric boundary conditions [1, 2] we require momentum matching between fermions and bosons

$$< q_g^2 >_{rec}^{1/2} + < q_f^2 >_{rec}^{1/2} = 0 \qquad (8)$$

as well as energy-momentum conservation

$$[< q_g^2 >^{1/2} + < q_f^2 >^{1/2}]\ (v/c) + E_g - x\ M_f = 0, \qquad (9)$$

where $x = \sqrt{2\tilde{m}/M_f}$ and (v/c) is taken as positive.

The momenta are given by $<q_g^2> = <q_g^2>_{rec}$ and $< q_{f_s}^2 > = < q_{f_s}^2 >_{rec}$, but for vector particles $< q_{f_v}^2 > = \int q^4 dq\ \psi_v(q) V_{3g}^v(q) / < q_{f_v}^0 >$, where the Fourier transformed quantities are given by $(\psi_v, V_{3g}^v)(q) = 4\pi \int r^2 dr\ j_1{}^2(qr)(\psi_v, V_{3g}^v)(r)$.

Further, a mass-radius condition has been derived from the potential $V_{2g}(r)$

$$Rat_{2g} = \frac{(\hbar c)^2\ (v/c)^2}{\tilde{m}(M_s/2) < r_{\psi_s}^2 >} = 1\ . \qquad (10)$$

Finally it is important to note that magnetically bound vector states (with radial node) are not stable. Nevertheless, energy-momentum conservation should be fulfilled for all states.

a) Existence of a complex magnetic bound state

A solution for magnetically bound hydrogen atoms (H-H) has been discussed in ref. [2], which led to a first-order equivalent coupling constant in agreement with Newton's gravitational constant G_N. Therefore, this type of bound state could be the origin of gravitation. However, in more detailed work it has been found that the boundary conditions are also satisfied, if both - the slope parameter b and the relative velocity factor $(v/c)^2$ - are multiplied with the same factor. This indicates that an extra constraint is needed to obtain an unambiguous solution.

Such a constraint can be defined by requiring that the velocity (v/c) is related to the kinetic energy by

$$(v/c) = \sqrt{\frac{2E^{kin}}{M_{tot}}}\ , \qquad (11)$$

where $M_{tot} = 2m_e + 2m_p$ is the total mass of the diatomic H-H or (e-p)^2 state. By imposing this constraint, an unambiguous solution is obtained, in which all boundary conditions are satisfied, see table 1. Even for the s-state energy-momentum conservation is fulfilled for bosons and fermions separately. Important to note that also in this case the first-order equivalent coupling constant

$$\alpha_{gr} = \frac{\int V_{3g}^s(r)\ dr}{\int \frac{\hbar c}{r}\ dr} \qquad (12)$$

Table 1: Solution of a (e-p)^2 state bound magnetically, using $\kappa = 1.35$ and $\alpha = 2.14$. All dimensional quantities are in GeV or fm.

system	$\tilde{m}$	b	$(v/c)^2$	$< r^2{}_s >^{1/2}$	M_s	Rat_{2g}	α_{gr}
$(ep)^2$	0.469	0.3425	$1.51\ 10^{-38}$	0.40	$2.6\ 10^{-38}$	1.0	$5.9\ 10^{-39}$

s	$< q_g^2 >^{1/2}\ (v/c)$	$< q_f^2 >^{1/2}\ (v/c)$	$\sum < q_{g,f}^2 >^{1/2}\ (v/c)$	E_g	xM_f	$xM_f - E_g$
0	$1.6 \pm 0.1\ 10^{-19}$	$1.6 \pm 0.2\ 10^{-19}$	$3.2 \pm 0.3\ 10^{-19}$	$-1.6\ 10^{-19}$	$1.6\ 10^{-19}$	$3.2\ 10^{-19}$
1	$2.2 \pm 0.2\ 10^{-19}$	$4.2 \pm 0.3\ 10^{-19}$	$6.4 \pm 0.5\ 10^{-19}$	$-2.6\ 10^{-19}$	$3.4\ 10^{-19}$	$6.0\ 10^{-19}$

is in good agreement with Newton's gravitational constant $G_N = 6.707\ 10^{-39} (\hbar c) GeV^{-2}$. This result may be taken as convincing evidence that the origin of gravitation is magnetic binding of many atoms.

The deduced scalar density and potentials are shown in fig. 1. In the upper part, the present interaction $v_v(r)$ is compared to a gravitational potential ~1/r, which shows the difference between a finite interaction and a divergent one. Below, the scalar density $w_s^2(r)$ and the potentials $V_{3g}^{s,v}(r)$ are given. One can see that $V_{3g}^v(r) \sim w_s^2(r)$, as required from a second geometric boundary condition [1, 2]. In the lower part of the figure the potential $V_{2g}(r)$ is displayed, which stabilizes the system. This potential has the same radial form as the "confinement" potential in hadrons and leptons.

This solution shows a fermion root-mean-square (rms) radius of 0.40 fm, indicating that the protons and electrons come close to each other (giving rise to a (e-p)^2 rather than a diatomic H-H state). This is consistent with the general observation from hadrons and leptons that magnetically bound systems have smaller radii than those bound electrically. Another point of interest, the ambiguity between *b* and $(v/c)^2$ without applying the condition (11) - indicates that the first-order equivalent coupling constant α_{gr} is the same - and thus universal - for all gravitational systems with increased or decreased central density relative to the basic (e-p)^2 state.

© 2018 Global Journals

b) Description of magnetic (gravitational) states of many (e-p) pairs

In the following, systems composed of many (e-p) pairs are discussed. These objects have to fulfill also boundary conditions concerning geometry, momentum and energy-momentum conservation. The geometry requires similar radii of the boson and fermion distributions

$$< r_f^2 >_{gal}^{1/2} \sim < r_g^2 >_{gal}^{1/2} \sim N_{gal}^r < r_{g,f}^2 >_s^{1/2} \quad (13)$$

where $< r_{f,g}^2 >_{gal}^{1/2}$ are the fermion and boson rms-radii of the composite systems and $< r_{g,f}^2 >_s^{1/2}$ the corresponding radii of the basic (e-p) pair. Further, momentum matching

$$< q_g^2 >_{gal}^{1/2} = < q_f^2 >_{gal}^{1/2} \quad (14)$$

as well as energy-momentum conservation should be satisfied. For bosons this reads

$$E_{gal}^g \sim (N_{gal})^3 < q_{g_s}^2 >^{1/2} (v/c) = (N_{gal})^3 E_s^g \,, \quad (15)$$

and for fermions

$$M_{gal}^f \sim (N_{gal})^3 < q_{f_s}^2 >^{1/2} (v/c)/x = (N_{gal})^3 M_s^f, \quad (16)$$

where N_{gal} is the average number of basic (e-p)^2 states in r-direction, which can be different from N_{gal}^r obtained from the geometrical relation (13), (v/c) the relative fermion velocity of the (e-p)^2 bound states, E_{gal}^g the boson binding energy, M_{gal}^f the mass and $x = \sqrt{2\tilde{m}/M_s^f}$, where $\tilde{m}$ is the reduced mass.

For a composite system of many particles the relation between potential and kinetic energy is non-trivial: an acceleration term for individual particles can be derived [6] from the Lagrangian (1), which allows to drive the random motion of the single particles to a coherent rotation of the whole system. In this case the kinetic energy will be lowered, the virial theorem is violated and leads to a collapse of the system[1].

However, formation of a stable system is possible under the special condition that also the magnetic (gravitational) attraction is reduced by the same amount. Such a lowering of the binding energy may be explained by assuming that a repulsive potential has been built up by the annihilation of matter during the former high density phase of the universe, from which all galactic matter originates.

The radial dependence of the rotation velocity of galactic systems may be calculated from a relation similar to eq. (11) by replacing the kinetic energy E_{gal}^{kin} by $N_{gal}\,(dE_s^{kin}(r)/dr)r_s$ and the (total) mass by $N_{gal}^r\, M_s$. In addition, we have to introduce a damping factor f_{damp}, which takes a reduction of coherent rotation into account. This yields

$$\frac{v_{rot}(r_{gal})}{c} = \sqrt{\frac{2}{dr}\frac{dE_s^{kin}(r)}{M_s}\, r_s \frac{N_{gal}}{N_{gal}^r}}\, f_{damp} \,, \quad (17)$$

where $dE_s^{kin}(r)/dr$ is the radial derivative of the kinetic energy of the magnetic state in sect. 2. a given by

$$\frac{dE_s^{kin}(r)}{dr} = 2\pi\psi_s^2(r) r^3 \left(\frac{dV_{2g}(r)}{dr} + \frac{dV_{3g}(r)}{dr}\right). \quad (18)$$

The ratio $\delta_{gal} = N_{gal}/N_{gal}^r$ can be understood as the average rms-radius of the basic (e-p) pairs in the galaxy divided by the rms-radius of the free (e-p)^2 state. But δ_{gal} can be considered also as the normalized central density of the galaxy with respect to that of the free (e-p)^2 state. For $\delta_{gal} < 1$ the average density is smaller than the basic magnetic state, whereas $\delta_{gal} > 1$ would indicate a system of higher density. In this respect it is important to mention that also for systems with $\delta_{gal} \neq 1$ all constraints (13) - (16) have to be satisfied, and also the first-order equivalent coupling constant is unchanged (universality of G_N). Finally it is important to note that for $f_{damp} \neq 1$ the virial theorem is not fulfilled, for $f_{damp} < 1$ the system will be driven to increased radii.

A second condition requires that the maximum rotation velocity of galaxies is related to (v/c) of the fundamental state by

$$\frac{v_{max}}{c} = (v/c)\,\sqrt{N_{gal}}\, f_{damp} \,. \quad (19)$$

By the geometric relation (13) and eqs. (17) and (19) the parameters δ_{gal} and f_{damp} are fixed, leading to an unambiguous determination of the galaxy masses, see eq. (16).

Finally, galaxy masses have been estimated using an (empirical) relation between maximum rotation velocity and galaxy mass - derived from gravitation theory

$$M^{gr} = v_{max}^2 R/G_N \,, \quad (20)$$

where R is the radius at v_{max}. A comparison of the deduced masses with this estimate will be made below.

III. Rotational Velocities of Galactic Systems

Although many aspects of gravitation can be well understood within Newton's theory of gravitation, the observation of galactic rotation velocities has led in the past to misleading interpretations. In the solar system, the orbital velocities of the different planets follow closely a Keplerian $\sqrt{1/r}$ behavior, which can be derived directly from Newton's law $V_{grav} \sim 1/r$. However, such a rapid fall-off of the velocity as a

[1] The collapse of gravitational systems has been worried about already by I. Newton after formulating the gravitational potential, see also Bentley's paradox [7].

© 2018 Global Journals

function of radius has commonly not been observed for galaxies. In contrary, for many galaxies velocities have been deduced, which increase from small radii towards the peripheral region. This fact has been interpreted as evidence for the existence of dark matter halos. There have been also alternative descriptions, e.g. by MOND [8], in which an empirical modification of Newtonian dynamics has been employed.

In the present formalism the rotation velocity has to go to zero for r → 0, a physical necessity for a system of finite density and interactions. This fact indicates clearly that the r-dependence of the velocity $v_{rot}(r) \sim \sqrt{G_N M/r}$, see eq. (20), can be only an approximation of the rotation velocities at larger radii.

In the upper part of fig. 2 the particle density and the potentials are shown for a galactic system with arms - radius of 3.2 kpc. The derived rotational velocity is given in the second part. One can see that the rotation curve starts from zero at r = 0 and reaches a maximum at a radius somewhat smaller than the rms-radius, then falls again to zero. A Keplerian $\sqrt{1/r}$ dependence is shown by dot-dashed line, which shows an unphysical divergence for $r \to 0$ and $r \to \infty$.

a) *Fit of various galaxies with different radii and rotation velocities*

In the lower part of fig. 2 a comparison of the calculated rotation curve is made with the rotation profile of the galaxy F583-1, which is typical of many low surface brightness galaxies [9]. By scaling the rotation curve in radius to the outside region, a reasonable fit is obtained with a rms radius of about 13 kpc (the deviations at smaller radii could indicate another galactic component of smaller radius). The results of the present analysis are given in table 2. The deduced mass of about 8 10^7 solar masses is two orders of magnitude smaller than estimated with the mass formula (20). Further, the deduced value of δ_{gal} of 0.015 indicates an average galactic density of about 70 times smaller than of the fundamental state. The damping factor of the rotation $f_{damp} \sim 0.1$ may indicate that about 90 % of the kinetic energy is in the form of random motion, whereas only 10 % of E^{kin}_{gal} contributes to the coherent rotation of the galaxy.

Rotation profiles for three other galaxies are shown in fig. 3, the two dwarf galaxies Draco and Fornax, and the elliptic galaxy NGC 3379, with data from refs. [10, 11]. Both, Draco and Fornax have rather small radii of about 0.4 and 1.3 kpc, respectively, whereas NGC 3379 shows a rms-radius of about 9 kpc. Apart from an increase of the rotation curves at small radius, the data are well described with the parameters given in table 2.

Table 2: Results for the galaxies in figs. 2-4, with root mean square radii $< r^2_{gal} >^{1/2}$ in kpc, maximum rotation velocities in km/s and masses in units of solar masses (M_{sol} =1.11574 10^{57} GeV/c^2). In the last column, the masses are given using the gravitational mass formula (20).

System	$< r^2_{gal} >^{1/2}$	v_{max}	N_{gal}	δ_{gal}	f_{damp}	M_{gal} (M_{sol})	M^{gr} (M_{sol})
F 583-1	13.0	78	1.5 10^{34}	1.5 10^{-2}	0.099	8.0 10^7	6.6 10^9
Draco	0.37	12.6	1.2 10^{31}	4.2 10^{-4}	0.034	4.2 10^{-2}	4.9 10^6
Fornax	1.25	14.5	1.4 10^{32}	1.4 10^{-3}	0.090	6.3 10^1	2.2 10^7
NGC 3379	8.5	230	4.8 10^{33}	7.3 10^{-3}	0.032	2.7 10^6	2.9 10^{10}
UGC 128	40.0	135	1.4 10^{35}	4.5 10^{-2}	0.026	6.7 10^{10}	6.1 10^{10}
NGC 2403	15.2	136	2.0 10^{34}	1.7 10^{-2}	0.017	2.0 10^8	2.4 10^{10}
NGC 5371	16.0	200	3.0 10^{34}	2.4 10^{-2}	0.010	6.4 10^8	7.1 10^{10}
" (2)	65.0	200	3.7 10^{35}	7.4 10^{-2}	0.009	1.2 10^{12}	2.2 10^{11}

Rotation velocities of three further galaxies, UGC 128, NGC 2403 from ref. [9] and NGC 5371 with data from ref. [12], are given in fig. 4. These have rather large radii of about 40 kpc and 20 kpc, respectively, with results given also in table 2. For all three galaxies there are indications for inner-galactic contributions with a rms-radius smaller by a factor 5. For the galaxy NGC 5371 the deduced velocities do not decrease for radii larger than 30 kpc, which may indicate a large-radius component given by dashed line in fig. 4, leading to the results marked (2) given separately in table 2.

The systematic behavior of the maximum rotation velocity and the extracted values of δ_{gal} and f_{damp} as a function of the galaxy mass is given in fig. 5, the galaxy masses as a function of radius are shown in fig. 6. Surprisingly, the deduced values of δ_{gal} (in the middle part of fig. 5) as well as the radius (in the lower part in fig. 6) show a very smooth mass dependence. Differently, v_{max} and f_{damp} show deviations from the average behavior, with values of f_{damp}, which follow closely the deviations of v_{max} from the solid line (for the Galaxy NGC 3379 results for a lower value of v_{max} of

© 2018 Global Journals

75 km/s are shown by open squares, which give a slightly larger mass of 6.1 10^6 M_{sol} , but f_{damp} reduced to 0.026). The larger values of f_{damp} could be related to uncertainties in the extracted absolute velocities, but more likely due to another galaxy component with increased radius (similar to that assumed for the galaxy NGC 5371).

Of large importance, in all cases the value of f_{damp} is significantly smaller than 1. This may indicate that only the compact galaxy fragments participate in a coherent rotation, whereas the motion within these fragments is quite random. Further, f_{damp} may include a damping due to interactions with other galaxies or galactic matter. Since the present results yield $f_{damp} < 1$, galaxies cannot be considered as real bound states: their radii increase permanently, in overall agreement with the observed expansion of the universe.

A really striking result is that the relative density $\delta_{gal} = N_{gal}/N_{gal}^r$ and the other quantities in fig. 5 show (after corrections, as discussed above) a very smooth mass dependence. Such a regular behavior can be expected only, if all galaxies originate from the same source, an early cosmic state of high density. An average value of δ_{gal} of 10^{-2} corresponds to a system, in which the rms-radius of the basic (e-p) pairs is increased to 40 fm, but this is still more than a factor 10^3 smaller than the size of hydrogen atoms. If we assume that galaxies are mainly composed of hydrogen atoms, its average density is rather high. This supports again the conclusion that galaxies have been created during the high-density phase of the cosmic evolution.

IV. Discussion

The analysis of galactic systems has shown that gravitation can be well described by magnetic binding of many (e-p) pairs (or hydrogen atoms). The following points are of particular interest:

a) *Constraints on the cosmic high-density phase of matter*

As discussed above, for the description of the rotation velocities of galaxies assumptions had to be make on the annihilation mechanisms of matter, which took place during the cosmic phase of high density. In radial direction, annihilation gave rise to an enormous flow of photons, resulting in heating the surrounding matter (transformation of kinetic energy in random motion) with subsequent disintegration into countless fragments of matter, from which galactic objects have been formed. However, in the galaxy fragments the kinetic energy is essentially due to random motion.

In transverse direction, annihilation photons could not be produced; instead a repulsive potential (opposite in sign to a binding potential) has been built up, which led to a reduction of binding, responsible for the generation of rather stable galaxies.

b) *Relation between fundamental description and first-order theories*

A surprising result of the present study is that for large galaxies the extracted masses are in rather good agreement with those obtained by using the gravitational mass formula (20). At first sight, this agreement appears to be accidental, if one considers the different mechanisms involved in the present analysis. However, one should realize that the present theory is based on the Lagrangian (1), which is an extension of the first-order Lagrangian of QED, see ref. [1]. By assuming $D_\nu D^\nu = 1$ the QED Lagrangian is restored, which gives rise to a Coulomb potential $V_{coul} = \alpha \hbar c/r$ and the correct binding energies of atomic states. As detailed in ref. [13], these binding energies are also reproduced in the present theory, but in a rather complicated way including many s- and p-states, which satisfy a linear quantum condition on the radius. In addition, the electric fine-structure constant $\alpha \sim 1/137$ is reproduced by the sum of first-order equivalent coupling constants α_{eq}^n.

For gravitation this appears to be similar, assuming $D_\nu D^\nu = 1$ leads to a first-order theory, which can be considered as a quantum description of Newton's theory of gravitation, which gives rise to a gravitation potential $V_{grav}(r) = \alpha_{gr}\, \hbar c/r$ with a coupling constant $\alpha_{gr} \simeq G_N\, m_1 m_2/\hbar c$. So, it is conceivable that also other features of Newton's theory of gravitation are recovered, as masses. This is confirmed for large galaxy masses by the present results.

However, as shown in the lower part of fig. 6, a strong fall-off of the deduced masses is obtained for decreasing radii, which is not found in the gravitational mass formula (20). This behavior can be well understood by the finiteness of the interaction $v_v(r)$, as shown in fig. 6. In the upper part the r-dependence of the Fourier transformed interaction $v_v(q)$ is compared to that of the gravitational potential $V_{grav}(q) \sim 1/q^2$. For small values of *r* (or *q*) the interaction $v_v(q)$ stays finite, whereas $V_{grav}(q)$ goes to infinity. The ratio $v_v(q)/V_{grav}(q)$ as a function of *r* drops to zero for $r \to 0$, as shown by the solid line.

Exactly this behavior is observed in the galaxy masses, see the lower part of fig. 6. By scaling the radii and momenta to the corresponding radii and masses of galaxies, the masses from gravitation theory (open squares) can be fitted by a function $m^{gr} \sim V_{grav}(q)\, q^{2.5}/V_{grav}(q)$ (given by the dot-dashed line). By multiplying m^{gr} with the ratio $v_v(q)/V_{grav}(q)$ given in the upper part, the solid line is obtained, which yields a good description of the radius dependence of the deduced galaxy masses. This agreement indicates that the strong drop-off of the deduced galaxy masses for smaller radii is due to the finiteness of the system.

© 2018 Global Journals

c) Evidence for dark matter?

An important topic, discussed extensively in the literature, is the possible existence of dark matter, which does not couple to known particles by electromagnetic forces. Corresponding particles have been proposed based on conclusions drawn from current particle theories [4], but the need for dark matter is also a requirement from general relativity. Therefore, large efforts have been made to detect these particles. Up to date the only experimental indication for the existence of dark matter comes from a comparison of observed galactic rotation velocities with Keplerian $\sim \sqrt{1/r}$ rotational curves, from which the possible existence of dark matter halo contributions has been inferred, see e.g. in ref. [14]. Based on the present results in sect. 3, however, such an interpretation should be abandoned.

A similar conclusion has been drawn from MOND [8], in which an empirical modification of the Newtonian dynamics is employed. Also in this approach the rotation velocities decrease for small radii (as detailed above, the condition $v_{rot}(r) \to 0$ is a physical necessity for a finite system). This property gives rise to a finite range of the gravitational force, yielding a natural solution of Bentley's paradox [7].

Further, it should be mentioned that also direct searches for dark matter in particle physics experiments have given negative results. From extensions of current theories [4] the existence of super-symmetric or other exotic particles has been predicted as a source of dark matter. In particular, super-symmetry has been proposed as a mechanism to understand the flavour degree of hadrons and leptons. But this degree can be well understood in the present theory [15] without the assumption of additional fields.

d) Deflection of light

General relativity predicts a relation between space and time (space-time), which does not exist in the present framework. Evidence for this property stems from the bending of light from solar and galactic systems (lensing). However, in the present formalism the bending of light on massive systems can be described by the deflection of photons from multi-atomic systems. This is similar to Compton scattering from the electron (which is also a magnetically bound system [2]), but also to optical deflections and the scattering of nuclei. These processes can be described in partial wave expansions (with an incoming spherical wave and an interference of outgoing scattering waves). So, we expect that all properties of gravitation can be described in the present theory based on first principles.

V. Summary

The present study of systems bound by magnetic forces has shown that rotation curves of galaxies can be well understood in a self-contained and fundamental theory.

The results may be summarized as follows:

1. The fact that a stable (e-p)^2 system has been found with a first-order equivalent coupling constant in agreement with Newton's gravitational constant G_N can be taken as evidence that the origin of the gravitational force is magnetic binding of (e-p) pairs.
2. This conclusion is confirmed by the analysis of galaxy rotation, which is well described in the present approach. The strong reduction of the rotation velocities may indicate that galaxies have been formed from strongly heated matter during the high-density phase of the universe. The deduced galaxy masses are consistent with the empirical relation $M^{gr} \sim v_{max} R/G_N$, if finite size effects are taken into account.
3. The fact that all boundary conditions can be fulfilled only by assuming $E_o = 0$ in eq. (3) indicates a coupling of the theory to the (absolute) vacuum, by which matter in its simplest form could be created out of the vacuum during the genesis of the universe. However, in this way only particles with equal fermion and antifermion content could be generated. The breaking of this symmetry in the collapse of the generated matter - leading to the high-density phase of the universe - is one of the most challenging puzzles to be explained.
4. Finally, from a study of the complex structure of the Lagrangian (1) – including derivative terms with $\partial\Psi$ and $\partial^2\Psi$ - a better understanding of the dynamics of these processes may be obtained.

The author thanks many colleges for important discussions. In particular, he is indebted to Benoit Loiseau for his help with the theoretical formulation.

References Références Referencias

1. H.P. Morsch, Brit. J. Math. and Comp. Sc. 17(6): 1-11 (2016) (open access)
2. H.P. Morsch and S. Ghosh, J. Adv. Math. and Comp. Sc. 24(4): 1-11 (2017) (open access)
3. see e.g. A. Einstein, "Über die spezielle und allgemeine Relativitätstheorie", Vieweg, Braunschweig 1920; A. Einstein, Z. Phys. 16, 228 (1923)
4. Review of particle properties, K. Nakamura et al., J. Phys. G 37, 075021 (2010); http://pdg.lbl.gov/ and refs. Therein
5. O. Aharony, S.S. Gubser, J. Maldacena, H. Ooguri, and Y. Oz, Phys. Rep. 323, 183 (2000).
6. H.P. Morsch: From the Lagrangian (1) an acceleration term $T_{acc} \sim \bar{\psi}(r)\, w_{s,v}(r)\, (v/c)^2\, d^2\psi(r)/dr^2$ has been derived, to be published in J. Adv. Math. and Comp. Sc. (2018)
7. Bentley's paradox: Correspondence between Isaac Newton and Richard Bentley after 1690: If all stars are drawn to each other by gravitation, they should collapse in a single point.

© 2018 Global Journals

8. M. Milgrom, Astrophys. J. 270, 365 (1983) and 698, 1630 (2009); and refs. therein
9. S.S. McGaugh and W.J.G. de Blok, Astrophys. J. 499, 41 (1998) and 499,66 (1998) (arXiv: astro-ph/9801102 and 9801123) and refs. Therein
10. J.W. Moffat, arXiv:astro-ph/0412195 (2005) and refs. Therein
11. J.T. Kleyna, M.I. Wikinson, N.W. Evans, and G. Gilmore, Mon. Not. R. Astron. Soc. (Febr.1, 2008) and arXiv: astro-ph/0109450
12. E. Battaner and E. Florido arXiv:astro-phys/0010475 (2000)
13. H.P. Morsch, Boson J. of Mod. Phys. 3(1):197 (2016) (open access)
14. W.J.G. de Blok, S.S. McGaugh and V.C. Rubin, Astron. J. 122, 2396 (2001).
15. H.P. Morsch, Univ. J. of Phys. and App. 7, 252 (2013) (open access) and arXiv:1112.6345 [gen-ph]

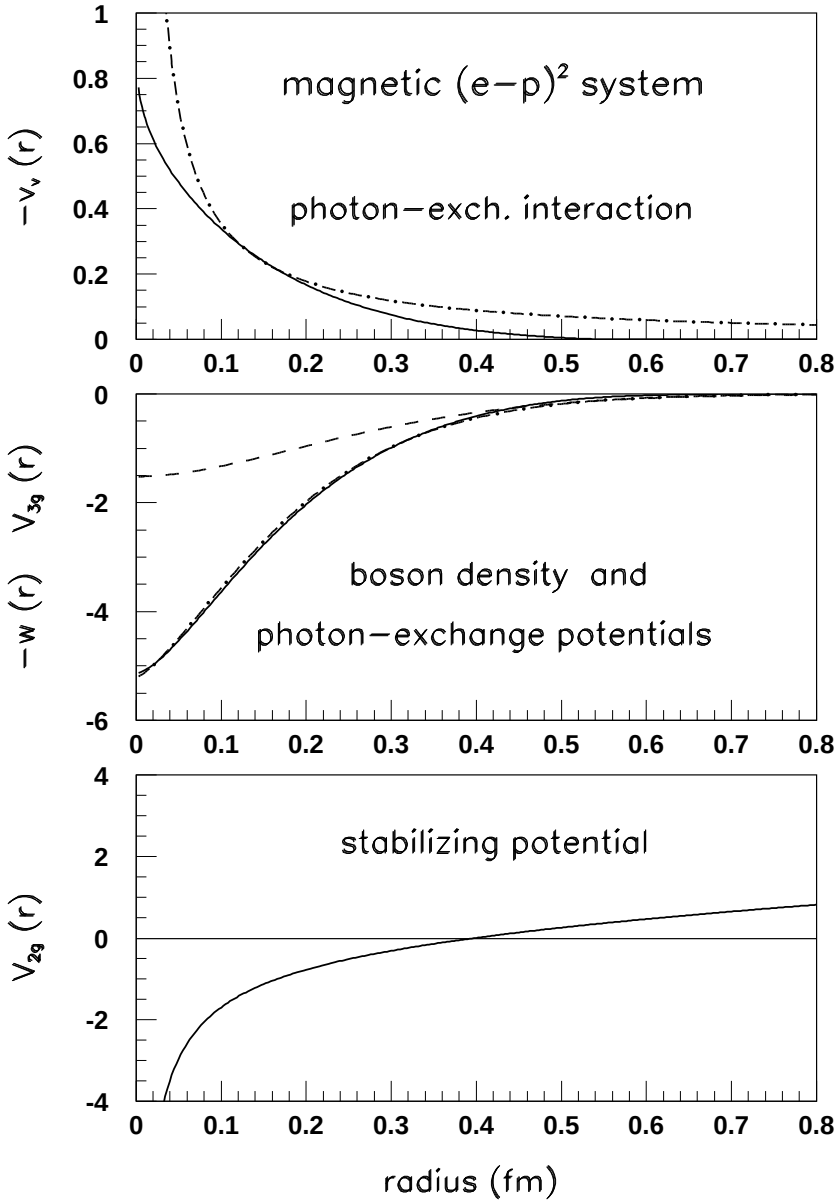


Figure 1: Radial dependence of scalar density and potentials of a magnetically bound (e-p)^2 state with a root mean square radius $< r_g^2 >^{1/2}$ of 0.4 fm. Upper part: Relative shape of the interaction $v_v(r)$, given by solid line, in comparison with the 1/r dependence of the gravitational potential (dot-dashed line). Middle part: Boson-exchange potentials $V_{3g}^{s,v}(r)$ and (negative) scalar boson density $w_s^2(r)$, given by dashed, solid and dot-dashed lines, respectively. Lower part: Stabilizing potential $V_{2g}(r)$.

© 2018 Global Journals

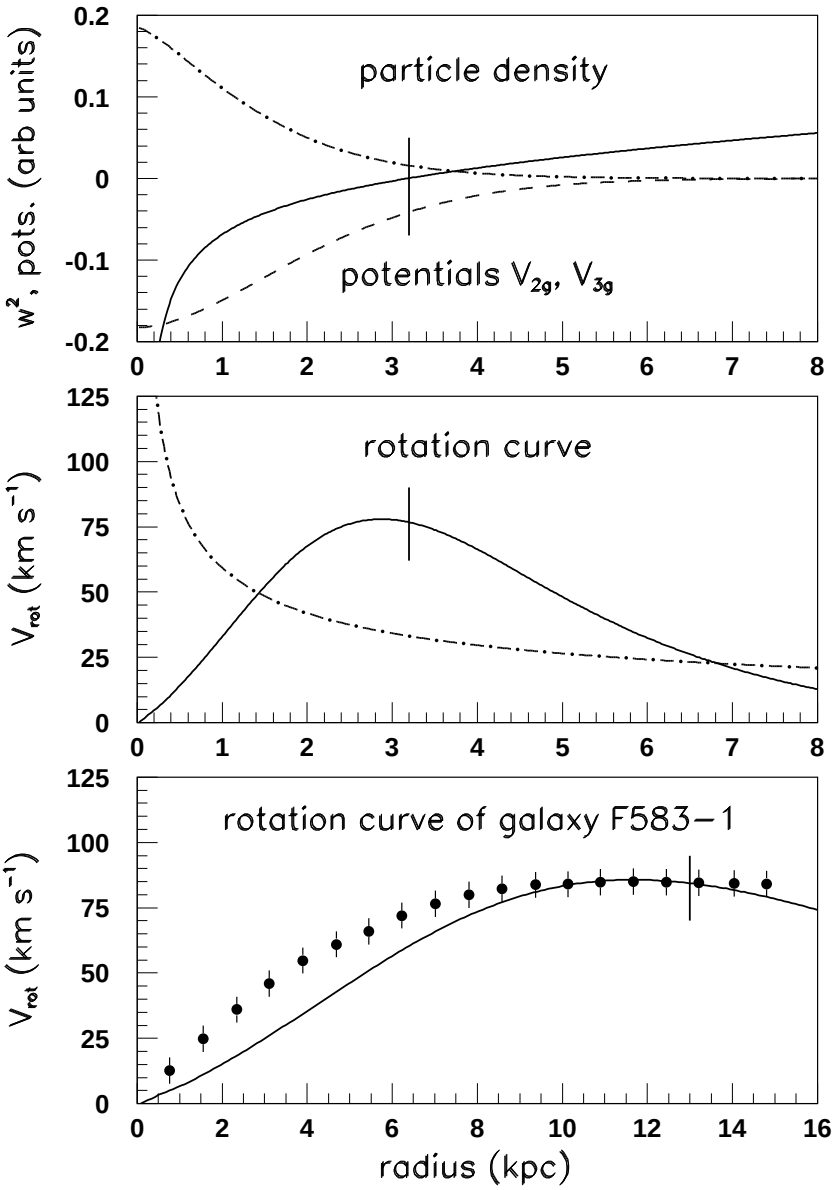


Figure 2: Upper part: Radial dependence of the density (dot-dashed line) and the potentials $V_{2g}(r)$ and $V_{3g}(r)$ of a galactic system with a rms-radius of 3.2 kpc, given by solid and dashed lines. Middle part: Deduced velocity distribution (solid line) in comparison to a Keplerian form (dot-dashed line), normalized to the same integral. Lower part: Velocity curve with radius fitted to the measured data of the galaxy F583-1 of ref. [9] (solid line). The vertical lines indicate the rms-radius of the density.

© 2018 Global Journals

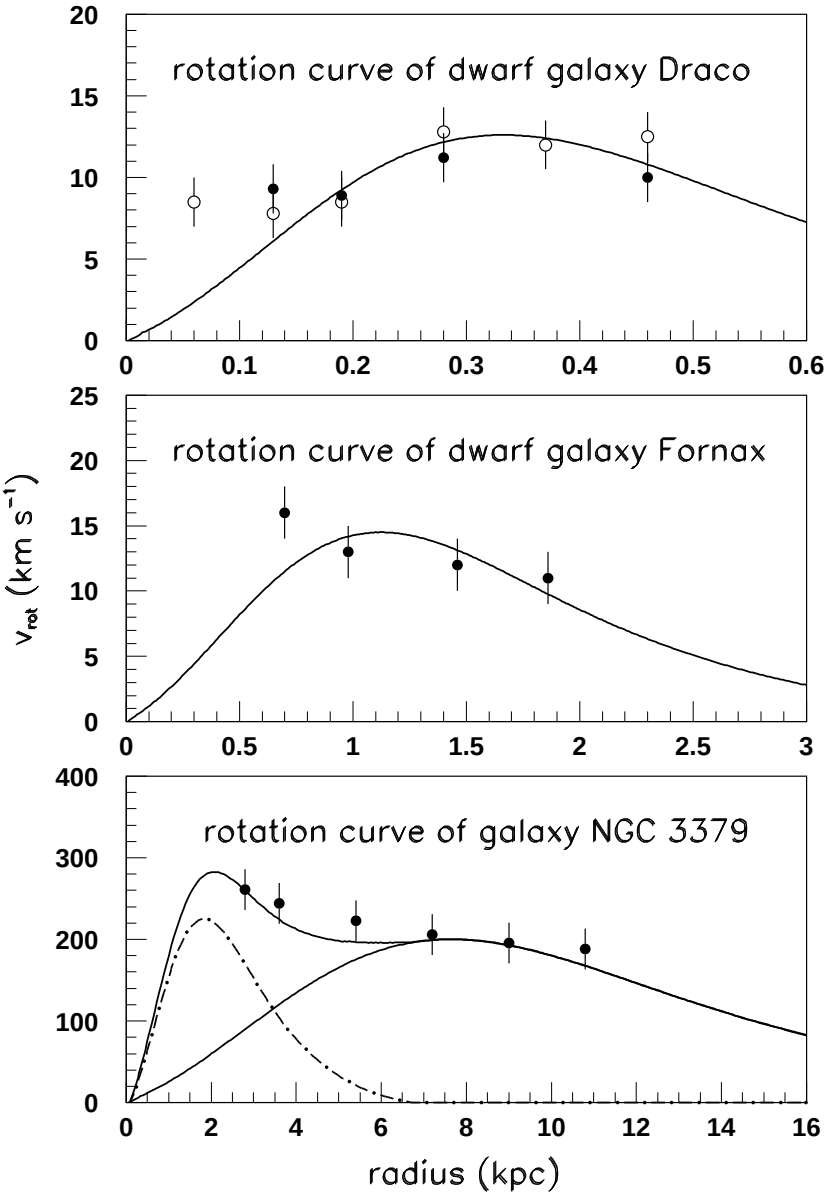


Figure 3: Radial dependence of the rotation velocities for the galaxies Draco, Fornax and NGC 3379 from ref. [10], for Draco see also ref. [11], together with rotation curves with the parameters in table 2. The increase in the rotation velocities at small radii, especially for NGC 3379, may indicate a second contribution with a radius smaller by a factor 4, shown by dot-dashed line.

© 2018 Global Journals

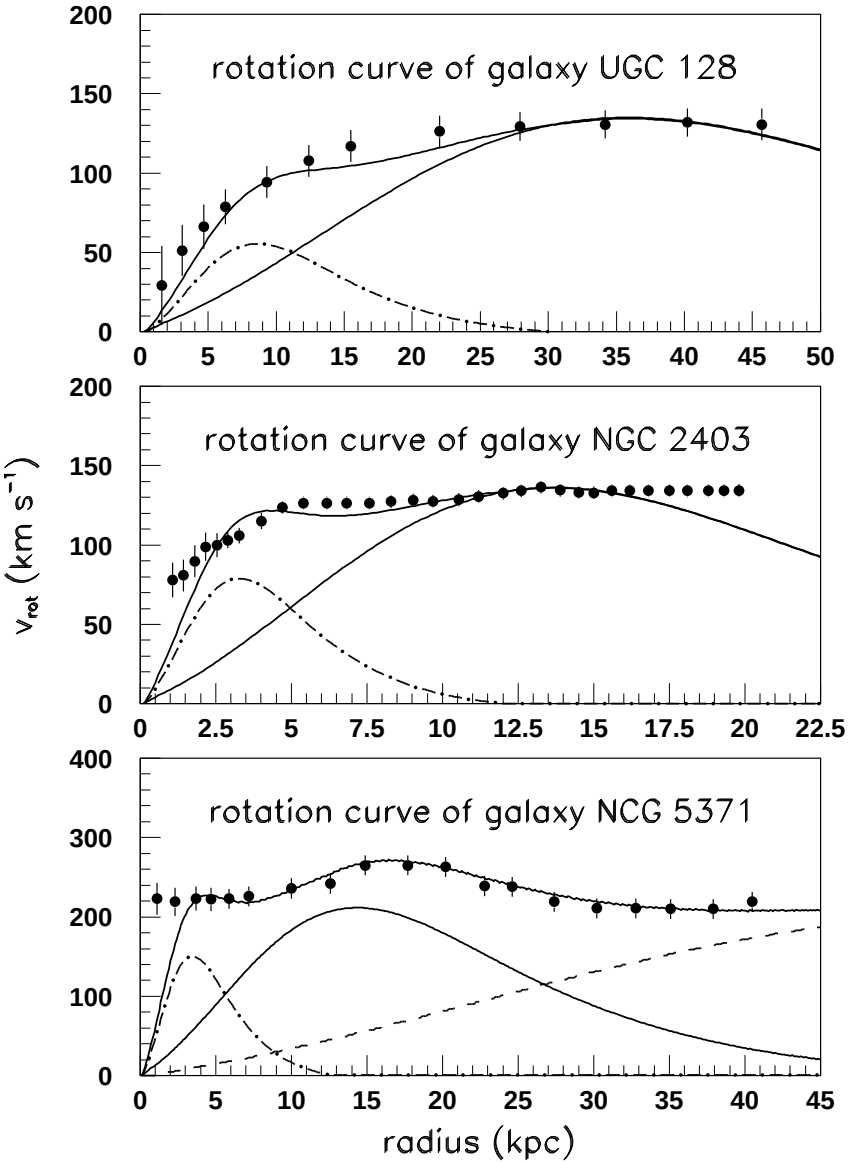


Figure 4: Rotation velocities for the galaxies UGC 128 and NGC 2403 from ref. [9], and NGC 5371 from ref. [12] as a function of radius, together with rotation curves with the parameters in table 2. The dot-dashed lines indicate a second component for each galaxy with a radius reduced to 24 %. An additional large radius component for NGC 5371 is given by dashed line.

© 2018 Global Journals

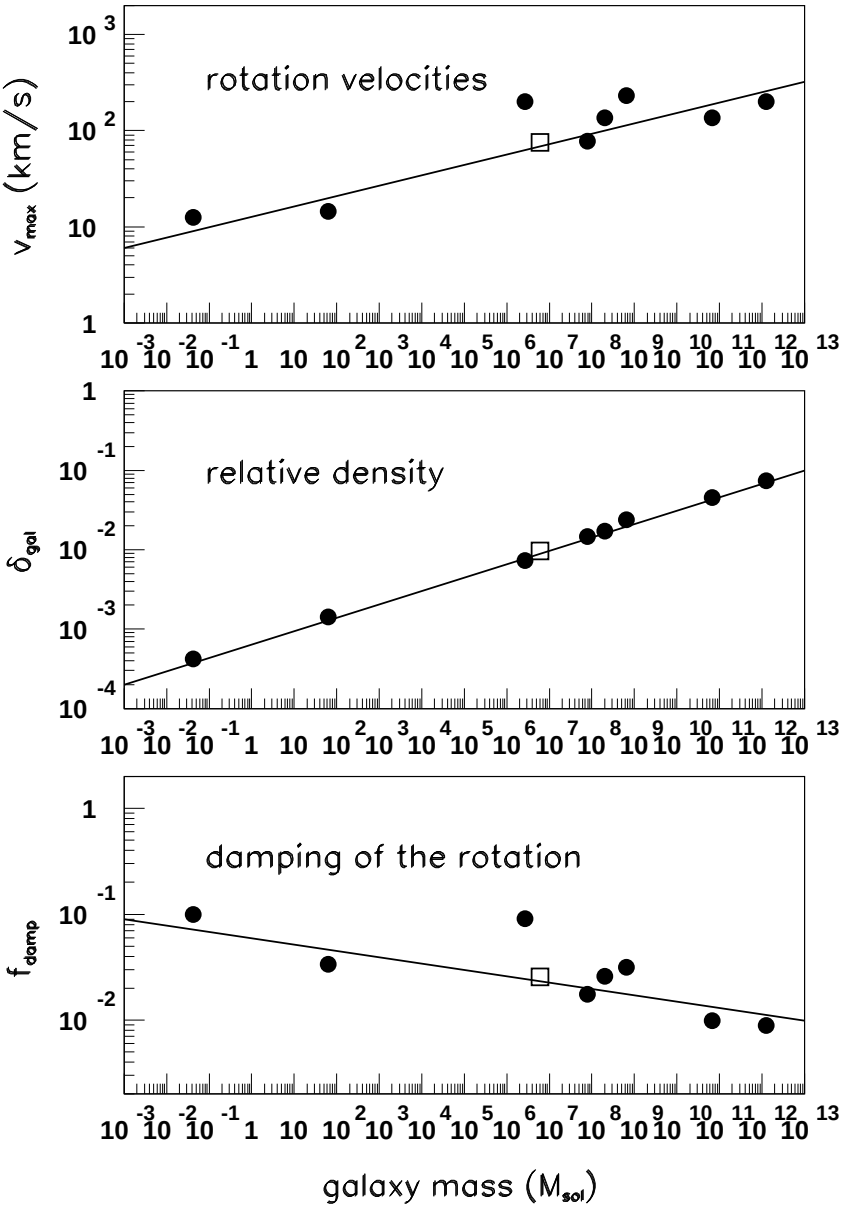


Figure 5: Mass dependence of the velocities v_{max} and deduced parameters δ_{gal} and f_{damp} for the galaxies in figs. 2-4, given by solid points. The solid lines show the average dependence of the different quantities. For the galaxy NGC 3379 the open squares are obtained by reducing v_{max} to 75 km/s, which gives a good agreement with the average dependencies given by solid lines.

© 2018 Global Journals

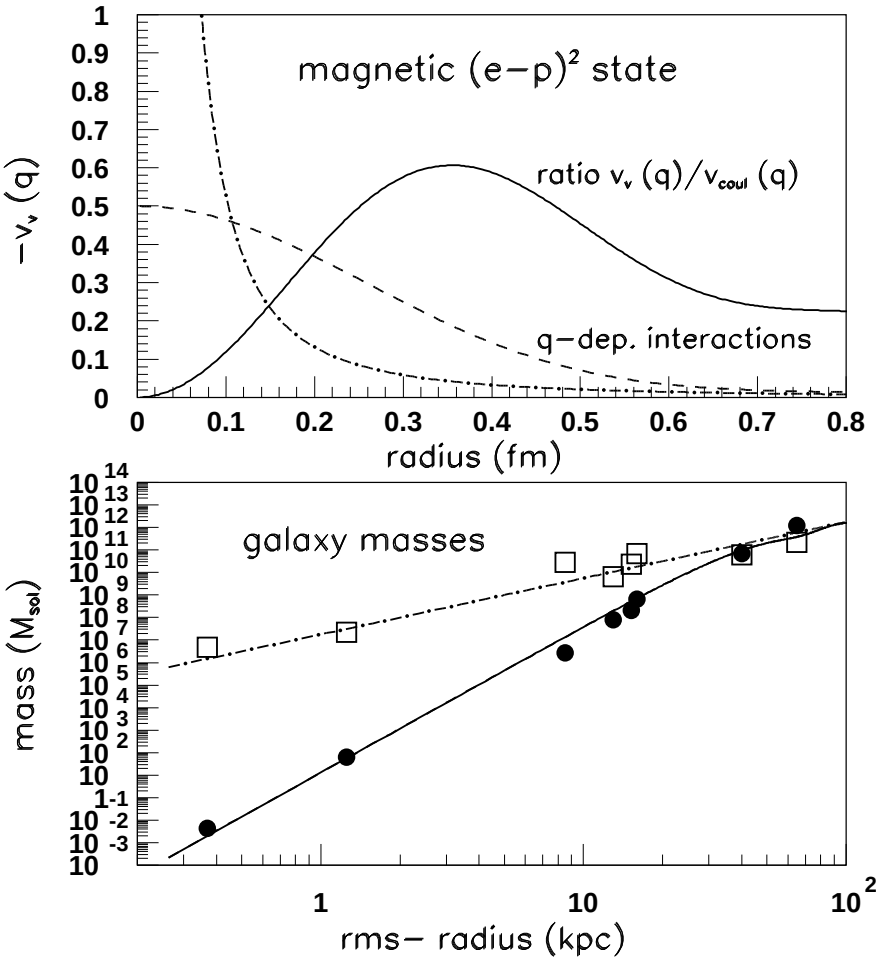


Figure 6: Upper part: Fourier transformed interaction vv(q) of the (e-p)^2 state in sect. 2.1 (dashed line), the gravitational potential $V_{grav}(q)$ (dot-dashed line) and the ratio $v_v(q)/V_{grav}(q)$ (solid line) as a function of radius. Lower part: Radius dependence of the deduced galaxy masses (solid points) and mass estimates using the gravitation mass formula (20) given by open squares. A fit of the latter is given by the dot-dashed line, whereas the solid line is obtained by multiplying this fit with the above $v_v(q)/V_{grav}(q)$ ratio.

© 2018 Global Journals

This page is intentionally left blank

© 2018 Global Journals

Global Journal of Science Frontier Research: a
Physics and Space Science
Volume 18 Issue 4 Version 1.0 Year 2018
Type: Double Blind Peer Reviewed International Research Journal
Publisher: Global Journals
Online ISSN: 2249-4626 & Print ISSN: 0975-5896

Current Self-Induction and Potential Well on the Superconductive Rings

By F. F. Mende

Abstract- Work examines new physical phenomenon potential well on the superconductive rings. This Phenomenon indicates that two superconducting the rings of different diameter, in which are frozen the flows, can be found with respect to each other in potential well, when their rapprochement or removal leads to the appearance of restoring force. The distance Between the rings, which determines this pit, corresponds to the minimum of potential energy of the system of the connected rings. This phenomenon can find a practical use for creating the standards of force and highly sensitive instruments for its measurement, such as gravimeters and accelerometers.

Keywords: self-induction, the law of conservation of flow, inductance, superconductivity, current generator, the voltage generator, potential well.

GJSFR-A Classification: FOR Code: 020404



Strictly as per the compliance and regulations of:

© 2018. F. F. Mende. This is a research/review paper, distributed under the terms of the Creative Commons Attribution-Noncommercial 3.0 Unported License http://creativecommons.org/licenses/by-nc/3.0/), permitting all non commercial use, distribution, and reproduction in any medium, provided the original work is properly cited.

Current Self-Induction and Potential Well on the Superconductive Rings

F. F. Mende

Abstract- Work examines new physical phenomenon potential well on the superconductive rings. This phenomenon indicates that two superconducting the rings of different diameter, in which are frozen the flows, can be found with respect to each other in potential well, when their rapprochement or removal leads to the appearance of restoring force. The distance between the rings, which determines this pit, corresponds to the minimum of potential energy of the system of the connected rings. This phenomenon can find a practical use for creating the standards of force and highly sensitive instruments for its measurement, such as gravimeters and accelerometers.

Keywords: self-induction, the law of conservation of flow, inductance, superconductivity, current generator, the voltage generator, potential well.

I. Introduction

To the laws of self-induction should be carried those laws, which describe the reaction of such elements of radio-technical chains as capacity, inductance and resistance with the galvanic connection to them of the sources of current or voltage. These laws are the basis of the theory of electrical chains. The motion of charges in any chain, which force them to change their position, is connected with the energy consumption from the power sources. The processes of interaction of the power sources with such structures are regulated by the laws of self-induction.

To the self-induction let us carry also that case, when its parameters can change with the presence of the connected power source or the energy accumulated in the system. This self-induction we will call parametric. Subsequently we will use these concepts: as current generator and the voltage generator. By ideal voltage generator we will understand such source, which ensures on any load the lumped voltage, internal resistance in this generator equal to zero. By ideal current generator we will understand such source, which ensures in any load the assigned current, internal resistance in this generator equally to infinity. The ideal current generators and voltage in nature there does not exist, since both the current generators and the voltage generators have their internal resistance, which limits their possibilities.

If we to one or the other network element connect the current generator or voltage, then opposition to a change in its initial state is the response reaction of this element and this opposition is always equal to the applied action, which corresponds to third Newton's law.

Author: Kharkov, Ukraine. e-mail: fedormende@gmail.com

II. Current Self-Induction and Potential Well on the Superconductive Rings

Let us introduce the concept of the flow of the current self-induction

$$\Phi_{L,I} = LI.$$

If inductance is shortened outed, and made from the material, which does not have effective resistance, for example from the superconductor, then

$$\Phi_{L,I} = L_1 I_1 = const,$$

where L_1 and I_1 - initial values of these parameters, which are located at the moment of the short circuit of inductance with the presence in it of current. Let us name this regime the law of the frozen flow for the short-circuited superconductive outlines [1-5]. In this case we have:

$$I = I_1 L_1 / L, \qquad (2.1)$$

where I and L - the instantaneous values of the corresponding parameters.

In flow regime examined of current induction remains constant, however, in connection with the fact that current in the inductance it can change with its change, this process falls under for the determination of parametric self-induction. The energy, accumulated in the inductance, in this case is equal

$$W_L = \frac{1}{2}\frac{\left(L_1 I_1\right)^2}{L} = \frac{1}{2}\frac{(const)^2}{L}.$$

Stress on the inductance is equal to the derivative of the flow of current induction on the time:

$$U = \frac{d\Phi_{L,I}}{dt} = L\frac{\partial I}{\partial t} + I\frac{\partial L}{\partial t}.$$

Let us examine the case, when the inductance L_1 is constant.

© 2018 Global Journals

$$U = L_1 \frac{\partial I}{\partial t}. \qquad (2.2)$$

Designating $\Phi_I = L_1 I$, we obtain $U = \frac{d\Phi_I}{dt}$. Let us integrate over (2.2) the time:

$$I = Ut/L_1. \qquad (2.3)$$

Thus, the capacity, connected to the source of direct current, presents for it the effective resistance

$$R = L_1/t, \qquad (2.4)$$

which decreases inversely proportional to time.

The power expended by source linearly depends on the time:

$$P(t) = U^2 t/L_1. \qquad (2.5)$$

Integral of (2.5) on the time is the accumulated in the inductance energy:

$$W_L = U^2 t^2/(2L_1). \qquad (2.6)$$

After substituting into expression (2.6) the value of stress from relationship (2.3), we obtain:

$$W_L = L_1 I^2/2.$$

This energy can be returned from the inductance into the external circuit, if we open inductance from the power source and to connect effective resistance to it.

Now let us examine the case, when the current I_1, which flows through the inductance, is constant, and inductance itself can change. Then we have:

$$U = I_1 \frac{\partial L}{\partial t}. \qquad (2.7)$$

Consequently, the value

$$R(t) = \partial L/\partial t, \qquad (2.8)$$

plays the role of the effective resistance [1-5]. As in the case of the electric flux, effective resistance can be (depending on the sign of derivative), and positive, and negative, i.e., inductance can how derive energy from without, so also return it into the external circuits.

Introducing the designation $\Phi_L = LI_1$ and, taking into account (2.7), we obtain:

$$U = \Phi d_L dt/. \qquad (2.9)$$

The relationship (2.1), (2.6) and (2.9) we will call the rules of current self-induction, or the flow rules of current self-induction. From relationships (2.6) and (2.9) it is evident that, as in the case with the electric flux, the method of changing the flow does not influence eventual result, and its time derivative is always equal to the applied potential difference. Relationship (2.6) determines the current self-induction, during which there are no changes in the inductance, and therefore it can be named simply current self-induction. Relationships (2.7-2.8) assume the presence of changes in the inductance; therefore we will call such processes current parametric self-induction.

The law of the frozen current (2.1) leads to not the known earlier phenomenon of magnetic potential pit on the superconductive rings.

Assume that in two coaxially located superconductive rings the currents are frozen; moreover current in the lower ring is considerably more than in the upper. In accordance with Savart law the magnetic induction of lower ring on the axis in the plane of upper ring takes the form:

$$B = \frac{\mu_0 I_1 R_1^2}{2\left(R_1^2 + z_0^{\,2}\right)^{3/2}},$$

where μ_0 - the magnetic constant, z_0 - the distance between the rings, R_1 - the diameter of lower ring, I_1 - the current, frozen in the lower ring.

If a radius of upper ring composes R_2, its diameter considerably smaller than a radius of lower ring, then the magnetic flux, created by lower ring and which penetrates upper ring, will comprise

$$\Phi_2 \cong \frac{\mu_0 I_1 R_1^2 R_2^2}{2\left(R_1^2 + z_0^{\,2}\right)^{3/2}}.$$

We will consider that the distance between the rings is considerably more than the diameter of lower ring, then

$$\Phi_2 \cong \mu_0 I_1 R_1^2 R_2^2/\left(2z_0^{\,3}\right).$$

If in the upper ring current is frozen I_2, that the flow is connected with it

$$\Phi_2 = L_2 I_2,$$

where L_2 - the inductance of upper ring.

Let us assume that in the initial position of rings direction of flow in them coincides, and rings are attracted. During lowering of lower ring the currents of induction will compensate currents in the upper ring, and current in it will reach the zero value, when the equality will be carried out

© 2018 Global Journals

$$\Phi_2 \cong \frac{\mu_0 I_1 R_1^2 R_2^2}{2 z_0^{\,3}}.$$

In this case the distance between the rings will comprise

$$z_0 = \left(\frac{\mu_0 I_1 R_1^2 R_2^2}{2\Phi_2} \right)^{1/3} = \left(\frac{\mu_0 I_1 R_1^2 R_2^2}{2 L_2 I_2} \right)^{1/3}.$$

With obtaining of this relationship the mutual inductance of rings is not taken into account, since the distance between the rings is great, and it was also considered that the current I_1 practically does not change with the approximation of upper ring to lower.

At point z_0 the currents of induction completely compensate the current, frozen in the upper ring; therefore, this ring will no longer interact with the lower ring. With further rapprochement of rings the current of induction in the upper ring changes its initial direction and it will be opposite in the direction of flow in the lower ring, and, therefore, it will begin from it to be repulsed. But if rings will be moved away from each other, then in the upper ring they will arise current, the coinciding in the direction with the currents in the lower ring, and rings will be attracted. Thus, the position of upper ring at point z_0 is potential well. Such properties of the superconductive suspensions in the literary sources are not described.

This analysis of the possibility in principle of obtaining potential well on the superconductive rings with the frozen currents does not consider the mutual inductance $M(z)$ of rings, which for two circular outlines of a radius R_1 and R_2 with the common axis and by the distance z between them is expressed as the complete elliptic integrals of the 1st $K(k)$ and 2nd $E(k)$ kind [6, 7]:

$$M(z) = \mu_0 f\left(k(z)\right)\sqrt{R_1 R_2},$$

$$f(k) = \left(\frac{2}{k} - k\right)K(k) - \frac{2}{k}E(k) = \frac{2}{k}\left[\left(1 - \frac{k^2}{2}\right)K(k) - E(k)\right],\ k^2 = \frac{4R_1R_2}{z^2 + \left(R_1 + R_2\right)^2},$$

$$K(k) = \int_0^{\frac{\pi}{2}} \frac{d\theta}{\sqrt{1 - k^2 \sin^2\theta}},\ E(k) = \int_0^{\frac{\pi}{2}} \sqrt{1 - k^2 \sin^2\theta}\, d\theta.$$

Subsequently for the calculations their own inductances of rings with radii of the section of wires will be used also r_1 and r_2:

$$L_{10} = \mu_0 R_1 \left(\ln\frac{8R_1}{r_1} - 1.75 \right),\ L_{20} = \mu_0 R_2 \left(\ln\frac{8R_2}{r_2} - 1.75 \right).$$

Let us freeze currents I_{10}, I_{20} in two secluded superconductive rings with its own inductances L_{10}, L_{20}. It will arrange these rings coaxially at a great distance so that the directions of flow in them again would coincide and let us begin to draw together them. Then we have relationships, which express the law of conservation of the frozen flows in the superconductive rings:

$$L_{10} I_1(z) + M(z) I_2(z) = L_{10} I_{10};\quad L_{20} I_2(z) + M(z) I_1(z) = L_{20} I_{10}. \tag{2.10}$$

From them we will obtain relationships for the currents:

$$I_1(z) = \frac{I_{10} L_{10} L_{20} - I_{20} L_{20} M(z)}{L_{10} L_{20} - M^2(z)};\quad I_2(z) = \frac{I_{20} L_{10} L_{20} - I_{10} L_{10} M(z)}{L_{10} L_{20} - M^2(z)}. \tag{2.11}$$

© 2018 Global Journals

From these relationships we will obtain the value of the mutual inductance, with which the current in the lower and upper rings is equal to zero:

$$M_1(z_1) = L_1 \frac{I_{10}}{I_{20}}; \quad M_2(z_2) = L_2 \frac{I_{20}}{I_{10}}.$$

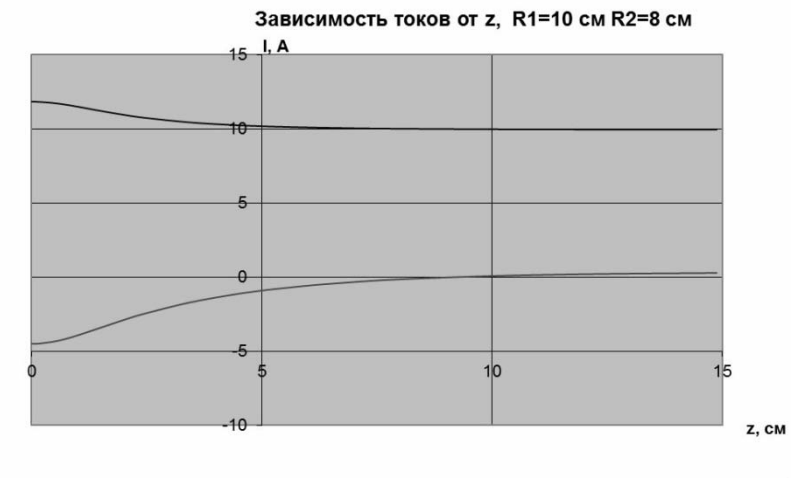


Fig. 1: Graphs of currents in the lower ring (upper curve) and in the upper ring (lower curve) with the initial values of current strength in the lower ring – 10 A and the value of current strength in the upper ring – 2 a.

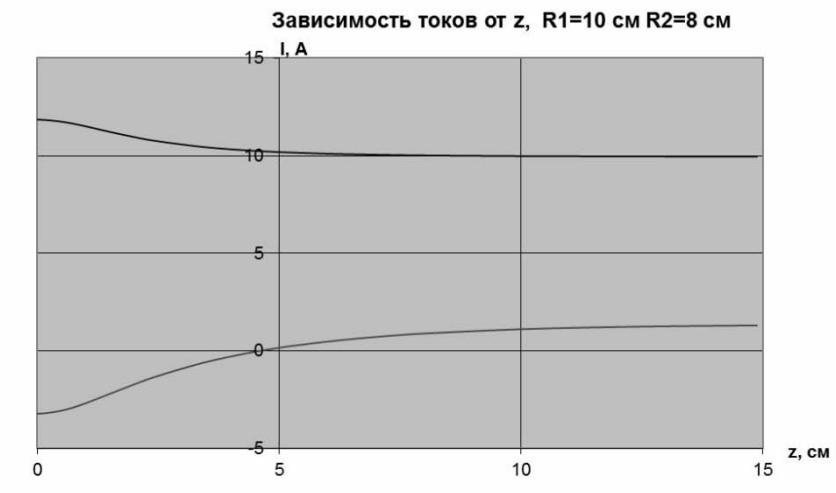


Fig. 2: Graphs of currents in the lower ring (upper curve) and in the upper ring (lower curve) with the initial values of current strength in the lower ring – 10 A and the value of current strength in the upper ring – 5 a.

Thus, assigning different initial values of inductances and currents frozen in them, it is possible to assign current zeros in that or other ring with different distances between them.

In Fig. 1 and Fig. 2 are depicted the drawings calculated by (2.11) formulas $I_1(z)$, also, $I_2(z)$ with different initial values of currents in the rings of radii $R_1 = 10$ cm, $R_2 = 8$ cm (radii of the section of wires $a_1 = a_2 = 0{,}1$ cm). It is evident that at the specific distance from the lower ring the current in the upper ring reverses the sign. They coincide at the great distance of direction of flow in the rings, and they are attracted. They are opposite on – smaller than the direction, and they are repulsed. Consequently, the point, at which the current in the upper ring reverses the sign, is a coordinate of potential well.

Let us examine the task, when the axes of two rings from the superconductive circular conductors coincide and are directed length wise Oz, in this case reference point O combined with the center of the first ring. Let us

© 2018 Global Journals

find currents in the rings and force of interaction of rings depending on the coordinate of the center of the second ring z, if with $z = z_0$ current in the second ring it is absent, and in the first it is equal I. Radii of rings r_1 r_2 are considerably more than radii a_1 and a_2 the section of wires.

Then in the first ring

$$I_1(z) = I\frac{b_1 b_2 - 4 f(\kappa_0) f(\kappa)}{b_1 b_2 - 4[f(\kappa)]^2}. \tag{2.12}$$

And the secondly

$$I_2(z) = 2Ib_1\sqrt{\frac{r_1}{r_2}}\frac{f(\kappa_0) - f(\kappa)}{b_1 b_2 - 4[f(\kappa)]^2}. \tag{2.13}$$

The force of interaction of the rings

$$F(z) = \mu_0 I^2 g(\kappa)\frac{[b_1 b_2 - 4 f(\kappa_0) f(\kappa)][f(\kappa_0) - f(\kappa)]}{[b_1 b_2 - 4[f(\kappa)]^2]^2}\frac{b_1 |z|}{r_2}. \tag{2.14}$$

Here μ_0 – magnetic constant, $b_1 = \ln(8r_1 / a_1) - 2$ and $b_2 = \ln(8r_2 / a_2) - 2$, A

$$\kappa = \kappa(z) = 2\sqrt{\frac{r_1 r_2}{(r_1 + r_2)^2 + z^2}}, \qquad \kappa_0 = \kappa(z_0) = 2\sqrt{\frac{r_1 r_2}{(r_1 + r_2)^2 + z_0^2}}.$$

In the expressions (2.12)–(2.14) the functions figure

$$f(\kappa) = \frac{1}{\kappa}[(1 - \kappa^2/2)K(\kappa) - E(\kappa)], \qquad g(\kappa) = \kappa\left[K(\kappa) - \frac{1 - \kappa^2/2}{1 - \kappa^2}E(\kappa)\right],$$

where $K(\kappa)$ and $E(\kappa)$ – the complete elliptic integrals of the 1st and 2nd kind:

$$K(\kappa) = \int_0^{\pi/2}\frac{d\theta}{\sqrt{1 - \kappa^2 \sin^2\theta}}, \qquad E(\kappa) = \int_0^{\pi/2}\sqrt{1 - \kappa^2 \sin^2\theta}\, d\theta.$$

As an example let us take the following radii of rings: $r_1 = 10$ cm and $r_2 = 8$ cm, and radii of the section of wires – $a_1 = a_2 = 0{,}1$ see. Let with the distance $z_0 = 5$ cm between the centers of rings the current strength in the first ring compose $I = 10$ A, and the secondly current is absent. Dependences $I_1(z)$, $I_2(z)$ and $F(z)$, calculated by formulas (2.12)–(2.14), are depicted in graphs (ris.3, Fig. 4 and Fig. 5) Current in the first ring I_1 is equal $I = 10$ to A with $z = \pm z_0$ and $z \to \pm\infty$. Current in the second ring I_2 is turned into zero with $z = \pm z_0$. Positive values I_2 correspond to identical directions of flow in the rings, and negative– opposite. Finally, the positive values of force F correspond to the repulsion of rings, and negative – to attraction. It is obvious that with $z = \pm z_0$ it becomes zero, in this case the rings are located in the position of stable equilibrium. Force F is absent also with $z = 0$ (when the planes of rings coincide), but in this case equilibrium – is unstable.

© 2018 Global Journals

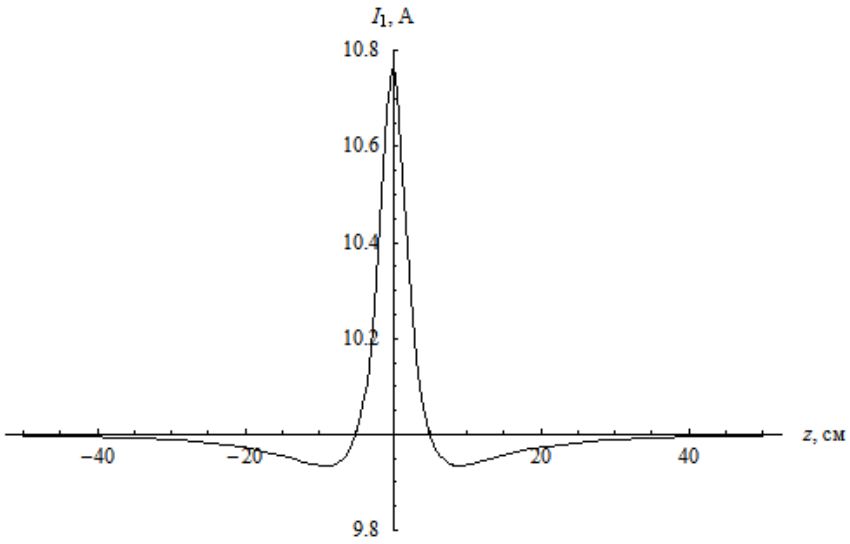


Fig. 3: Dependences $I_1(z)$

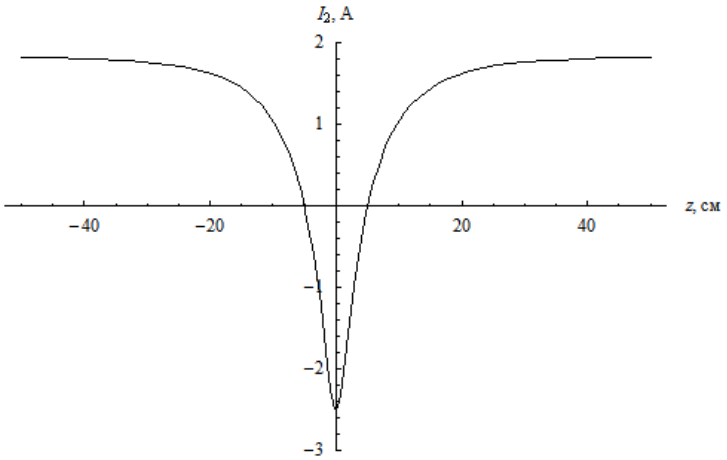


Fig. 4: Dependences $I_2(z)$

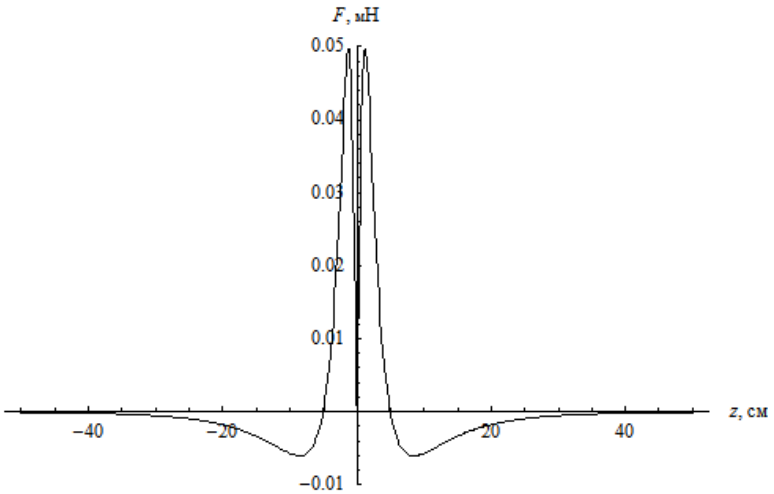


Fig. 5: Dependences $F(z)$

© 2018 Global Journals

III. Conclusion

Work examines new physical phenomenon potential well on the superconductive rings. This phenomenon indicates that two superconducting the rings of different diameter, in which are frozen the flows, can be found with respect to each other in potential well, when their rapprochement or removal leads to the appearance of restoring force. The distance between the rings, which determines this pit, corresponds to the minimum of potential energy of the system of the connected rings. This phenomenon can find a practical use for creating the standards of force and highly sensitive instruments for its measurement, such as gravimeters and accelerometers.

References Références Referencias

1. Ф. Ф. Менде, А. С.Дубровин.Особые свойства реактивных элементов и потоков заряженных частиц. Инженернаяфизика, №11, 2016, с. 13-21.
2. F. F. Mende. Induction and Parametric Properties of Radio-Technical Elements and Lines and Property of Charges and Their Flows, AASCIT Journal of Physics Vol.1, No. 3, Publication Date: May 21, 2015, Page: 124-134.
3. F. F. Mende. New Properties of Reactive Elements, Lines of Transmission of Energy and the Relaxation Properties of Electronic Fluxes and Conductors, AASCIT Journal of Physics, Vol.1, No. 3, Publication Date: June 12, 2015, Page: 190-200.
4. F. F. Mende, New Properties of Reactive Elements and the Problem of Propagation of Electrical Signals in Long Lines, American Journal of Electrical and Electronic Engineering, Vol. 2, No. 5, (2014), 141-145.
5. F. F. Mende. Nominal and Parametric Self-Induction of Reactive Elements and Long Lines, Engineering and Technology, Vol.2, No. 2, Publication Date: April 3, 2015, Page: 69-73.
6. Менде Ф. Ф., Дубровин А. С.Альтернативная идеология электродинамики. Монография. М.: Перо, 2016. – 198 с. ISBN 978-5-906927-22-4.
7. Mende F. F., Dubrovin A. S. Alternative ideology of electrodynamics. Monograph. M.: Перо, 2016.- 216 p. ISBN 978-5-906927-23-1.

© 2018 Global Journals

This page is intentionally left blank

© 2018 Global Journals

Global Journal of Science Frontier Research: a
Physics and Space Science
Volume 18 Issue 4 Version 1.0 Year 2018
Type: Double Blind Peer Reviewed International Research Journal
Publisher: Global Journals
Online ISSN: 2249-4626 & Print ISSN: 0975-5896

Variations in the Aerosol Optical Depth above the European Russia Territory from the Data Obtained at the Russian Actinometric Network in 1976-2016 Years

By I. N. Plakhina
Obukhov Institute of Atmospheric Physics

Abstract- Investigation results of the atmospheric aerosol over the Russia territory are of great interest for the ecology and climate developments. The regularities of spatial and temporal variations in the Aerosol Optical Depth (AOD) can be received by the Russian actinometric network data (Russian Hydrometeorological Research Center). Our analysis will be based on the "Atmosphere Transparency" special-purpose database created at the Voeikov Main Geophysical Observatory on the basis of observational actinometric data. Author has many years cooperation with MGO in the region of the processing and analysis of these observation data.

GJSFR-A Classification: FOR Code: 040199



Strictly as per the compliance and regulations of:

© 2018. I. N. Plakhina. This is a research/review paper, distributed under the terms of the Creative Commons Attribution-Noncommercial 3.0 Unported License http://creativecommons.org/licenses/by-nc/3.0/), permitting all non commercial use, distribution, and reproduction in any medium, provided the original work is properly cited.

Variations in the Aerosol Optical Depth above the European Russia Territory from the Data Obtained at the Russian Actinometric Network in 1976–2016 Years

I. N. Plakhina

Abstract- Investigation results of the atmospheric aerosol over the Russia territory are of great interest for the ecology and climate developments. The regularities of spatial and temporal variations in the Aerosol Optical Depth (AOD) can be received by the Russian actinometric network data (Russian Hydrometeorological Research Center). Our analysis will be based on the "Atmosphere Transparency" special-purpose database created at the Voeikov Main Geophysical Observatory on the basis of observational actinometric data. Author has many years cooperation with MGO in the region of the processing and analysis of these observation data.

I. Section 1

Network observation stations system and empirical data will be described in section 1. A map showing the location of 53 actinometric stations of the Russian network for which the AOD of vertical atmospheric column were estimating for a wavelength of 0.55 μ. These stations cover a large part of Russia and are located outside the zones of direct local anthropogenic sources of industrial and municipal aerosol emissions (suburbs, rural areas, uplands, etc.). An analysis of the AOD of a vertical atmospheric column can be made on the basis of data on the integral atmosphere transparency (P), because P variations are, to a great extent, determined by the aerosol component of the attenuation of direct solar radiation; other components of the attenuation (water vapor and other gases) have little effect on its time variations.

The integral air transparency:

$$P = (S/S_0)^{1/2} \quad (1)$$

where S is the direct solar radiation to the normal to flux surface, reduced to the average distance between the Earth and the Sun and a solar altitude of 30°; S_0 is the solar constant equal to 1.367 kW/m^2. On the basis of 1) data on the homogeneous (calibrated against a single standard and obtained with a unified method) observational series of direct solar-radiation fluxes at the land surface, 2) some semi-empirical approximations, 3) evaluations of the integral (total) and aerosol transparency, it is possible to analyze variations in the AOD of a vertical atmosphere. I shall analyze variations in the AOD of a vertical atmosphere on the basis of the 1976–2016 observational data obtained at 21 actinometric stations.

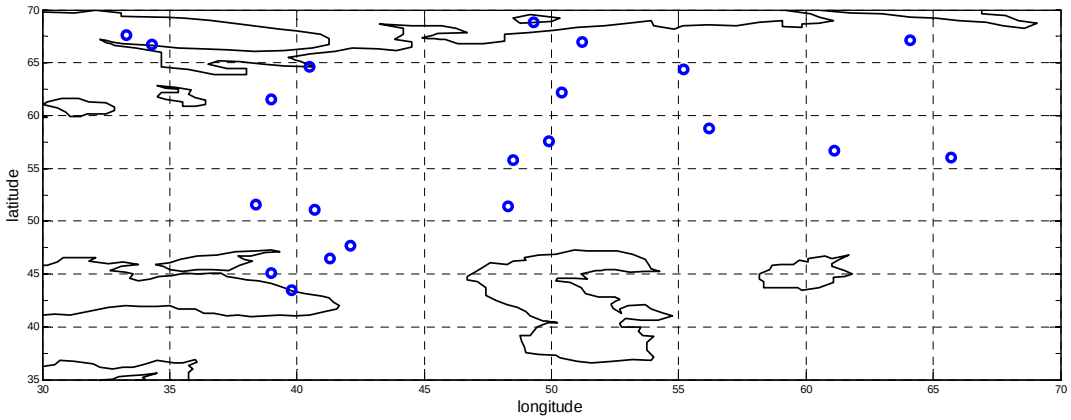


Fig. 1: Layout of 21 actinometric stations whose data will be analyzed in the article

Author: *Obukhov Institute of Atmospheric Physics, Russian Academy of Sciences, Pyzhevskii per. 3, Moscow, 119017 Russia.*
e-mail: inna@ifaran.ru

© 2018 Global Journals

II. Section 2

The method of estimations of AOD, its limitations and errors will be described in section 2. Aerosol optical density of the vertical atmosphere is calculated with a method specially developed, using S -- direct solar radiation near earth surface reduced to the average distance between the Earth and the Sun, W/m^2 and some meteorological values (surface humidity et. al) above the earth surface.

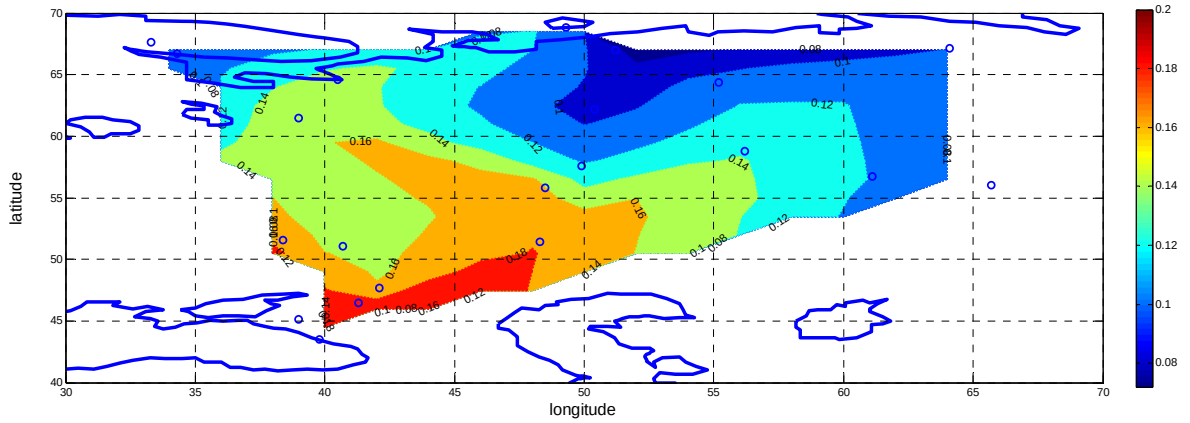
III. Section 3

The character of multiyear seasonal variations in AOD will be presented in section 3. The main statistical parameters (means, extremes, and variation coefficients) of the multiyear variations in annual and seasonal AOD means will be also assessed.

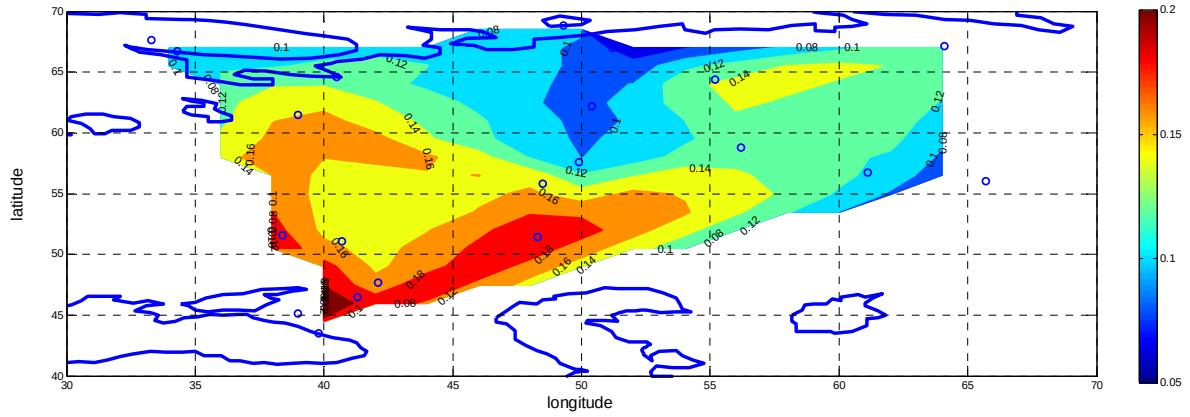
IV. Section 4

The results of an analysis of variations in the AOD of a vertical atmospheric column on the basis of a 21-year (1995–2016) series of observations will be presented in section 3. The general regularities of spatial variations in the aerosol optical depth over Russia are revealed: a monotonic decrease from the southwest to the northeast (see Fig.2), with localized areas having different aerosol loads due to the global and regional factors of their formation.

a) Years (1995-2016)



b) April (1995-2016)



© 2018 Global Journals

c) *July (1995-2016)*

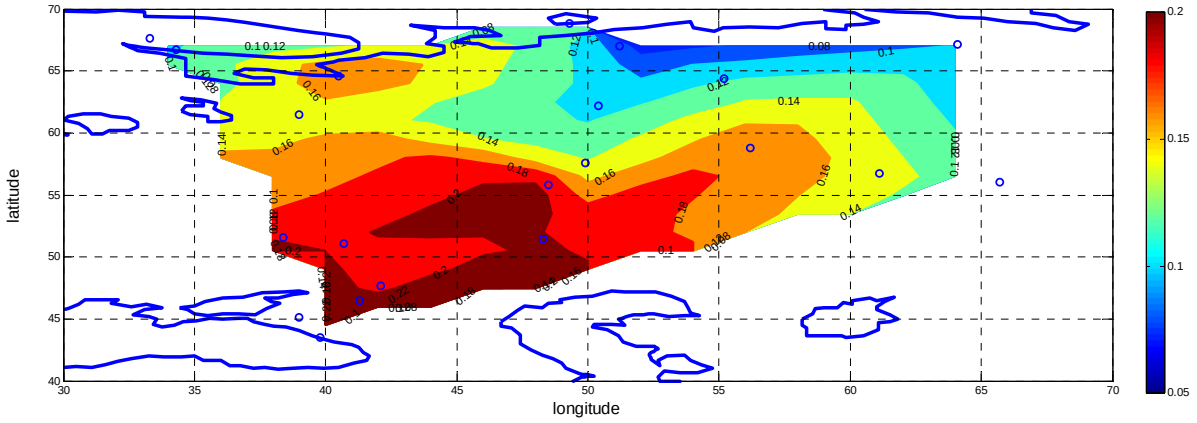


Fig. 2: Spatial distributions (east longitude - horizontal axis, north latitude – vertical axis) of the multiyear means of AOD over the observation periods: 1995–2016 for different seasons

V. Section 5

A spatiotemporal structure of the anomalies of AOD annual values within the time interval under consideration, including the El Chichon (1982) and Pinatubo (1991) eruptions and events of summer 2010 (abnormal heat and forest and peat bog fires) evidently changed both the average values of air turbidity and the character of its spatial variations will be studied in section 5. Two intensive volcano eruptions: (El Chichon – 1982 year, Pinatubo – 1991 year) affected on the atmosphere transparency regime during the analyzed period. Maximal effect of both volcano eruptions are revealed during the next year (1983 and 1992 years). It is evident that the periods of anomaly high turbidity are connected with the volcano eruptions cases. From the 1994 year the decreasing of integral (T_2) and aerosol (AOD) turbidity of the atmosphere in the different Russia regions is observed.

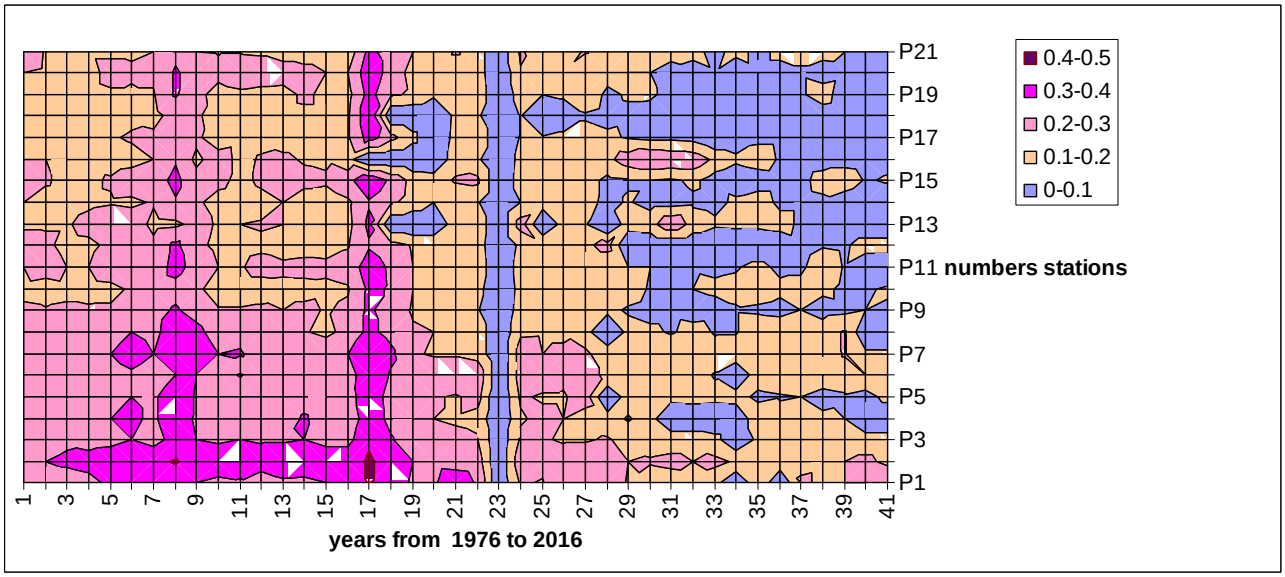
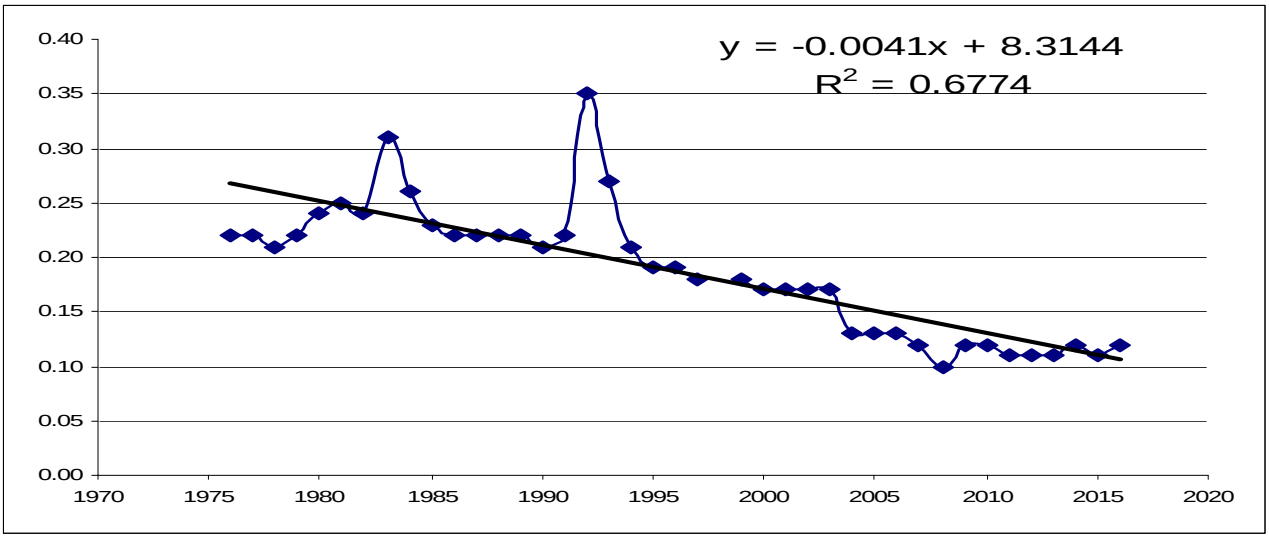


Fig. 4: Spatiotemporal distributions of the annual values of AOD over Russia during 1976–2006 (Year - horizontal axis, Number station – vertical axis)

© 2018 Global Journals

A)



B)

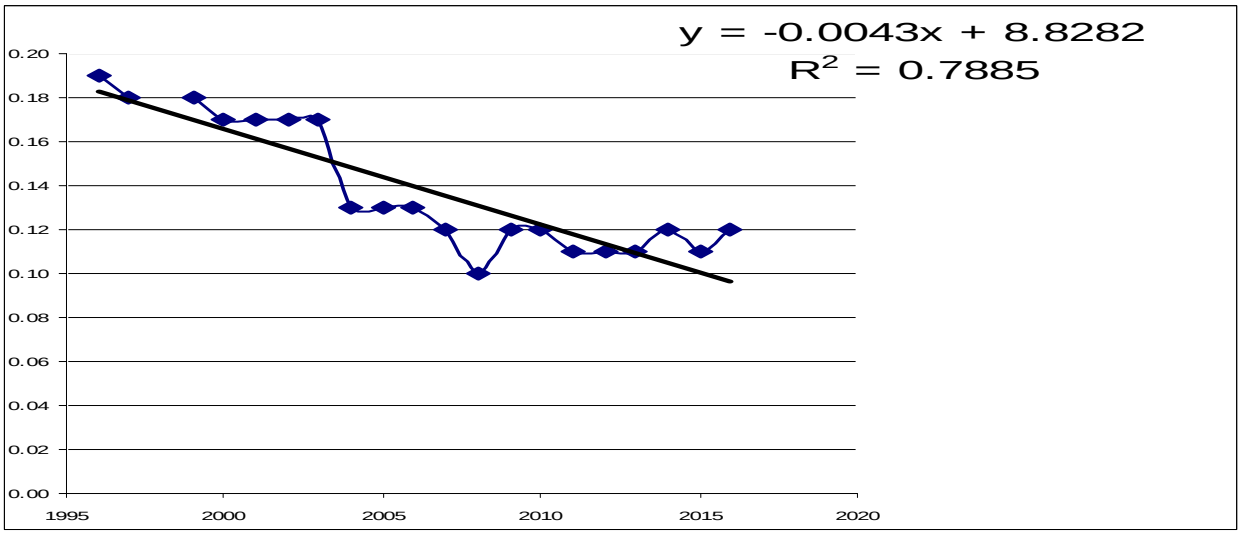


Fig. 5: Trends of the annual values of AOD over Russia during a) 1976–2016 and b) 1995 – 2016 (Year - horizontal axis, Number station – vertical axis)

VI. Some Conclusions

The aerosol optical thickness is an important characteristic of the atmospheric climate. The application of the AOT estimation technique for processing the results of observations at the actinometric network stations allows obtaining qualitatively new and detailed information on the level of aerosol pollution of the atmosphere in separate regions and in Russia as a whole. The analysis of AOT variations during the last 35 years shows the following results:

(1) The character of the long-period annual cycle of AOT did not change as compared with the preceding decades. For most stations, the AOT typically increases in spring and summer by 60–80% with respect to its minimum values in November–December. The AOT increase in spring and summer is associated with a seasonal increase in temperature and humidity and with changes in the underlying surface, as well as with a more intense photochemical and condensational generation of aerosol and with a flux of aerosol from the soil to the atmosphere;

(2) The main factors of space changes in the AOT annual cycle are a latitudinal succession of climatic and landscape zones, in combination with higher industrial loading of the southern regions of European Russia, as compared with the northern ones, and with higher industrial and urban

© 2018 Global Journals

development of European Russia as compared with Asian Russia;

(3) Total averaged AOT over all stations and the whole period under study (0.19 or 0.14) is very close to the annual mean global AOT value (0.14) calculated from the ECHAM-HAM model and to the estimates obtained from satellite data (0.16);

(4) Average and maximum annual AOT values increase at the stations located from north to south in European Russia and decrease from west to east in the whole of Russia;

(5) "Purification" of the atmosphere from aerosol is caused by the absence of large volcanic eruptions and by industrial "calm" conditions during the last decade. The mean AOT for the last two decades is 30% lower than in the preceding ones, both for maximum and average values. Negative tendencies are almost similar for remote and urban (as well as for rural) stations; they are less pronounced in the fall than in spring and summer;

(6) Local effect of the AOT increase due to volcanic eruptions can reach 100%, while the average effects, within our consideration, are minimal.

© 2018 Global Journals

This page is intentionally left blank

© 2018 Global Journals

Global Journal of Science Frontier Research: a
Physics and Space Science
Volume 18 Issue 4 Version 1.0 Year 2018
Type: Double Blind Peer Reviewed International Research Journal
Publisher: Global Journals
Online ISSN: 2249-4626 & Print ISSN: 0975-5896

Activity Concentrations and Gamma Dose Rate Levels in Poultry Feeds and Manure used in Ibadan, Nigeria

By B. U., Nwaka & N. N., Jibiri
Alvan Ikoku Federal College of Education Owerri

Abstract- Workers and dealers in poultry feeds, and commercial farmers may be exposed to elevated gamma radiation doses via internal and external exposure during handling of feeds and manure in farming operations. The measurement and evaluation of internal and external exposure to gamma radiation doses due to the distribution of activity concentrations of ^{40}K, ^{226}Ra and^{232}Th in starter/grower poultry feeds, finisher poultry feeds and resulting poultry manure is therefore necessary from the radiation protection point of view. The measurement was done using Sodium Iodide activated with Thallium $\boldsymbol{NaI\ (Tl)}$ gamma–ray spectrometer. The mean activity concentrations of ^{40}K, ^{226}Ra and^{232} Th in finisher poultry manure were 382.33±67.12 $\boldsymbol{Bq\,kg^{-1}}$ 8.92±3.48 $\boldsymbol{Bq\,kg^{-1}}$, 39.20±5.58 $\boldsymbol{Bq\,kg^{-1}}$ respectively, and in finisher poultry feeds were 284.31±27.46 $\boldsymbol{Bq\,kg^{-1}}$, 15.21±8.88 $\boldsymbol{Bq\,kg^{-1}}$, 38.43±4.08 $\boldsymbol{Bq\,kg^{-1}}$. The distribution of ^{226}Ra was more heterogeneous in all the samples than homogeneous distributions obtained in ^{40}K and ^{232}Th. The significant radiation exposure pathway to the farmers is from internal exposure due to inhalation of poultry and manure dust particles.

Keywords: poultry feeds, poultry manure, primordial radionuclides, activity concentrations, effective radiation doses.

GJSFR-A Classification: FOR Code: 030702



Strictly as per the compliance and regulations of:

© 2018. B. U., Nwaka & N. N., Jibiri. This is a research/review paper, distributed under the terms of the Creative Commons Attribution-Noncommercial 3.0 Unported License http://creativecommons.org/licenses/by-nc/3.0/), permitting all non commercial use, distribution, and reproduction in any medium, provided the original work is properly cited.

Activity Concentrations and Gamma Dose Rate Levels in Poultry Feeds and Manure used in Ibadan, Nigeria

B. U., Nwaka [α] & N. N., Jibiri [σ]

Abstract- Workers and dealers in poultry feeds, and commercial farmers may be exposed to elevated gamma radiation doses via internal and external exposure during handling of feeds and manure in farming operations. The measurement and evaluation of internal and external exposure to gamma radiation doses due to the distribution of activity concentrations of ^{40}K, ^{226}Ra and^{232}Th in starter/grower poultry feeds, finisher poultry feeds and resulting poultry manure is therefore necessary from the radiation protection point of view. The measurement was done using Sodium Iodide activated with Thallium $NaI(Tl)$ gamma–ray spectrometer. The mean activity concentrations of ^{40}K, ^{226}Ra and^{232}Th in finisher poultry manure were 382.33±67.12 $Bq\,kg^{-1}$, 8.92±3.48 $Bq\,kg^{-1}$, 39.20±5.58 $Bq\,kg^{-1}$ respectively, and in finisher poultry feeds were 284.31±27.46 $Bq\,kg^{-1}$, 15.21±8.88 $Bq\,kg^{-1}$, 38.43±4.08 $Bq\,kg^{-1}$. The distribution of ^{226}Ra was more heterogeneous in all the samples than homogeneous distributions obtained in ^{40}K and ^{232}Th. The significant radiation exposure pathway to the farmers is from internal exposure due to inhalation of poultry and manure dust particles. The mean annual effective dose of 3.62±0.23 $\mu Sv\,y^{-1}$, 3.73±0.38 $\mu Sv\,y^{-1}$, 2.25±0.23 $\mu Sv\,y^{-1}$ were obtained for starter/grower feeds, finisher feeds, and finisher poultry manure respectively. The total annual effective dose calculated from the three major pathways for finisher poultry manure (2.94±0.48 $\mu Sv\,y^{-1}$) were lower than the results obtained for starter/grower (4.70±0.37 $\mu Sv\,y^{-1}$) and finisher feeds (4.80±0.64 $\mu Sv\,y^{-1}$). Lower values of internal and external dose rate ($\mu Sv\,y^{-1}$) of the samples showed that workers, dealers in poultry feeds, and commercial farmers are not significantly exposed to elevated gamma doses. A very weak and negative linear relationships in the activity concentrations was found between finisher poultry manure and finisher poultry feed for ^{40}K and ^{40}K ($R = 0.16$); ^{226}Ra and ^{226}Ra ($R = 0.19$); and between ^{232}Th and ^{232}Th ($R = 0.29$). This is an indication that the radionuclide contents in poultry feeds contributed but not significantly to the level of radionuclides in poultry manure.

Keywords: poultry feeds, poultry manure, primordial radionuclides, activity concentrations, effective radiation doses.

Author α: Department of Physics, Alvan Ikoku Federal College of Education Owerri, PM B 1033, Imo state, Nigeria.
e-mails: ben_de_req@yahoo.com, nwakabenjaminu@gmail.com
Author σ: Radiation and Health Physics Research Laboratory, Department of Physics, University of Ibadan, Nigeria.
e-mail: jibirinn@yahoo.com

I. Introduction

Most farm crops such as maize, wheat, and beans mixed with some ingredients like crayfish, fishmeal and bone meal are importantly used in processing animal feeds. Organic manure and chemical fertilizers are applied to farm soil to replenish the lost nutrients which as a consequence boost the crop yield. Crops harvested from fertilized farm soil used in the manufacturing of poultry feeds may contain elevated doses of ionizing radiation due to the activity concentrations of natural radionuclides present in the materials. Dealers and users of the products, commercial farmers, as well as poultry workers may significantly be exposed to elevated doses of ionizing radiation. This has created undue anxiety among people especially those who are not in the field of environmental radioactivity. The possible pathways of exposure to radiation doses are internal exposure via inhalation and external exposure through handling, packing in bags, transportation, and application to farm soil. Sometimes, accidental internal exposure due to ingestion is likely possible from feeds and manure particles during handling.

Studies on environmental radioactivity have reported ^{40}K, ^{226}Ra and^{232}Th radionuclides in rocks, soil, farm soil and soil of quarry sites (Jankovic *et al.,* 2008; Jibiri *et al.,* 2009; Okeyede *et al.,* 2014; Feroz *et al.,* 2015; Faanu *et al.,* 2016), solid minerals (Ademola *et al.,* 2014; Kolo *et al.,* 2016), food crops and vegetables (Jibiri *et al.,* 2007; Ghosh *et al.,* 2011 Avwiri *et al.,* 2013; Tchokossa *et al.,* 2013), surface and ground water (Aziz *et al.,*2014; Aydan *et al.,* 2015; Ogundare and Adekoya, 2015) and agrochemicals for crop production (Saueia and Mazzilli, 2006; Ibeanu *et al.,* 2009; Tahir *et al.,* 2009; Jibiri and Fasae, 2012; Alharbi, 2013).

In other countries, Boukhenfouf and Boucenna (2011) for ^{226}Ra, ^{232}Th and ^{40}K radionuclides in NPK fertilizer one (1) and NPK fertilizer two (2) collected from Outlying Setif region Algeria, found 134.7±14.1 $Bq\,kg^{-1}$, 131.8±16.7 $Bq\,kg^{-1}$, 11644±550 $Bq\,kg^{-1}$ and 190.3±30 $Bq\,kg^{-1}$, 117.2±10.3 $Bq\,kg^{-1}$, 5321±249 $Bq\,kg^{-1}$ respectively. El –Taher and Althoyaib (2011) established that activity concentrations of ^{226}Ra, ^{232}Th and ^{40}K in natural fertilizers from cow, sheep, and chicken were lower than corresponding

© 2018 Global Journals

values in chemical fertilizers used in Kingdom of Saudi Arabia; also the range of Ra_{eq} in chemical fertilizers (100. 37 to 161.43 $Bq\,kg^{-1}$) and organic fertilizers (34 .07 to 102.19 $Bq\,kg^{-1}$) were lower than the standard limit of 370 $Bq\,kg^{-1}$ (Beretka and Mathew, 1985). Alharbi *et al.* (2013) in Saudi Arabia established mean activity of 31.6±1.6 $Bq\,kg^{-1}$, 6.3±0.3 $Bq\,kg^{-1}$, 277.3±12 $Bq\,kg^{-1}$ for ^{226}Ra, ^{232}Th and ^{40}K radionuclides and, absorbed dose rate and annual outdoor effective dose of 28.6 $\eta Gy\,h^{-1}$ and 0.03 $mSv\,y^{-1}$ for sheep fertilizer manure; corresponding result of 41.14±1.7 $Bq\,kg^{-1}$, 7.5±0.3 $Bq\,kg^{-1}$, 284.5±8 $Bq\,kg^{-1}$, 35.3 $\eta Gy\,h^{-1}$, 0.04 $mSv\,y^{-1}$ for cow fertilizer; and 54.2±1.3 $Bq\,kg^{-1}$, 16.9±3 $Bq\,kg^{-1}$, 410.7±14 $Bq\,kg^{-1}$, 51.0 $\eta Gy\,h^{-1}$, 0.06 $mSv\,y^{-1}$ respectively for natural organic.

In Nigeria, Ibeanu *et al.* (2009) reported high activity concentration of ^{40}K and ^{226}Ra in Nitrogen Phosphorus and potassium fertilizers (NPK 15 – 15 – 15, and NPK 16 – 16 – 16 – 16) than cow dropping and chicken droppings. Jibiri and Fasae (2012) recorded the high activity of concentrations of ^{40}K in NPK fertilizers comparable to the work of Ibeanu *et al.* (2009) in Zaria, Kaduna State. Njing *et al.* (2016) found gross alpha and gross beta activity concentrations of 0.262±0.052 $Bq\,kg^{-1}$ and 3.210±1.636 $Bq\,kg^{-1}$ in goat dung (manure) sold in Turaku area of Minna, Niger State, Nigeria. The scarcity of available data set and limited information on internal and external ionizing radiation doses received by dealers of poultry feeds, poultry workers, and farmers in the use of poultry manure for crop production necessitated the need for the study. Hence, it was carried out to fill in the gap in the existing knowledge on internal and external exposure to radiation doses emanating from the materials.

The study whose focus was on poultry feeds and poultry manure was aimed at providing the information on the concentrations of radionuclide ^{40}K, ^{226}Ra and^{232}Th in poultry feeds and poultry manure and to evaluate the associated internal and external exposure to the handlers. The objectives were (i) to evaluate if poultry workers, farmers, and dealers of these products are really exposed to high doses of ionizing radiation doses due to internal and external exposure; (ii) to determine whether the poultry manure collected in this study could be a less radionuclide content than other organic manure and chemical fertilizer reported in the literature; (iii) to provide the data and relevant radiometric information needed for future references and further studies in poultry manure management.

II. Materials and Method

a) Sample collection

In order to ensure that sampling relatively covers a good number of the poultry feeds, a pre–field survey was carried out to identify common poultry feed purchased by poultry farmers and major marketers for their poultry business. Twenty seven (27) samples comprising of nine (9) Starter/grower feeds, nine (9) finisher poultry feeds and consequent nine (9) finisher manures were randomly purchased and used for this study. The poultry feed were produced in Abeokuta, Ogun State; a high background radiation area in Southwestern Nigeria (Jibiri *et al.,* 2010; Okedeye *et al.,* 2014), and distributed to local marketers in Bodija Market in Ibadan, Oyo State. While finisher poultry manure were purchased from Student Research Farm at the University of Ibadan, Ibadan, Nigeria.

b) Sample preparation

The poultry feeds and manure samples were collected in nylon bags and properly labeled. They were then taken to the laboratory where they were dried in an oven at temperature of 90°C for 2 hours each to maintain constant weight. The dried samples were pulverized, homogenized and allow to pass through ~ 1.5 mm mesh sieve, weighed about 200 g each and packed into empty plastic containers which was earlier certified to be non – radioactive. The sample containers were of uniform size 66 mm height by 62 mm diameter which fitted well in the detector holder. Thereafter the sample containers were hermetically sealed and kept in the laboratory for a period of about 30 days to enable the short–lived members of uranium and thorium series attain secular radioactive equilibrium prior to gamma counting.

c) Radioactivity measurements

A well calibrated, 7.60 cm × 7.60 cm $NaI(Tl)$ gamma–ray spectrometry detector enclosed in thick lead–shied to reduce the effects of laboratory background radiation was used as the set – up for radionuclide measurements. The detector was earlier used by Jibiri *et al.* (2010) in the measurement of radionuclides in water samples in high background radiation area of Abeokuta, Nigeria. It was coupled with a computer–based Multichannel Analyser (MCA) which was used for data acquisition and analysis of gamma spectra. The detector has a resolution of 8% at 0.665 MeV gamma line of ^{137}Cs, capable of distinguishing the gamma–ray energies of the radio nuclides of interest in this work.

To ensure that the radiation indices or parameters in the poultry feed and poultry manure samples could be expressed in physical radiometric units, two stages of calibration was done before the detector was used for analyses; these are energy calibration and efficiency calibration which was done using reference standard source materials. The energy calibration converts channel numbers to gamma–ray energy in MeV. This was carried out by placing different gamma sources of known energy or energies on the detector after a preset time of 900 seconds (15 minutes). The channel numbers of the various photopeaks corresponding to the gamma energies were

© 2018 Global Journals

identified and recorded. The reliability of the measuring instrument (detector) was determined from the regression plot ($R^2 = 0.99$) of channel number versus corresponding energies which gave correlation coefficient value of $R = 0.99$, considered very strong enough. The efficiency calibration was carried out to determine the gamma–ray counting efficiencies using a set of gamma sources of known radio nuclides supplied by the International Atomic Energy Agency (IAEA) Vienna, with well-defined energies (0.511 – 2.615 MeV) within the range of interest. This was carried out by converting the count per seconds (cps) under the photopeaks to activity concentrations in $Bq\ kg^{-1}$.

The counting time for accumulating the spectral for both background and samples was 36, 000 s which was good enough for the detector to analyze the spectrum with peaks of interest clearly shown and well distinguished (Jibiri *et al.,* 2010; Isinkaye and Emelue, 2015). Each of the empty containers as well as the containers that contained the samples was placed directly in the detector holder to determine the net count. The processes followed that; the background count was determined by counting an empty container of the same dimension as those containing the poultry feed and poultry manure samples. The gross count was also determined by counting the pulverized samples inside plus that of empty container. Thereafter, the net count was determined by subtracting the background count from the gross count. Both the background count and gross count were repeated at regular interval for quality control while each sample was counted for 36, 000 seconds to reduce the statistical uncertainty (Ademola *et al.,* 2014).

d) Determination of Activity Concentrations of the Radionuclides

The activity concentrations of ^{40}K in the individual poultry feeds and manure samples was determined by measuring the 1.460 MeV gamma–ray line of ^{40}K emitted during it decay, the activity of ^{226}Ra was estimated from 1.765 MeV gamma–ray line of ^{214}Bi while 2.165 MeV gamma–ray line of ^{208}Tl was used for the determination of activity concentration of ^{232}Th. The count rate under the photopeaks of each of the three radionuclides of interest is related to activity concentrations of the samples using equation 1 (Ademola *et al.,* 2014; Isinkaye and Emelue, 2015).

$$A_c = \frac{C_n}{P_\gamma\ M\ \varepsilon} \quad (1)$$

Where A_c, is the activity concentration of the radionuclide in each of the samples measured in $Bq\ kg^{-1}$, C_n is the net count rate under the corresponding peak, P_γ is absolute transition probability of the specific gamma ray, M is the mass of the sample (kg), and ε is the detector efficiency at specific gamma ray energy.

III. Results

Table 1 presents the energy gamma line and minimum detection activity (MDA) for the radio nuclides of interest. Table 2 presents the dose coefficient and some risk parameters for radionuclide of interest adopted in this work. Descriptive statistical results for the activity concentrations of radio nuclides ^{40}K, ^{226}Ra, and ^{232}Th contained in starter/grower poultry feeds, finisher poultry feeds and finisher poultry manure were presented in Tables 3 to 5 respectively. Figures 1 to 3 represent the frequency distribution histogram of ^{40}K, ^{226}Ra, and ^{232}Th radio nuclides for starter/grower poultry feeds; Figure 4 to 6 represented the frequency distribution histogram ^{40}K, ^{226}Ra, and ^{232}Th radio nuclides for finisher poultry feeds, while Figure 7 to 9 represent the frequency distribution histogram^{40}K, ^{226}Ra, and ^{232}Th radio nuclides for finisher poultry manure respectively. The frequency distribution histogram and curves were acquired from Software Package for Social Sciences (SPSS) version 20.0.

Table 1: Energy Gamma Line and Minimum Detection Activity (MDA) for Radio nuclides of interest

Radio nuclides of Interest	Energy (MeV)	Conversion Factor	Minimum Detection Activity, MDA ($Bq\ kg^{-1}$)
^{40}K	1.460	0.075	9.67
^{226}Ra	1.765	0.061	3.06
^{232}Th	2.615	0.029	3.00

a) Estimation of Annual Effective Doses (Internal and external exposures)

During handling, packing of materials in bags, transportation of poultry feeds and application of poultry manure to farm soil workers are exposed to ionizing radiation doses present in the material through three major pathways: external exposure to gamma–ray during the packing in bags and handling of the materials, internal exposure from inhalation of dust and contaminated air due to the practice and possible internal exposure from any accidental ingestion of the materials. These computed doses are summed up to get the total effective doses delivered by ^{40}K, ^{226}Ra and ^{232}Th radionuclides.

The ionizing radiation impacted on exposed workers, marketers and farmers through these exposure pathways were estimated from the activity concentrations of radionuclides^{40}K, ^{226}Ra and ^{232}Th in different samples investigated. This was carried out by applying relevant conversion coefficient doses supply by

© 2018 Global Journals

the International Commission on Radiological Protection (ICRP). According to Kolo *et al.* (2016), the health risk of any adverse induced radiation exposure is dependent on the total effective dose. The dose from external exposure to gamma radiation is estimated from equation 2 (Mustapha *et al.,* 2007; Ademola and Oyema, 2014):

$$D_{Ext} = \sum_i A_i \, C_{Ext,\,i} \, T_{exp} \quad (2)$$

Where A_i is the activity concentrations of nuclide, i $(Bq\ kg^{-1})$,$C_{Ext,\,i}$ is the effective dose coefficient for nuclides, i as presented in Table 2, T_{exp} is the duration of exposure in number in a year. For a poultry worker and markers who work for eight (8) hours per day in twenty (20) working days per month, the duration of exposure per year is therefore calculated as $20 \times 8 \times 12$ which equals 1920 hours per year. In this study, we assume that for a farmer who works for 8 hours per day for three (3) days per a week which gives a total of twelve (12) days per month. The duration of exposure for such farmer per year is thus given as $12 \times 8 \times 12$ which equals 1152 hours per year as presented in Table 2.

Internal exposure from inhalation of poultry/manure dust and contaminated air due to the practice was calculated using equation 3 (Mustapha *et al.,* 2007)

$$D_{Inh} = \sum_i A_i \, C_{Inh,\,i} \eta_{Inh} D_f \, T_{exp} \quad (3)$$

Where A_i is the activity concentrations of nuclide, i $(Bq\ kg^{-1})$, T_{exp} is the duration of exposure in number of years (which for this study, has been corrected for 1920 for poultry feeds exposure and 1152 for poultry manure exposure), $C_{Inh,\,i}$ is the dose coefficient for inhalation of nuclide i measured in $Sv/_{Bq}$, η_{Inh} is the breathing rate measured in $m^3/_h$ with coefficient of 1.69 (Mustapha *et al.,* 2007) and D_f is the dust loading factor measured in $g/_{m^{-3}}$ with coefficient of 1.0×10^{-3} (Degrand and Lepicard, 2005).

Internal dose from accidental ingestion of radionuclides was calculated from equation 4 (Kolo *et al.,* 2016)

$$D_{Ing} = \sum_i A_I C_{Ing,\,i} \, \eta_{ing} \, T_{exp} \quad (4)$$

Where A_i is the activity concentrations of nuclide i $(Bq\ kg^{-1})$, $C_{Ing,\,i}$ is the dose coefficient for ingestion of nuclide, i, measured in $Sv/_{Bq}$, η_{ing} is the ingestion rate for adults, measured in $kg/_h$ whose value is 5.0×10^{-6} (Mustapha *et al.,* 2007) and T_{exp} is the duration of exposure in a years, which for this study has been corrected for 1920 for poultry feeds exposure and 1152 for poultry manure exposure.

Table 2: Dose coefficient and some risk parameters for radionuclide of interest adopted in this work

Dose coefficient parameters	^{40}K $(Bq\ kg^{-1})$	^{226}Ra $(Bq\ kg^{-1})$	^{232}Th $(Bq\ kg^{-1})$	T_{exp} $(h\ y^{-1})$	References
Effective dose coefficient, C_{ext} $(\eta Sv\ h^{-1}/Bq\ kg^{-1})$	1.175	9.929	0.003		Mustapha *et al.* (2007)
Dose coefficient for inhalation, C_{Inh} $(Sv\ Bq^{-1})$	3.0 E-09	2.2 E-06	2.9 E-05		1CRP, 119 (2012)
Dose coefficient for ingestion C_{Ing} $(Sv\ Bq^{-1})$	6.2 E-09	2.8 E-07	2.2 E-07		1CRP, 119 (2012)
Duration of exposure for poultry workers				1920*	
Duration of exposure for commercial farmers				1152**	

Source: Kolo et al. (2016), except for 1920 and 1152** which were computed for this study*

© 2018 Global Journals

Table 3: Some descriptive statistics of radionuclides and dose rates for starter/grower poultry feeds

Statistics	Minimum value	Maximum value	Mean	Standard Deviation	Coefficient of variation (CV)
^{40}K $(Bq\ kg^{-1})$	339.29±17.27	388.35±19.76	362.87	16.28	0.04
^{226}Ra $(Bq\ kg^{-1})$	3.28±6.88	14.62±4.02	7.15	4.13	0.58
^{232}Th $(Bq\ kg^{-1})$	33.33±0.53	41.18±0.55	37.92	2.28	0.06
$D_{Ext.}$ $(\mu Sv\ y^{-1})$	0.83	1.16	0.96	0.12	0.13
$D_{Inh.}$ $(\mu Sv\ y^{-1})$	3.16	3.98	3.62	0.23	0.06
$D_{Ing.}$ $(\mu Sv\ y^{-1})$	0.09	0.15	0.12	0.02	0.17
Total annual effective dose $(\mu Sv\ y^{-1})$	**4.08**	**5.29**	**4.70**	**0.37**	**0.08**

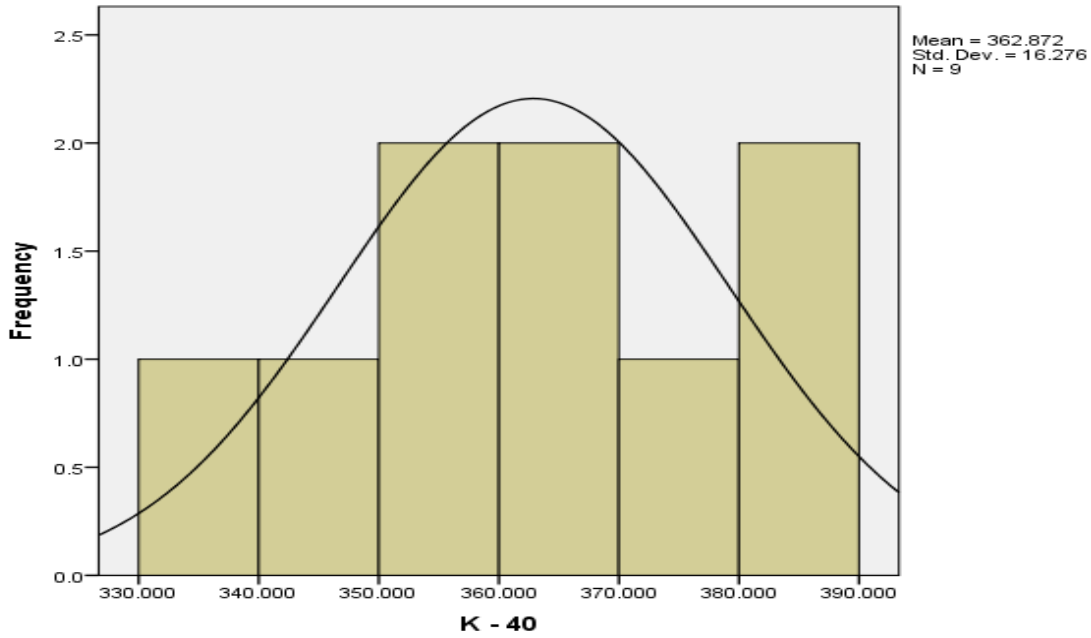


Figure 1: Frequency distribution histogram for activity concentration of ^{40}K in $Bq\ kg^{-1}$ for starter/grower poultry feeds

© 2018 Global Journals

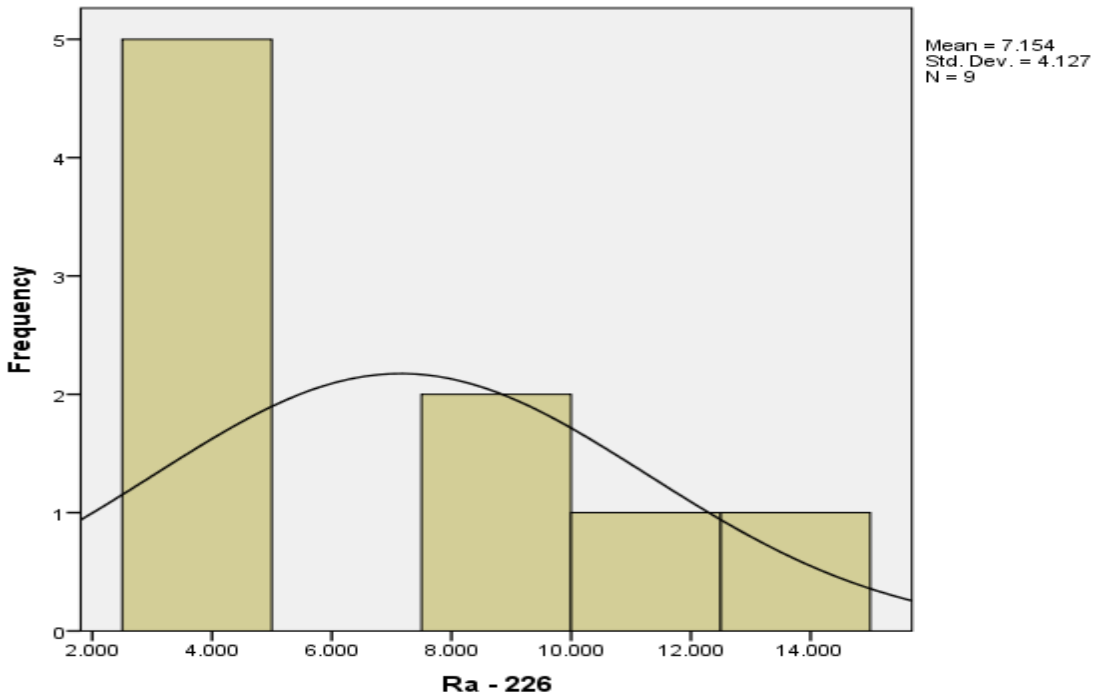


Figure 2: Frequency distribution histogram for activity concentration of ^{226}Ra in $Bq\ kg^{-1}$ for starter/grower poultry feeds

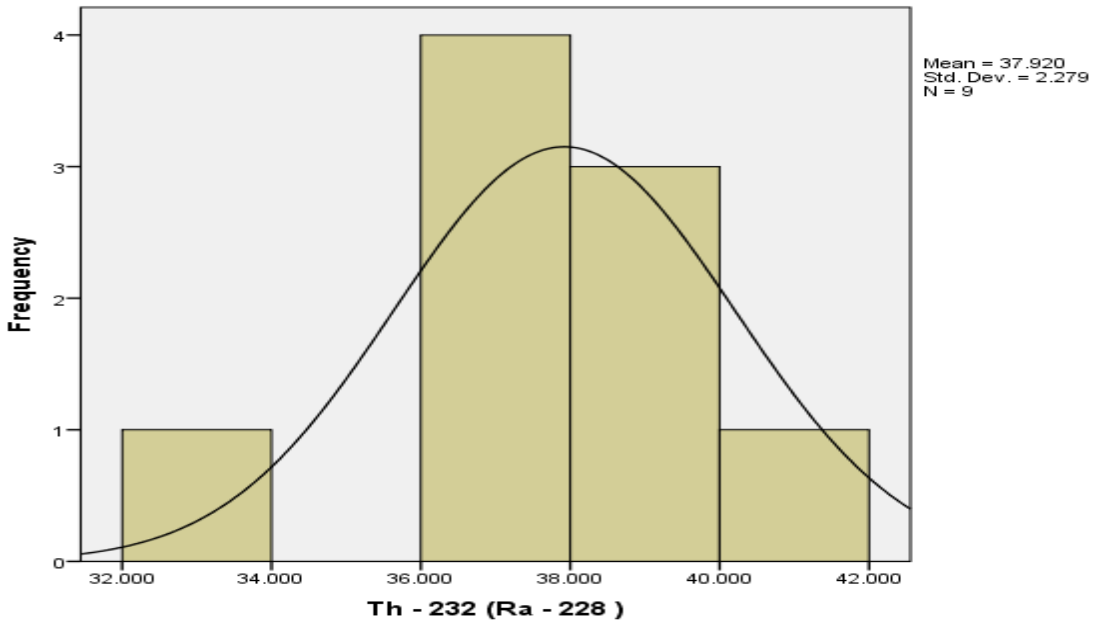


Figure 3: Frequency distribution histogram for activity concentration of ^{232}Th (^{228}Ra) in $Bq\ kg^{-1}$ for starter/grower poultry feeds

© 2018 Global Journals

Table 4: Some descriptive statistics of radio nuclides and dose rates for finisher poultry feeds

Statistics	Minimum value	Maximum value	Mean	Standard Deviation	Coefficient of variation (CV)
^{40}K $(Bq\ kg^{-1})$	269.66±13.73	353.24±17.98	284.31	27.46	0.01
^{226}Ra $(Bq\ kg^{-1})$	3.82±11.06	29.42±3.24	15.21	8.88	0.58
^{232}Th $(Bq\ kg^{-1})$	33.33±0.53	44.59±0.57	38.43	4.08	0.11
$D_{Ext.}$ $(\mu Sv\ y^{-1})$	0.68	1.36	0.93	0.23	0.25
$D_{Inh.}$ $(\mu Sv\ y^{-1})$	3.17	4.41	3.73	0.38	0.10
$D_{Ing.}(\mu Sv\ y^{-1})$	0.10	0.19	0.14	0.03	0.21
Total annual effective dose $(\mu Sv\ y^{-1})$	3.95	5.96	4.80	0.64	0.56

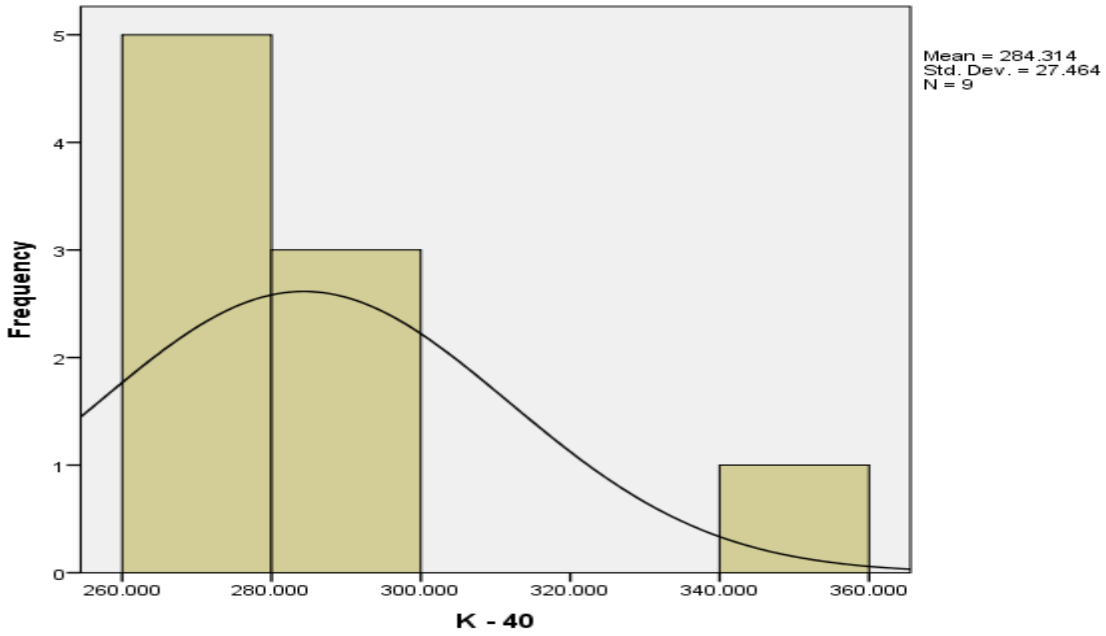


Figure 4: Frequency distribution histogram for activity concentration of ^{40}K in $Bq\ kg^{-1}$ for finisher poultry feeds

© 2018 Global Journals

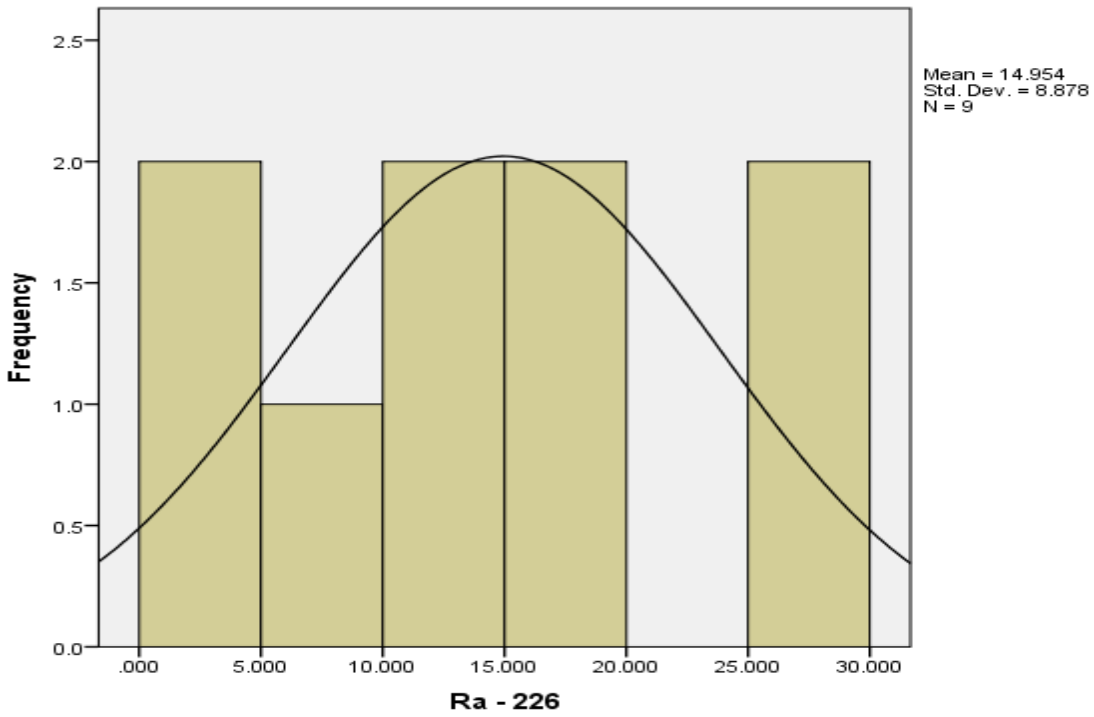


Figure 5: Frequency distribution histogram for activity concentration of ^{226}Ra in $Bq\,kg^{-1}$ for finisher poultry feeds

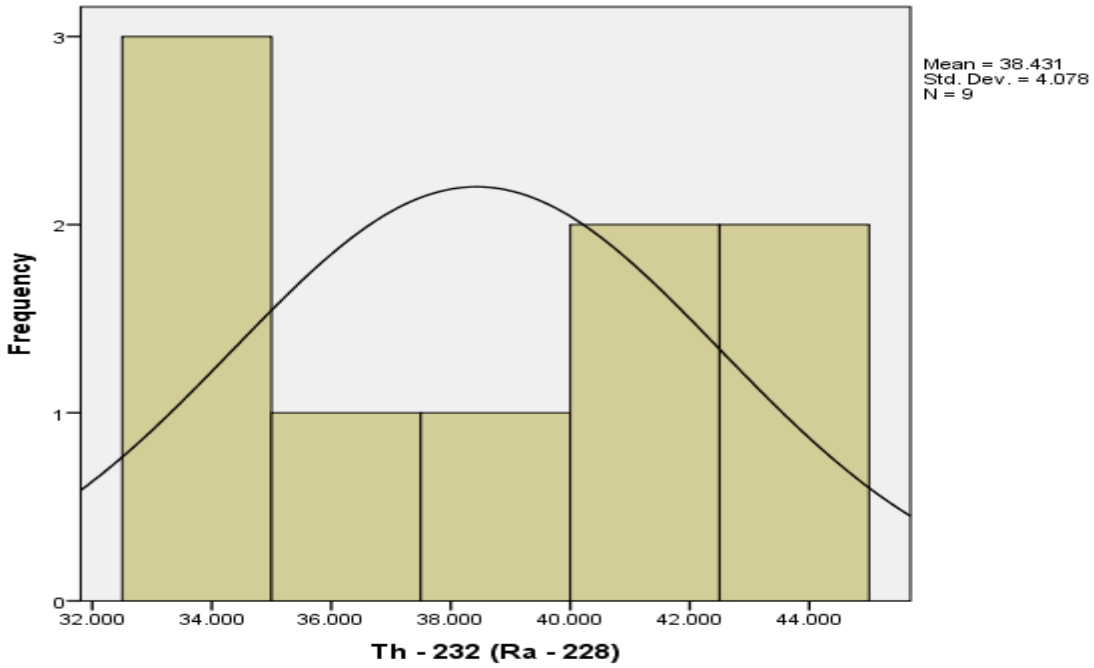


Figure 6: Frequency distribution histogram for activity concentration of ^{232}Th (^{228}Ra) in $Bq\,kg^{-1}$ fo finisher poultry feeds

© 2018 Global Journals

Table 5: Some descriptive statistics of radionuclides and dose rates for finisher poultry manure

Statistics	Minimum value	Maximum value	Mean	Standard Deviation	Coefficient of variation (CV)
^{40}K ($Bq\ kg^{-1}$)	288.04±14.64	509.68±25.93	382.33	67.12	0.18
^{226}Ra ($Bq\ kg^{-1}$)	4.43±6.39	14.74±6.14	8.92	3.48	0.39
^{232}Th ($Bq\ kg^{-1}$)	28.83±0.54	46.14±0.63	39.20	5.58	0.14
$D_{Ext.}$ ($\mu Sv\ y^{-1}$)	0.44	0.86	0.61	0.13	0.21
$D_{Inh.}$ ($\mu Sv\ y^{-1}$)	1.65	2.67	2.25	0.33	0.15
$D_{Ing.}$($\mu Sv\ y^{-1}$)	0.05	0.10	0.08	0.02	0.25
Total annual effective dose ($\mu Sv\ y^{-1}$)	2.14	3.63	2.94	0.48	0.16

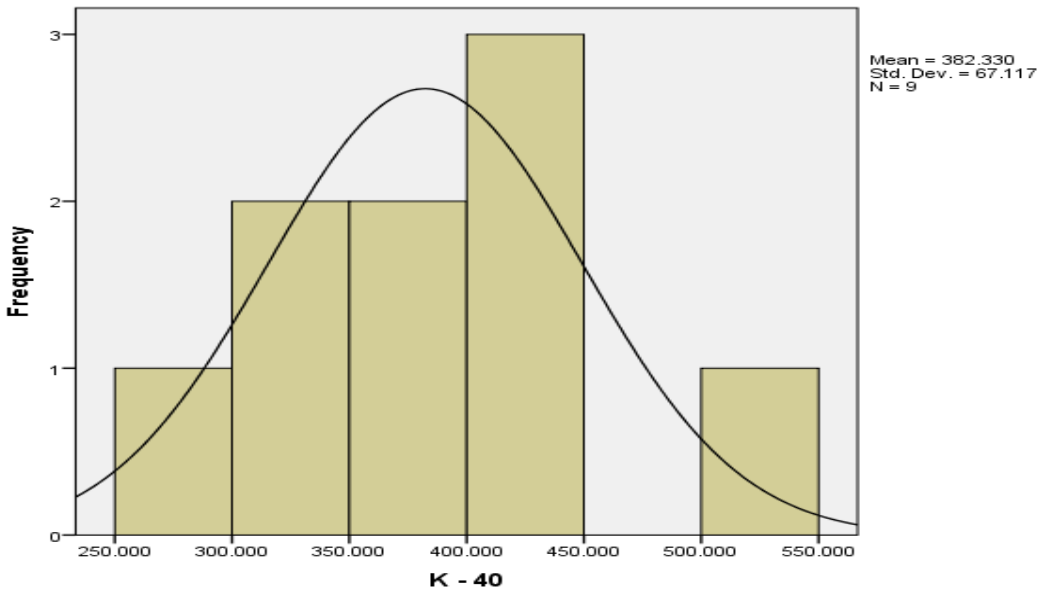


Figure 7: Frequency distribution histogram for activity concentration of ^{40}K in $Bq\ kg^{-1}$ fo finisher poultry manure

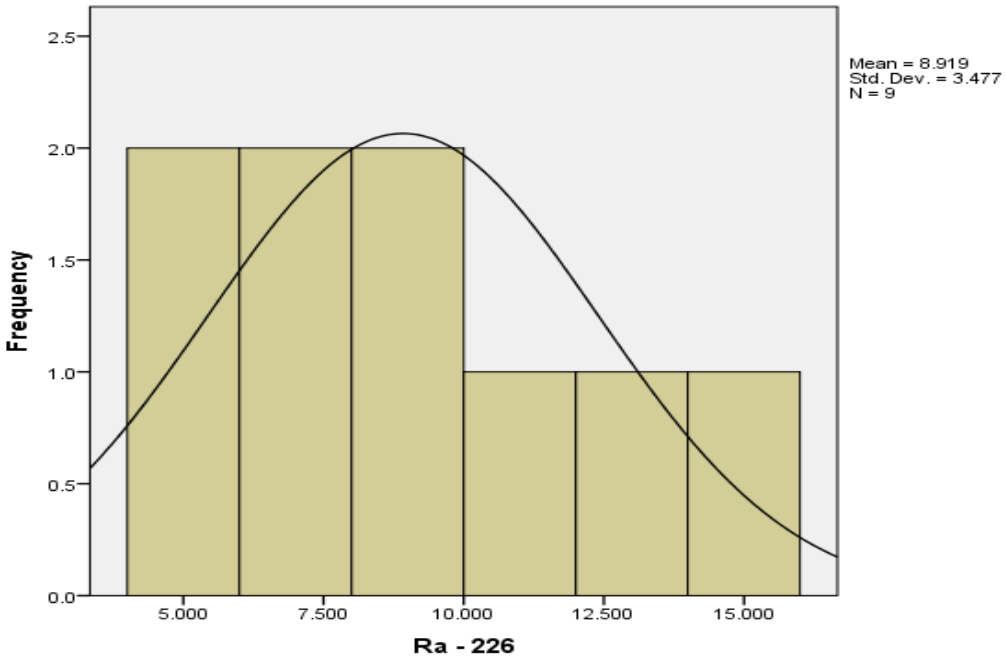


Figure 8: Frequency distribution histogram for activity concentration of ^{226}Ra in $Bq\ kg^{-1}$ fo finisher poultry manure

© 2018 Global Journals

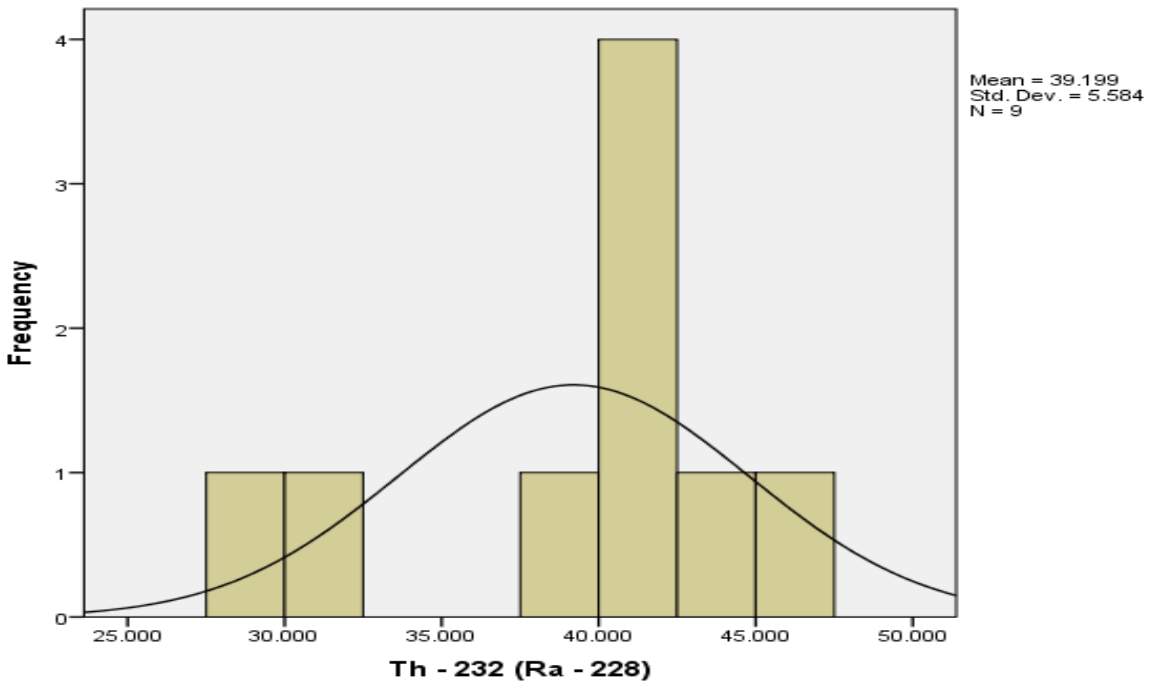


Figure 9: Frequency distribution histogram for activity concentration of ^{232}Th (^{228}Ra) in $Bq\ kg^{-1}$ fo finisher poultry manure

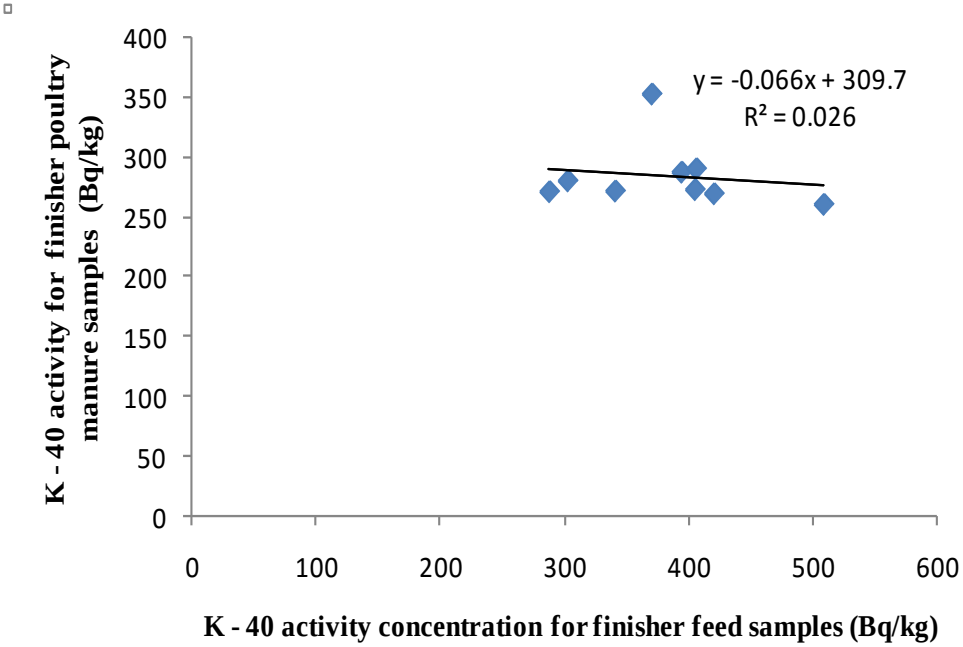


Figure 10: Regression plot to determine correlation coefficient between ^{40}K and ^{40}K for poultry manure and poultry feeds

© 2018 Global Journals

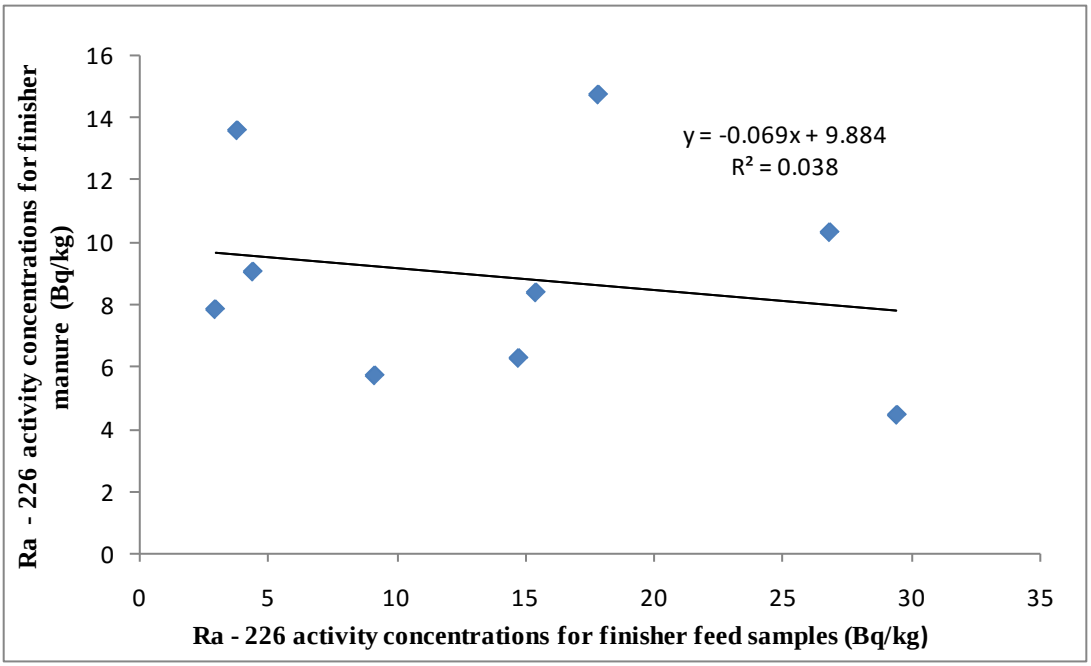


Figure 11: Regression plot to determine correlation coefficient between ^{226}Ra and ^{226}Ra for poultry manure and poultry feeds

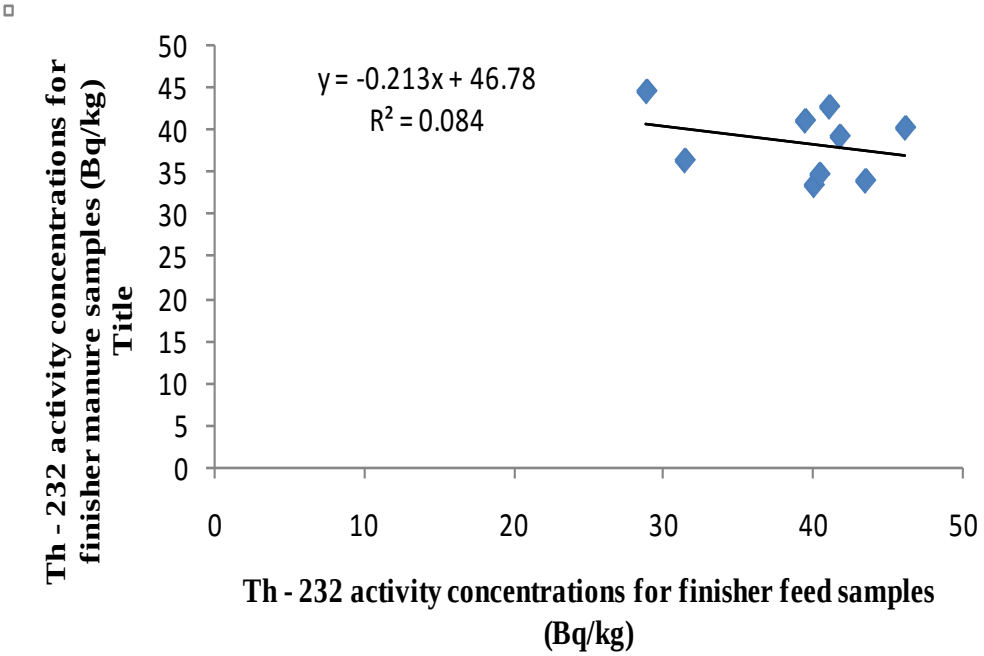


Figure 12: Regression plot to determine correlation coefficient between ^{232}Th and ^{232}Th for poultry manure and poultry feeds

IV. Discussion

a) Range, mean, standard deviations and coefficient of variation for Radionuclides

The range of activity concentrations obtained in starter/grower feed samples for ^{40}K, ^{226}Ra, and ^{232}Th radionuclides respectively presented in Table 3 were from 339.29 to 388.35 $Bq\ kg^{-1}$; 3.28 to 14.63 $Bq\ kg^{-1}$; 33.33 to 41.18 $Bq\ kg^{-1}$, with mean and standard deviation of 362.87±16.28 $Bq\ kg^{-1}$; 7.15±4.13 $Bq\ kg^{-1}$; and 37.92±2.28 $Bq\ kg^{-1}$ respectively. The distribution of ^{226}Ra (CV = 0.58) was observed to be more varied than ^{40}K (CV = 0.04) and ^{232}Th (CV = 0.06) radionuclides in the starter/grower feed samples.

© 2018 Global Journals

As Observed from Table 4, the activity concentrations obtained in finisher feed samples for ^{40}K, ^{226}Ra, and ^{232}Th radionuclides respectively ranged from 269.66 to 353.25 $Bq\ kg^{-1}$; 3.82 to 29.42 $Bq\ kg^{-1}$; 33.33 to 44.59$Bq\ kg^{-1}$, with mean and standard deviation of 284.31±27.46 $Bq\ kg^{-1}$; 15.21±8.88 $Bq\ kg^{-1}$; and 38.43±4.08 $Bq\ kg^{-1}$ respectively. The distribution of ^{226}Ra (CV = 0.59) was observed to be more dispersed than ^{40}K (CV = 0.01) and^{232}Th (CV = 0.11) radionuclides in the finisher feed samples.

As shown in Table 5, the activity concentrations obtained in finisher poultry manure samples for ^{40}K, ^{226}Ra, and ^{232}Th radionuclides respectively ranged from 288.04 to 509.68 $Bq\ kg^{-1}$; 4.43 to 14.74 $Bq\ kg^{-1}$; 28.83 to 46.14 $Bq\ kg^{-1}$, with mean and standard deviation of 382.33±67.12 $Bq\ kg^{-1}$; 8.92±3.48 $Bq\ kg^{-1}$; and 39.20±5.58 $Bq\ kg^{-1}$ respectively. Observation from the table showed the distribution of ^{226}Ra (CV = 0.39) was widely spread than ^{40}K and ^{232}Th radionuclides in the finisher feed samples.

Observation from Tables 3, 4 and 5 revealed finisher poultry manure contained the highest ^{40}K activity (382.33±67.12 $Bq\ kg^{-1}$) while the lowest was found in finisher poultry feeds (284.31±27.46 $Bq\ kg^{-1}$). Also, finisher poultry feeds recorded the highest ^{226}Ra activity concentrations (15.21±8.88 $Bq\ kg^{-1}$) among the three materials investigated while the lowest was found in starter/grower feeds (7.15±4.13 $Bq\ kg^{-1}$). While the activity concentrations of ^{232}Th radionuclides in the three materials were highest in finisher poultry manure (39.20±5.58 $Bq\ kg^{-1}$) with the lowest result obtained in starter/grower feed samples (37.92±2.28 $Bq\ kg^{-1}$). Radionuclide content of ingredient used in processing the feeds, the lithology and geochemical composition of agricultural farm soil from where the materials were sourced could likely be a major contributor to radionuclides found in the materials.

The mean result for ^{40}K contained in finisher poultry manure was found higher than 277.3±12 $Bq\ kg^{-1}$, and 284.5±8 $Bq\ kg^{-1}$ reported in Sheep and Cow fertilizers in Saudi Arabia (Alharbi, 2013); BDL and 336.3±13.9 $Bq\ kg^{-1}$ established in Chicken droppings and Cow droppings collected from Zaria, Kaduna State (Ibeanu *et al.,* 2009). However, the mean activity concentrations of ^{226}Ra found in the poultry manure were lower than the corresponding 31.6±1.6 $Bq\ kg^{-1}$ and41.1±1.7 $Bq\ kg^{-1}$ recorded in Sheep and Cow fertilizer in Saudi Arabia (Alharbi, 2013), and 134.7±24.1 $Bq\ kg^{-1}$ and 190.3±30 $Bq\ kg^{-1}$ contained in Chicken droppings and Cow droppings obtained in Zaria, Kaduna State, Nigeria (Ibeanu *et al.,* 2009). Though the poultry manure contains some levels of ^{40}K, ^{226}Ra and ^{232}Th radionuclides, its application to farm soil may not significantly increase the radioactivity levels.

b) Total mean annual effective dose

The levels of total mean annual effective doses were directly associated with the activity concentrations of radionuclides in the poultry feeds and poultry manure samples. The calculated effective dose due to external exposure to the two poultry feeds ranged from 0.68 $\mu Sv\ y^{-1}$ (finisher poultry feeds) to 1.36 $\mu Sv\ y^{-1}$ (finisher poultry feeds) with the mean and standard deviation of 0.93±0.23 $\mu Sv\ y^{-1}$; while for finisher poultry manure it ranged from 0.44 $\mu Sv\ y^{-1}$ to 0.86 $\mu Sv\ y^{-1}$ with the mean and standard deviation of 0.61±0.13 $\mu Sv\ y^{-1}$. The effective dose delivered to the workers, dealers of the two poultry feeds via inhalation pathway ranged from 3.16 $\mu Sv\ y^{-1}$ (starter poultry feeds) to 4.41 $\mu Sv\ y^{-1}$ (finisher poultry feeds) with the mean of 3.68±0.31 $\mu Sv\ y^{-1}$; while for finisher poultry manure, it ranged from 1.65 $\mu Sv\ y^{-1}$ to 2.67 $\mu Sv\ y^{-1}$ with the mean and standard deviation of 0.08±0.02 $\mu Sv\ y^{-1}$. Mean effective doses from accidental ingestion for starter/grower poultry feeds (0.12±0.02 $\mu Sv\ y^{-1}$), finisher poultry feeds (0.14±0.03 $\mu Sv\ y^{-1}$) and finisher poultry manure (0.08±0.02 $\mu Sv\ y^{-1}$) were considered to be in good agreement. The most significant radiation exposure pathway in all the three materials investigated as observed in Tables 3, 4, and 5 was the internal exposure from inhalation of poultry feeds dust particles associated with air. Considering the distribution of the total mean annual effective dose due to internal and external exposures, workers in poultry environment and dealers of poultry feeds are more exposed to radiation risk than farmers in farm soil environment. Relatively lower values of internal and external doses rate ($\mu Sv\ y^{-1}$) of the samples investigated showed that workers, dealers in poultry feeds, and commercial farmers are not significantly exposed to elevated gamma doses.

c) Frequency histogram distribution, skewness, and kurtosis

Figures 1 to 9 showed the distributions of frequency histogram of activity concentrations of ^{40}K, ^{226}Ra, and ^{232}Th radionuclides respectively in starter/grower poultry feeds, finisher poultry feeds and finisher poultry manure. Skewness is a measure of asymmetry or departure from the symmetry of distribution while kurtosis measures the tailedness (outliers) of the probability distribution. Close observation showed that about 77.8% of the distributions was moderately symmetric (bell–shape) while 22.2% was asymmetric about the mean. Few of the frequency distribution curves were heavy–tailed, while others were light – tailed.

d) Regression and correlation analysis

To find out the strength and degree of associations between the pair of radionuclides for poultry feeds and poultry manure, correlation studies were carried out between each pair of radionuclides.

© 2018 Global Journals

The regression analyses were between ^{40}K and ^{40}K; ^{226}Ra and ^{226}Ra; and ^{232}Th and ^{232}Th activity concentrations of finisher poultry manure and feed respectively. The scatter plots from the regression analyses are shown in Figures 10, 11 and 12 respectively. Close observation from plots revealed very weak and negative linear association/relationship existed between the activity concentrations for finisher poultry manure and finisher poultry feed for ^{40}K and ^{40}K ($R = 0.16$); ^{226}Ra and ^{226}Ra ($R = 0.19$); and between ^{232}Th and ^{232}Th ($R = 0.29$) respectively which shows that data set move in opposite directions for each pair of radionuclides; in other words, for every positive increase in data set for finisher feed there is a corresponding decrease in finisher manure for the pairs of radionuclides investigated which signify that the radionuclide contents of poultry feeds did not contribute significantly to the level of radionuclides in poultry manure. It could be from other sources such as the water they drink, and other food supplements were given to the poultry bird.

V. Conclusion

Measurement and evaluation of internal and external exposure to ionizing radiation doses due to the distribution of activity concentrations of radionuclide ^{40}K, ^{226}Ra and ^{232}Th in starter/grower poultry feed, finisher poultry feed and resulting poultry manure was carried out. The ^{40}K concentration, in all the samples, investigated recorded the highest mean activity concentration than ^{226}Ra and ^{232}Th. The distribution of ^{226}Ra was more heterogeneous in all the samples than homogeneous distributions obtained in ^{40}K and ^{232}Th. Activity concentrations of ^{40}K in poultry manure were found higher than reported works for animal manure in Saudi Arabia and Zaria (Nigeria). In all, about 77.8% of the distribution was moderately symmetric while 22.2% were asymmetric about the mean. Most significant exposure pathway in all the three materials investigated was the internal exposure from inhalation of poultry and manure dust particles. Considering the distribution of the total mean annual effective dose due to internal and external exposures, workers in poultry environment and dealers of poultry feeds are more exposed to ionizing radiation risk than farmers in farm soil environment. A very weak and negative linear relationship found between the activity concentrations of pairs of radionuclide recorded in finisher poultry manure and finisher poultry feed could suggest radionuclide contents in poultry feeds contributed but not significantly to the level of radionuclides in poultry manure. The radiometric information from this study could serve as baseline in the study area and as a reference material for similar studies in the future within the country and beyond in situations of environmental radioactivity contaminations from uncontrolled releases of radiation sources into the environment.

References Références Referencias

1. Ademola, A.K., Bello, A.K., Adejumobi, A.C. (2014). Determination of natural radioactivity and hazard in soil samples in and around gold mining area in Itagunmodi, South – Western, Nigeria, *Journal of Radiation Research and Applied Sciences.* 7: 249 – 255.
2. Ademola, J.A. and Oyema, U.C. (2014). Assessment of natural radionuclides in fly ash produced at Orji River Thermal Power Stataion, Nigeria and the associated radiological impact. *Natural Science,* 6 : 752 -759.
3. Ahmed, N.K., El – Arabi, A.M. (2005). Natural radioactivity in farm soil and phosphate fertilizer and its environmental implications in Qena Governorate Upper Egypt. *Journal of Environmental Radioactivity,* 84(1):51 - 64
4. Alharbi, W.R., (2013). Natural radioactivity and dose assessment for brands of chemical and organic fertilizers used in Saudi Arabia. *Journal of Modern Physics,* 4: 344 – 348.
5. El – Taher, A. and Althoyaib, S.S (2011). Natural radioactivity levels and heavy metals in chemical and organic fertilizers used in Kingdom of Saudi Arabia. *Applied Radiation and Isotopes,* 70(1): 290 – 295.
6. Avwiri, G.O., Osarolube, E., Alao, A.A. (2013). Assessment of natural radionuclide content in some commonly consumed vegetables and fruits in Oil Mining Lease (OML) 58 and 6, Oil and Gas Producing Area in the Niger Delta Region of Nigeria using gamma – ray. *International Journal of Scientific Research,* 2(2): 376 – 379.
7. Aydan A.Ş. and Turhan, H.G. (2015).Natural and artificial radionuclides in drinking water samples and consequent population doses. *Journal of Radiation Research and Applied Sciences,* 8(4): 578 – 582.
8. Aziz, A.Q., Shahina, T., KamelUd Din., Shahid M., Chiara C., Abdul W. (2014). Evaluation of excessive life time cancer risk due to natural radioactivity in the rivers sediments of Northern Pakistan. *Journal of Radiation Research and Applied Sciences,* 7(4): 438 – 477.
9. Boukhenfouf, W. and Boucenna, A. (2011).The radioactivity measurement in soil and fertilizers using gamma spectrometry technique. *Journal of Environmental radioactivity,* 102(4):336 – 339.
10. Degrange, J., Lepicard, S. (2005). Naturally occurring radioactive materials (NORM IV). Proceedings of an International Conference, Szezkyrk, 17 – 21 May, p. 230.
11. Faanu, A., Adukpo, O.K., Tettey – Larbi, L., Lawluvi, H., Kpeglo, D.O., Darko, E.O., Emi – Reynolds, G.,

© 2018 Global Journals

et al., (2016). Natural radioactivity levels in soil, rocks and water at a mining concession of Persus gold mine and surrounding towns in Central Region of Ghana. *Springer Plus,* 5:98, doi: 10.1186/s40064 – 016 – 0716 – 5. PMCID: PMC435091

12. Farai, I.P. (2014). Physics in radiation application and safety for national technological advancement. A Plenary Lecture delivered at the 37th Annual Conference of the Nigerian Institute of Physics, held at Oduduwa University, Ipetumodu, Osun State, 27 – 31,October.
13. Feroz, A. M., and Sajad, A.R. (2015). Measurement of radioactive nuclides present in soil samples of district Ganderbal of Kashmir Province for radiation safety purposes. *Journal of Radiation Research and Applied Sciences,* 8(2):155 – 159.
14. Ghosh, D., Deb, A., Sengupta, R., Bera, S., Hardar, S., Maitaii, S. (2011).Measurement of alpha radioactivity and dose assessment in common food crops with SSNTD.*J. Environ. Sci. Eng.,* 53(1): 51 – 56.
15. Ibeanu, I.G.E., Akpan T.C., Mallam, S.P., Chatta, C. (2009). Evaluation of chemical fertilizer in Nigeria for NORMs Using NAI gamma spectrometry technique. *Nigerian Journal of Physics,* 21(1): 130 – 134.
16. International Commissinm on Radiological Protection. (2012). ICRP Publication 119: Compendium of dose coefficients based on ICRP Publication 60. Annals of the ICRP41 (Suppl).42(4); e1 – e130.
17. Isinkanye, M.O. and Emelue, H.U. (2015). Natural radioactivity measurements and evaluation of radiological hazards in sediments of Oguta Lake, South East Nigeria. *Journal of Radiation Research and Applied Sciences,* 8(3): 459 – 469.
18. Jankovic, M., Todorovic, D., Savanovic, M. (2008). Radioactivity measurement in soil samples collected in the republic of Sipska. *Radiation Measurement,* 43:1448 – 1452.
19. Jibiri, N.N., Alausa, S.K., Owofolaju, A.E. and Adeniran, A.A. (2011).Terrestrial gamma dose rates and physicochemical properties of farm soils from ex – tin mining locations in Jos – Plateau, Nigeria. *African Journal of Environmental Science and Technology,* 5(12): 1039 – 1049.
20. Jibiri, N.N., Amakom, C.M., Adewuyi, G.O.(2010). Radionuclide content and physicochemical water quality indicator in stream, well and borehole water sources in high background radiation area of Abeokuta, South western Nigeria. *J. water Resource and Protection,* 2: 291 – 297.
21. Jibiri, N.N., and Fasae, K.P. (2012).Activity concentrations of ^{226}Ra, ^{232}Th and ^{40}K in brands of fertilizers used in Nigeria. *Radiation Protection Dosimetry,* 148(1):132 – 137.
22. Jibiri, N.N., Farai, I.P., Alausa, S.K. (2007). Activity concentrations of ^{226}Ra, ^{228}Th and^{40}K in different food crops from high background radiation area in Bitsichi, Jos – Plateau, Nigeria. *Radiat. Environ Biophys.,* 46(1): 53 – 59.
23. Kolo, M.T., Khandarker, M.U., Amin, Y.M., Abdullah, W.H.B. (2016). Quantification and radiological risk estimation due to the presence of natural radionuclides in Maiganga Coal, Nigeria. *Plos ONE,* 11(6): e0158100, doi:10.1371/journal.pone. 0158100.
24. Mustapha, A., Mbuzukongira, P., Mangala, M. (2007).Occupational radiation exposure of artisans mining columbite – tantalite in Eastern Democratic Republic or Cogo. *Journal of Radiological Protection,* 27(2): 187: PMID: 17664663.
25. Njing, R.L., Tshivhase, V.M., Onoja, R.A. and Aisha, I. P. (2016). Evaluation of gross alpha and beta activity concentration in five vital organs of some goats. *Journal of Animal & Plant Science,* 27(2): 4219 – 4229.
26. Ogundare, F.O., and Adekoya, O.I. (2015).Gross alpha and beta radioactivity in surface soil and drinkable water around a steel processing and facilities. *Journal of Radiation Protection and Applied Sciences,* 8(3): 411 – 417.
27. Okedeye, A.S., Gbadebo, A.M., Mustapha, A.O. (2014). Effects of Physical and chemical properties of quarry sites in Ogun State, Nigeria. *Journal of Applied Sciences,* 14: 691 – 696.
28. Saueia, C.H., Mazzilli, M.P. (2006). Distribution of natural radionuclide in the production and use of phosphate fertilizers in Brazil. *Journal of Environmental Radioactivity,* 89(3): 229 – 239.
29. Shanthi, G., Maniyan, C.G., Allen, G.A.G., Kumaran, J.T.T. (2009). Radioactivity in food crop from high background radiation areas in Southwest, India.*Current Science,* 97(9): 1331 – 1335.
30. Taskin, H., Karravus, M., Ay P., Topuzoglu, A., Hidiroglu, S., Karahan, G. (2009). Radionuclide concentration in soil and Kirklareli, Turkey. *Journal of Environmental Radioactivity,* 100: 49 – 53.
31. Tchokossa, P., Olomo, J.B., Balogun, F.A., and Adesanmi, C.V. (2013). Assessment of radioactivity content of food in oil and gas producing area in Delta State, Nigeria. *International Journal of Science and Technology,* 3(4): 245 – 250.
32. World Health Organisation, WHO, (2016). Ionizing Radiation, Health Effects and Protective Measures. Fact Sheet.medianinquiries@who.int.

© 2018 Global Journals

Global Journal of Science Frontier Research: A
Physics and Space Science
Volume 18 Issue 4 Version 1.0 Year 2018
Type: Double Blind Peer Reviewed International Research Journal
Publisher: Global Journals
Online ISSN: 2249-4626 & Print ISSN: 0975-5896

Hexamethylenetetramine Assisted Wet Chemical Route to Synthesize Nanostructured Cadmium Sulfide Thin Film

By S. A. Vanalakar

Abstract- Nano-structured thin films of cadmium sulfide (CdS) have been wet chemically deposited on soda lime glass substrate and, fluorine-doped tin oxide (FTO) coated conducting glass substrates by using non-ionic surfactant; Hexamethylenetetramine (HMTA). The structural, optical and surface morphological properties of the CdS films was investigated through the analysis of the x-ray diffraction, optical spectroscopy and, scanning electron microscopy. The structural and optical study showed that the CdS thin films are polycrystalline in nature having cubic crystal structure. The optical study revealed that the CdS films have a direct band gap energy of 2.44 eV. The SEM images show interconnected nano-plates like morphology with a well-defined surface area. Finally, the photoelectrochemical (PEC) performance of HMTA mediated CdS thin film samples were studied. The CdS based solar cell shows PEC performance with maximum short circuit current density of (I_{sc}) 1.25 mA/cm^2.

Keywords: *cadmium sulfide, surfactant, nanowalls morphology, pec performance.*

GJSFR-A Classification: *FOR Code: 030302*

HEXAMETHYLENETETRAMINEASSISTEDWETCHEMICALROUTETOSYNTHESIZENANOSTRUCTUREDCADMIUMSULFIDETHINFILM

Strictly as per the compliance and regulations of:

OPEN ASSOCIATION OF RESEARCH SOCIETY, USA
RESEARCH | DIVERSITY | ETHICS

© 2018. S. A. Vanalakar. This is a research/review paper, distributed under the terms of the Creative Commons Attribution-Noncommercial 3.0 Unported License http://creativecommons.org/licenses/by-nc/3.0/), permitting all non commercial use, distribution, and reproduction in any medium, provided the original work is properly cited.

Hexamethylenetetramine Assisted Wet Chemical Route to Synthesize Nanostructured Cadmium Sulfide Thin Film

S. A. Vanalakar

Abstract- Nano-structured thin films of cadmium sulfide (CdS) have been wet chemically deposited on soda lime glass substrate and, fluorine-doped tin oxide (FTO) coated conducting glass substrates by using non-ionic surfactant; Hexamethylenetetramine (HMTA). The structural, optical and surface morphological properties of the CdS films was investigated through the analysis of the x-ray diffraction, optical spectroscopy and, scanning electron microscopy. The structural and optical study showed that the CdS thin films are polycrystalline in nature having cubic crystal structure. The optical study revealed that the CdS films have a direct band gap energy of 2.44 eV. The SEM images show interconnected nano-plates like morphology with a well-defined surface area. Finally, the photoelectrochemical (PEC) performance of HMTA mediated CdS thin film samples were studied. The CdS based solar cell shows PEC performance with maximum short circuit current density of (I_{sc}) 1.25 mA/cm^2.

Keywords: cadmium sulfide, surfactant, nanowalls morphology, pec performance.

I. Introduction

Now-a-days, nanostructured materials are extensively explored due to their superior physico-chemical properties in various applications, including photovoltaic, electro-optical, and sensor devices [1-4]. Nanotechnology becomes advantageous to make inexpensive and efficient solar cells on a large scale. To this end, nanostructured layers in thin film solar cells offer three significant advantages. First, due to multiple reflections, the actual optical path for absorption is much larger than the definite film thickness [5]. Second, light generated electrons and holes need to travel over a much shorter path, so, the recombination losses are greatly reduced. As a result, the absorber layer thickness in nano-structured solar cells is very thin in few nanometers (nm) instead of several micrometers in the traditional thin-film solar cells (TFSCs) [6]. Third, the energy band gap of different layers of TFSCs can be improved to the preferred design value by simply varying the size of nano-particles [7]. The altered energy band gap energies allows for more design flexibility in the absorber and window layers in the solar cells. In particular, nano-structured cadmium sulfide (CdS), zinc oxide (ZnO), cadmium telluride (CdTe), Cu_2ZnSnS_4, Cu_2FeSnS_4, etc. are of great interest as window and absorber layers in thin film solar cells [8-11].

Among various semiconductors, CdS is one of the most vital semiconductor compounds which is used widely as a photo-electrochemical (PEC) solar cell element due to its optimum band gap energy [12]. Also, to PEC solar cell, CdS has also been exploited in diode lasers, gas sensors, and catalytic applications [13, 14]. Meanwhile, the specific properties of CdS have been correlated with growth conditions and methods. In this direction, CdS have been prepared via a number of physical and chemical techniques. Out of various techniques, chemical bath deposition (CBD) is one of the simplistic and easy methods to prepare CdS thin films with a variety of surface morphologies [15, 16].

In the present paper, attempts were made to engineer the morphology of the CdS thin films by using ionic surfactant; hexamethylenetetramine (HMTA). In this direction, thin films of CdS in assistance with HMTA were prepared at 90°C by using simplistic CBD method. The surface morphological study revealed the interconnected nanoplate-like structure of as synthesized CdS thin films. Further, these interconnected nanowalls of CdS thin films were characterized for their structural, and optical studies through the techniques including X-ray diffraction (XRD), and optical absorption spectroscopy. Finally, the photoelectrochemical (PEC) performance such as J-V characteristics in dark and under illumination, ideality factor of prepared CdS films was studied.

II. Experimental Details

All chemical were purchased from S. D. fine-chemicals and used without any further purification. The cadmium sulfate ($CdSO_4{\cdot}H_2O$) were used as cadmium (Cd) source and thiourea ($H_2N{\cdot}CS{\cdot}NH_2$) as sulfur (S) source. HMTA and liquor ammonia (NH_3) were used as an organic surfactant and a complexing agent, respectively. The experimental parameters like the precursor's concentration, operating temperature, pH, and deposition time were varied to produce a good quality CdS thin films. Initially, the matrix solution was prepared by adding aqueous solution (1 wt %) of an organic surfactants (HMTA) to 1.25 M $CdSO_4$. Then, to

Author: Department of Physics, Shree Mouni Vidhyapeeth's Karmaveer Hire College, Gargoti, Kolhapur-416209, M.S., India.
e-mail: sharad.vanalakar@gmail.com

© 2018 Global Journals

maintain 11 pH of the solution, the aqueous ammonia (NH_4OH) added to the solution. The initial turbid solution becomes transparent by adding the excess ammonia. Finally, 1.1 M thiourea was added into above solution with constant stirring. The CdS films were deposited by dipping the soda lime glass into the above solution at 90 C for 10 min. Finally, the synthesized CdS thin films were rinsed in distilled water and kept for drying at room temperature overnight.

The X-ray diffractometer (Philips, PW 3710, Almelo, Holland Make) operated at 25 kV, 20 mA with CuKα radiation (1.5407 Å) was used for study of the structural properties of the CdS thin films. Optical absorbance was measured using a UV–vis spectrophotometer (UV1800, Shimadzu, Japan). The surface morphology of the films was examined by SEM (Model JEOL-JSM-6360, Japan), operated at 20 kV. Meanwhile, the thickness of the resulting CdS films was measured using a surface profiler (Ambios XP-1). The J-V characteristics were measured using Semiconductor Characterization System (SCS-4200, Keithley, Germany) using two electrode configurations.

III. Result and Discussion

X-ray diffraction (XRD) patterns of CdS thin films were used for its structural characterization and the assessment of stoichiometry. Fig. 1 shows XRD pattern of HMTA mediated CdS interconnected nanowalls network on soda lime glass substrate. The films deposited were stoichiometric and did not show peaks related to elemental cadmium or sulfur or carbon. CdS peaks in XRD pattern are (111), (200), (220), (311), (222), (400) and (331) appears at 2θ = 26.45, 31.71, 44.13, 51.87, 54.97, 62.67 and 70.23 degree, respectively. The formation of CdS phase was confirmed by comparing the observed XRD pattern with the standard JCPDS data (80-0019). In addition, the standard JCPDS data suggest the cubic crystal structure of as-synthesized CdS thin films. The lattice parameter 'a' is calculated using the following Eq. (1),

$$\frac{1}{d^2} = \frac{h^2 + k^2 + l^2}{a^2} \quad (1)$$

The mean values of 'a' observed in our study (5.810 Å) is in good agreement with the reported value a=5.811Å.

Further, using the breadth of (111) peak, the average crystallite size was estimated using Scherrer's formula given below Eq. (2)

$$D_{(111)} = \frac{k\lambda}{\beta \cos\theta} \quad (2)$$

where k is the dimensionless constant (0.95), λ is wavelength having value 1.5406Å and, β is the broadening of the diffraction line at half of its maximum intensity (taken in radians by multiplying a factor of $\pi/360$). The D the diameter of crystallite and θ is diffraction angle. The calculated crystallite size is found to be 20 nm for (111) plane. Meanwhile, the broadened peaks indicate the nanocrystalline nature of the films [17].

Due to the nanocrystalline thin films, UV-Vis spectroscopy has become an effective tool in determining the size and optical properties. Fig. 2 shows the room temperature optical absorption spectrum of the CdS thin film recorded in the range of 450–750 nm without taking into account scattering and reflection losses. The optical absorption peak appeared at ~ 522 nm gives band gap energy value of about 2.44 eV. This band gap energy is suitable for the light energy capturing and its conversion to electrical energy [18]. The present UV-visible spectrum reveals as-synthesized CdS thin film has a high absorbance of light in the visible region, indicating applicability as a captivating material in solar cell applications.

The surface morphology of as-synthesized HMT assisted CdS thin films were examined by SEM technique and presented in Fig. 3. The low magnification SEM image as shown in Fig. 3(a) reveals the porous surface structure and the formation of CdS interconnected nanoplates-like assembly over the complete substrate. Also, no overgrowth, pinholes, voids or cracks on the substrate was seen. In addition, the nano-plates like structure covers over the entire substrate. Fig. 3(b) shows the high magnification SEM image of CdS thin films. The high magnification images clearly show the nanoplates connected with each other forming nanoconduits. Such plates having ~70 nm thickness are seen in the SEM image Fig. 3(b). Due to these interconnected nanowalls, the HMT mediated CdS thin film sample provides noticeable surface area. The higher surface area is beneficial for the enhancement of surface activities such as effective permeability of electrolytes into the inner structure of the film, and light absorption [19]. Also, the peculiar interconnected nanoplate-like structure scatters the light internally, which may lead to improvement in the effective light absorption [20]. The light absorption path length of photons can be increased as it is trapped in the nanoconduits. These mechanisms boost the PEC performance of CdS electrode.

For the PEC characterization of the HMT mediated CdS thin film sample (CdS), the measurements were performed in an electrolyte of 1 M polysulfide (Na_2S-NaOH-S) in a two-electrode arrangement of the following configuration:

Glass/FTO/CdS/Na_2S-NaOH-S/G

In the photo-electrochemical cell, poly-sulfide solution acts as an electrolyte and the CdS thin film deposited on the FTO acts as a working electrode. The

© 2018 Global Journals

graphite (G) acts as a counter electrode. The active area of working and counter electrode was about 1 cm^2. The J-V characteristics were measured by a SCS-4200 unit in the dark and under light illumination at 30 mW/cm^2. Fig. 4 suggest that, the J-V characteristics is like diode characteristics for the PEC cells fabricated with CdS thin film samples. Under illumination, shifting of the J–V curve in the fourth quadrant of the graph suggests that the electrons are the majority carriers, confirming the n-type conductivity of CdS thin films [21]. The CdS cell shows the photo-electric conversion efficiency (η) of 0.34 % with (J_{SC}) =1.25 mA/cm^2, open-circuit voltage (V_{OC}) =435 mV and fill factor (FF) =0.31.

The ideality factor 'n_d ' of CdS films is determined under forwarding bias by using following equation (Eq. (3)) as,

$$I = I_O\,(e^{qV/ndkT}) - 1 \qquad (3)$$

Where Io is the reverse saturation current, V is forward bias voltage, k is Boltzmann's constant, and T is ambient temperature. Usually, the value of 'n_d' is found to be in between 1 to 2. This value depends on the relation between diffusion current and recombination current. When diffusion current is more, then, ideality factor becomes 1 and, it becomes 2 when the diffusion current is less than recombination current. The ideality factor in our CdS film was found to be 1.6. The value of 'n_d' is a suitable parameter that describes how closely the diode's behavior matches the behavior predicted by theory.

IV. Conclusion

In summary, CdS composed of a uniform interconnected nanoplate-like network have been successfully prepared via a non-ionic surfactant-assisted chemical bath deposition at ambient atmosphere. The as-deposited CdS film showed a cubical crystal structure. The well-covered porous structure with the interconnected nanoplates network morphology leads to a high surface area which is observed by SEM studies. Further, this structure is a good prospective way for PEC solar cell application.

References Références Referencias

1. J. Jeevanandam, A. Barhoum, Y. S. Chan, A. Dufresne, M. K. Danquah, Review on nanoparticles and nanostructured materials: history, sources, toxicity and regulations, Beilstein Journal of Nanotechnology, 9 (2018) 1050–1074
2. S. A. Vanalakar, S. S. Mali, E. A. Jo, J. Y. Kim, J. H. Kim, P. S. Patil, Triton-X mediated interconnected nanowalls network of cadmium sulfide thin films via chemical bath deposition and their photoelectrochemical performance, Solid State Sciences, 36 (2014) 41-46
3. V. L. Patil, S. A. Vanalakar, P. S. Patil, J. H. Kim, Fabrication of nanostructured ZnO thin films based NO2 gas sensor via SILAR technique, Sensors and Actuators B: Chemical, 239 (2017) 1185-1193
4. H. Gleiter, Nanostructured materials: basic concepts and microstructure, Acta Materialia, 48 (2000) 1-29
5. S. A. Vanalakar, S.S. Mali, R.C. Pawar, N. L. Tarwal, A.V. Moholkar, Jin A. Kim, Ye-bin Kwon, J.H. Kim, P.S. Patil, Synthesis of cadmium sulfide spongy balls with nanoconduits for effective light harvesting, Electrochimica Acta, 56 (2011) 2762–2768
6. V. K. Sethi, M. Pandey, P. Shukla, Use of nanotechnology in solar PV cell, International Journal of Chemical Engineering and Applications, 2 (2011) 77-80
7. M.C. McAlpine, R.S. Friedman, Song Jin, Keng-hui Lin, Wayne U. Wang, C.M. Lieber, High-Performance Nanowire Electronics and Photonics on Glass and Plastic Substrates, Nano Letters, 3 (2003) 1531–1535
8. S. A. Vanalakar, S. S. Mali, R. C. Pawar, D. S. Dalavi, A. V. Mohalkar, H. P. Deshamukh, P. S. Patil, Farming of ZnO nanorod-arrays via aqueous chemical route for photoelectrochemical solar cell application, Ceramics International, 38 (2012) 6461–6467.
9. S. Chander, A. Purohit, C. L. Saini, M.S. Dhaka, Enhancement of optical and structural properties of vacuum evaporated CdTe thin films, Materials Chemistry and Physics 185 (2017) 202-209
10. S. A. Vanalakar, P. S. Patil, J. H. Kim, Recent advances in synthesis of Cu2FeSnS4 materials for solar cell applications: A review, Solar Energy Materials and Solar Cells, 182 (2018) 204-219
11. K. C. Lai, C. C. Liu, C. H. Lu, C. H. Yeh, M. P. Houng, Characterization of ZnO:Ga transparent contact electrodes for microcrystalline silicon thin film solar cells, Solar Energy Materials and Solar Cells, 94 (2010) 397-401
12. A. Kamble, B. Sinha, G. Agawane, S. Vanalakar, J. Y. Kim, S. S. Kale, P. Patil, J. H. Kim, Sulfur ion concentration dependent morphological evolution of CdS thin films and its subsequent effect on photo-electrochemical performance, Physical Chemistry Chemical Physics, 18 (2016) 28024-28032
13. L. Borrell, S. Cervera-March, J. Giménez, R. Simarro, J. M. Andújar, A comparative study of CdS-based semiconductor photocatalysts for solar hydrogen production from sulphide + sulphite substrates, Solar Energy Materials and Solar Cells, 25 (1992) 25-39
14. S. A. Vanalakar, V. L. Patil, P. S. Patil, J. H. Kim, Rapid synthesis of CdS nanowire mesh via a simplistic wet chemical route and its NO2 gas sensing properties, New Journal of Chemistry 42 (2018), 4232-4239

© 2018 Global Journals

15. S. M. Pawar, B. S. Pawar, J. H. Kim, O. S. Joo, C. D. Lokhande, Recent status of chemical bath deposited metal chalcogenide and metal oxide thin films, Current Applied Physics, 11 (2011) 117-161
16. K. Mokurala, L. L. Baranowski, F. W. de Souza Lucas, S. Siol, M. F. A. M van Hest, S. Mallick, P. Bhargava, A. Zakutayev, Combinatorial Chemical Bath Deposition of CdS Contacts for Chalcogenide Photovoltaics, ACS Combinatorial Science, 18 (2016) 583–589
17. S. Rajathi, K. Kirubavathi, K. Selvaraju, Preparation of nanocrystalline Cd-doped PbS thin films and their structural and optical properties, Journal of Taibah University for Science, 11 (2017) 1296-1305
18. S. A. Vanalakar, M. P. Suryawanshi, S. S. Mali, A. V. Moholkar, J. Y. Kim, P. S. Patil, J. H. Kim, Simplistic surface active agents mediated morphological tweaking of CdS thin films for photoelectrochemical solar cell performance, Current Applied Physics, 14 (2014) 1669-1676
19. S. A. Vanalakar, P. S. Patil, J. H. Kim, Polymer assisted synthesis of CdS nanostructure for photoelectrochemical solar cell applications, Book: Advanced Polymeric Materials: From Macro-to Nano-Length Scales, CRC Publication, 2016, 174-203
20. A. Niv, M. G. Koren, H. Dotan, G. Bartal, A. Rothschild, Separation of light confinement and absorption sites for enhancing solar water splitting, Journal of Material Chemistry A, 4 (2016) 3043-3051.
21. J. J. Vijila, J. Henry, T. Daniel, K. Mohanraj, G. Sivakumar, Photoresponse of novel mixed metal chalcogenide MoSb2-xCuxSe4/CdS thin film solar cells fabricated by CBD method using citric acid, International Journal of Energy Research, 41 (2017) 1295-1309.

Figure Captions

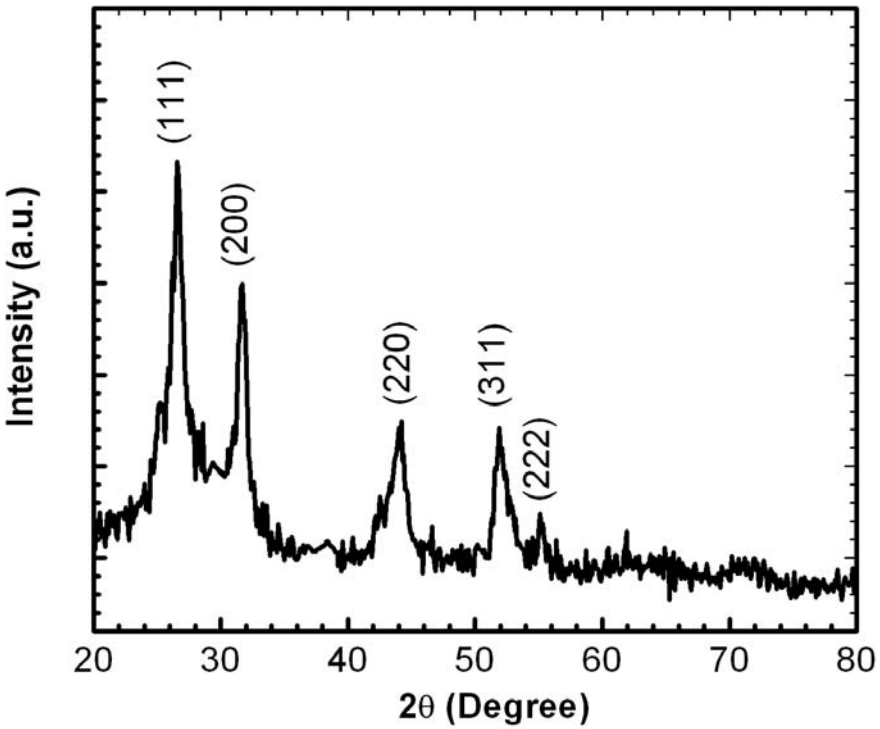


Fig. 1: X ray diffraction pattern of HMTA mediated CdS thin film

© 2018 Global Journals

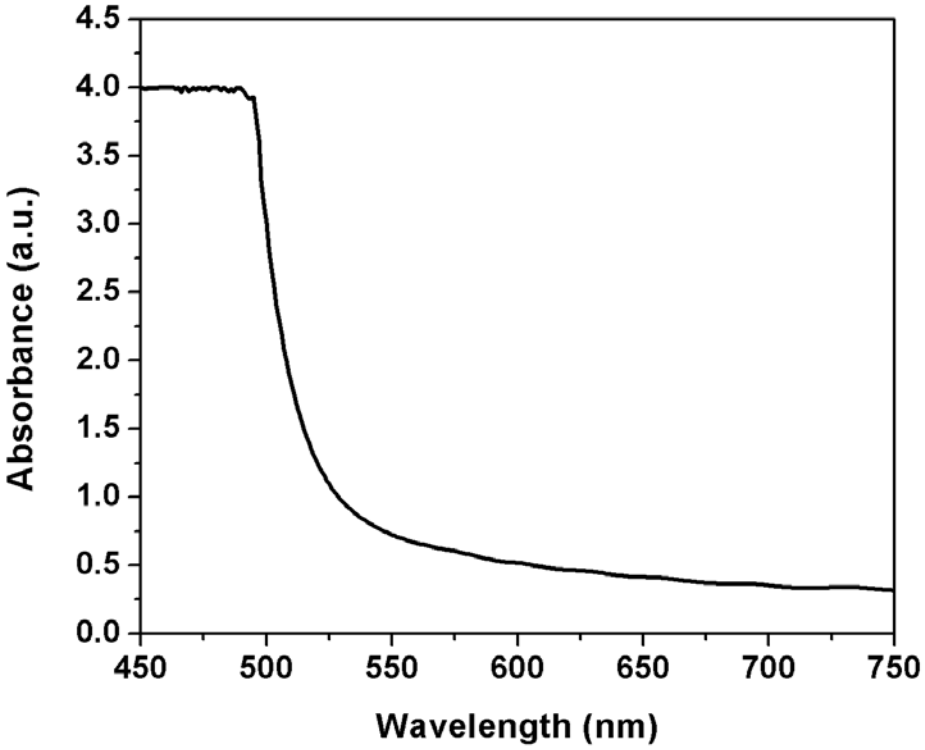


Fig. 2: Optical absorption spectrum of HMTA mediated CdS thin film

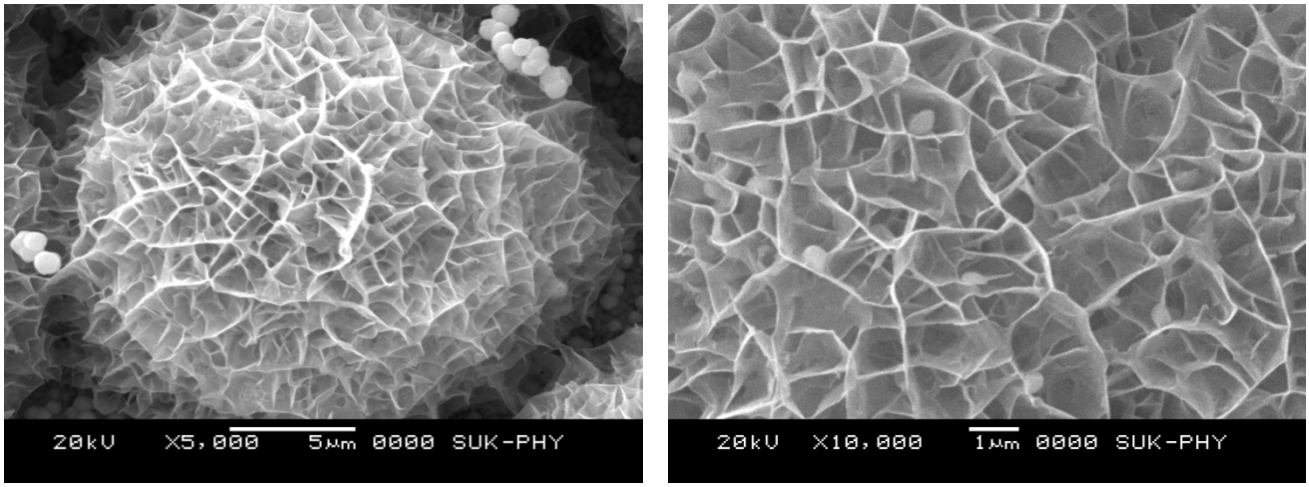


Fig. 3: (a) Low magnification SEM images of HMTA mediated CdS thin films sample

(b) SEM images show the formation of interconnected nanowall network of HMTA mediated CdS over the substrate

© 2018 Global Journals

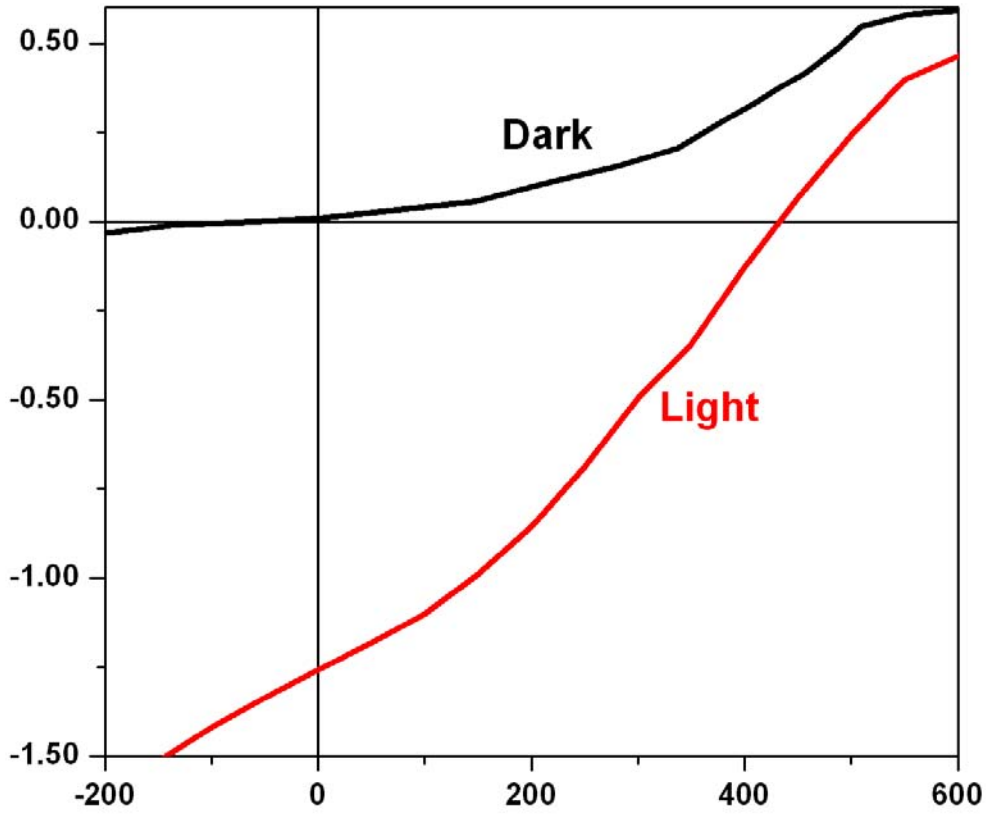


Fig. 4: The J-V characteristics of interconnected nanowall network of HMTA mediated CdS thin film sample

© 2018 Global Journals

Global Journal of Science Frontier Research: a
Physics and Space Science
Volume 18 Issue 4 Version 1.0 Year 2018
Type: Double Blind Peer Reviewed International Research Journal
Publisher: Global Journals
Online ISSN: 2249-4626 & Print ISSN: 0975-5896

External and Internal Radiation Doses from Chemical Fertilizers used in Ibadan, Oyo State, Nigeria

By B. U., Nwaka & N. N., Jibiri
Alvan Ikoku Federal College of Education Owerri

Absract- The knowledge of external and internal doses of radiation emitted from radionuclides contained in different chemical fertilizers sold in Ibadan, Nigeria is very important. Therefore, activity concentrations of 40K, 226Ra and 232Th radionuclides in Urea, NPK (15 – 15 – 15), NPK (16 – 16 – 16) and Single Super Phosphate (SSP) fertilizer brands sold in the area for agricultural purposes were determined using gamma–ray spectroscopy. Radium equivalent activity (Raeq), gamma radiation or representative index (I_γ), alpha index (I_α), annual gonadal dose equivalent (AGDE), external exposure (D_{ext}) to gamma radiation as well as internal exposure (D_{int}) to doses of radiation to the marketers and users of the products were calculated. The calculated Ra_{eq} for the four brands of chemical fertilizers were 80.90 $Bqkg^{-1}$, 295.95 $Bqkg^{-1}$, 293.93 $Bqkg^{-1}$ and 706.17 $Bqkg^{-1}$ respectively. External gamma doses were 0.60 $mSvy^{-1}$, 6.73 $mSvy^{-1}$, 6.65 $mSvy^{-1}$ and 13.00 $mSvy^{-1}$ while the sum of the internal doses due to inhalation and ingestion were found as 3.93 μSvy^{-1} , 4.51 μSvy^{-1} , 3.61 μSvy^{-1} and 8.97 μSvy^{-1} respectively. More external and internal doses of radiation were calculated for marketers of the products than farmers.

Keywords: *chemical fertilizers, ionizing radiation, external exposure, somatic effects, radium equivalent activity.*

GJSFR-A Classification: *FOR Code: 250604*



Strictly as per the compliance and regulations of:

© 2018. B. U., Nwaka & N. N., Jibiri. This is a research/review paper, distributed under the terms of the Creative Commons Attribution-Noncommercial 3.0 Unported License http://creativecommons.org/licenses/by-nc/3.0/), permitting all non commercial use, distribution, and reproduction in any medium, provided the original work is properly cited.

External and Internal Radiation Doses from Chemical Fertilizers used in Ibadan, Oyo State, Nigeria

B. U., Nwaka [α] & N. N., Jibiri [σ]

Abstract- The knowledge of external and internal doses of radiation emitted from radionuclides contained in different chemical fertilizers sold in Ibadan, Nigeria is very important. Therefore, activity concentrations of ^{40}K, ^{226}Ra and ^{232}Th radionuclides in Urea, NPK (15 – 15 – 15), NPK (16 – 16 – 16) and Single Super Phosphate (SSP) fertilizer brands sold in the area for agricultural purposes were determined using gamma–ray spectroscopy. Radium equivalent activity (Ra_{eq}), gamma radiation or representative index (I_γ), alpha index (I_α), annual gonadal dose equivalent (AGDE), external exposure (D_{ext}) to gamma radiation as well as internal exposure (D_{int}) to doses of radiation to the marketers and users of the products were calculated. The calculated Ra_{eq} for the four brands of chemical fertilizers were 80.90 $Bq\,kg^{-1}$, 295.95 $Bq\,kg^{-1}$, 293.93 $Bq\,kg^{-1}$ and 706.17 $Bq\,kg^{-1}$ respectively. External gamma doses were 0.60 $mSv\,y^{-1}$, 6.73 $mSv\,y^{-1}$, 6.65 $mSv\,y^{-1}$ and 13.00 $mSv\,y^{-1}$ while the sum of the internal doses due to inhalation and ingestion were found as 3.93 $\mu Sv\,y^{-1}$, 4.51 $\mu Sv\,y^{-1}$, 3.61 $\mu Sv\,y^{-1}$ and 8.97 $\mu Sv\,y^{-1}$ respectively. More external and internal doses of radiation were calculated for marketers of the products than farmers. The order of SSP > NPKs > Urea fertilizers was observed for external exposure to gamma radiation. The results could serve as important radiometric data and information upon which future environmental monitoring of external and internal exposure to gamma radiation and alpha particles associated with chemical fertilizers could be based.

Keywords: chemical fertilizers, ionizing radiation, external exposure, somatic effects, radium equivalent activity.

I. Introduction

Fertilizers, whether chemical (inorganic) or animal manure (organics) are used to replenish micro and macro elements lost by crops through leaching, erosion and continuous cropping in farm soil. The widespread inorganic fertilizers in use in Nigeria are Nitrogen Phosphorus and Potassium (NPK) fertilizers, Urea fertilizer and Single Supper Phosphate fertilizer (SSP). NPK fertilizers are of different formulations including NPK (15 – 15 – 15), NPK (20 – 10 – 10) and NPK (16 – 16 – 16). Using x–ray fluorescence spectrometric technique, heavy metals of silicon, vanadium, chromium, nickel, zinc, iron, titanium and copper were identified in inorganic fertilizers sold in Samaru, Zaria, Nigeria (Elisha, 2014).

The phosphorus content of chemical fertilizers originates from phosphate rocks which contain varying levels of natural radionuclides Uranium (^{238}U), Thorium (^{232}Th) and Potassium (^{40}K) (Hassan *et al.,* 2016) that emit alpha particles, beta particles, and gamma radiations. According to Sahu *et al.* 2014 rock phosphate ore and phosphogypsum contributes to enhanced concentrations of natural radionuclides in the environment. High activity concentrations of radionuclides in fertilizers may result to increase in redistribution of radionuclides in farm soil, and via plant tissues, are deposited in steam, leaves, and fruits. Moreover, the health status of factory workers, marketers or dealers of the product as well as farmers may be at risk due to handling and packing in bags, inhalation and accidental ingestion which are the possible pathways of exposure.

The study of gamma radiation and alpha particles emitted from the radionuclides ^{226}Ra, ^{232}Th and ^{40}K present in fertilizers is very important in environmental radioactivity. This is because high doses of radiation deposited directly on tissues and lunges could cause cancerous growth. External gamma radiation exposure occurs directly by the handling of fertilizer which could cause skin cancer if the gamma doses are higher than safe limit recommended by radiation protection and measurement agencies. Whereas, internal exposure to alpha particles arises from the inhalation of radon gas and its progenies as well as ingestion of doses of radiation either intentionally or accidentally. During radioactive decay, ^{226}Ra and ^{232}Th radionuclides release short–lived decay products of radon gas ($t_{1/2} = 3.8$ days) and thoron ($t_{1/2} = 55.6$ seconds) in the air which deposit their alpha particle energies in tissues and lungs. Radionuclide ^{226}Ra has high potential, due to continuous irradiation, causing biological damages once it is deposited in tissues.

Hassan *et al.* (2017) had established that the average value of ^{226}Ra (^{238}U), ^{232}Th and ^{40}K in Japanese fertilizers were less than their corresponding values in Egyptian fertilizers. Jabbar and Abdul (2014) in Basrah Governorate, Iraq found the mean specific activity

Author α: Department of Physics, Alvan Ikoku Federal College of Education, Owerri, PMB 1033, Imo state, Nigeria.
e-mails: ben_de_req@yahoo.com; nwakabenjaminu@gmail.com;
Author σ: Radiation and Health Physics Research Laboratory, Department of Physics, University of Ibadan, Nigeria.
e-mail: jibirinn@yahoo.com

© 2018 Global Journals

concentrations 107.0±8.7 $Bq\,kg^{-1}$, 108.0±7.6 $Bq\,kg^{-1}$ and 1207.0±9.8 $Bq\,kg^{-1}$ respectively for ^{226}Ra, ^{232}Th and ^{40}K. Though not too recently, activity concentrations of radionuclides ^{226}Ra, ^{232}Th and ^{40}K present in chemical fertilizers in Nigeria were reported (Ibeanu *et al.,* 2009; Jibiri and Fasae, 2012) but the results did not consider at the time the radiation dose contribution of the various brand of fertilizers investigated. External and internal radiation dose contributions due to chemical fertilizers had not been given attention in Nigeria, therefore, the need to have current data and information on gamma radiation doses from external exposure as well as inhalation and accidental ingestion of doses of radiation due to alpha and possibly beta particles and the health implication. These were carried out by determining the activity concentrations of ^{226}Ra, ^{232}Th and ^{40}K radionuclides, radium equivalent activity (Ra_{eq}), the gamma radiation or representative hazard index (I_γ) and the alpha index (I_α) contained in NPK (15 – 15 – 15), NPK (16 – 16 – 16), SSP, and Urea fertilizers used in Ibadan, Nigeria for different purposes.

II. Materials and Method

a) Sample preparation

The four (4) brands of chemical fertilizers commonly in use in Ibadan were purchased from local marketers in the locality which comprises of NPK (15 – 15 – 15), NPK (16 – 16 – 16), Urea, and SSP fertilizers. Thirty – six (36) samples comprising of nine (9) samples from each brand were purposively selected and collected for the study, put in polythene bags, labeled and transported to the laboratory for preparation and analysis. They were pulverized in agate mortar to fine grain size and sieved through ~ 1.5 mm mesh sieve to be more homogeneous. The samples were then dried in a temperature controlled oven at 100°C to completely remove the moisture content until they attained constant weight. They were cooled in a desiccator, weighted (200±1g) and transferred in plastic containers, sealed using adhesives masking tape with each lid fastened on each container to prevent radon escape. The 36 sealed containers were stored for 30 days to establish radioactive secular equilibrium between long–lived ^{238}U and ^{232}Th and its daughters. Thereafter, an empty plastic container of the same geometry as the prepared homogeneous fertilizer samples was sealed and kept for 30 days to measure the background radiation of the laboratory environment.

b) Gamma–ray spectroscopy detector and characteristics

Measurement of ^{226}Ra, ^{232}Th and ^{40}K radionuclides was done using a 6 cm lead – shielded 7.6 cm by 7.6 cm sodium iodide activated with thallium, NaI(Tl), gamma ray spectrometer detector (Model number 802 series CANBERRA Inc.). The detector is lead shielded to minimize the effect of background radiation in the laboratory. The measuring instrument was coupled to a CANBERRA series 10 plus Multichannel Analyser (Model number 1104) through a preamplifier base and a photomultiplier tube which converts the visible light photons produced in the crystal into amplified electrical pulses, and then an amplifier. It has a modest resolution of 8% full–width at half maximum (FWHM) at ^{137}Cs energy of 0.662 MeV (Jibiri *et al.,* 2011), which suggests the choice of its use for measurement, which is capable of distinguishing the gamma–ray energies of the radionuclide of interest. The detector was connected to a personal computer (PC) with data acquisition system. A software programme was used to collect and analyse the data to compute the radionuclide concentrations in the samples. The procedure used in this study was similar to that followed by Isinkaye and Emelue (2015).

c) Energy and efficiency calibration of the detector

To ensure the radiation parameters in the samples could be expressed in physical radiometric units, the detector was calibrated before it was used for analyses. Since the performance of a gamma–ray spectroscopy depends on the high resolving power and high value of efficiency, the calibration was done in two stages: energy calibration and efficiency calibration. Energy calibration converts channel numbers in the spectrum to gamma–ray energies in MeV by placing different gamma sources of known energy in the detector volume after a preset counting time so as to identify channels of various photopeaks corresponding to the different gamma energies. ^{137}Cs (0.662 MeV), ^{60}Co (1.173 MeV), ^{22}Na (1.274 MeV), ^{60}Co (1.333), ^{40}K (1.460 MeV) ^{214}Bi (1.765 MeV) and ^{208}Ti (2.615 MeV) sources were used for energy calibration. A linear graph with empirical relation between the channel number and energies was obtained as the reliability of the measuring instrument, which was very strong enough (with correlation coefficient, $R = 0.99$) as shown in Figure 1. The efficiency calibration of the detector was done in other to determine the gamma–ray counting efficiencies over energy range of 0.662 – 2.615 MeV covering all gamma energies of radionuclide of interest in the study. This was carried out by converting the count per seconds under the photopeaks to activity concentrations in $Bq\,kg^{-1}$ of certified reference standard samples. The counting time for accumulating the spectral line for both background and each fertilizer sample was set for 36, 000 seconds which was good enough for the detector to analyse the spectrum with the peaks of interest clearly shown and well distinguished (Isinkaye and Emelue, 2015).

© 2018 Global Journals

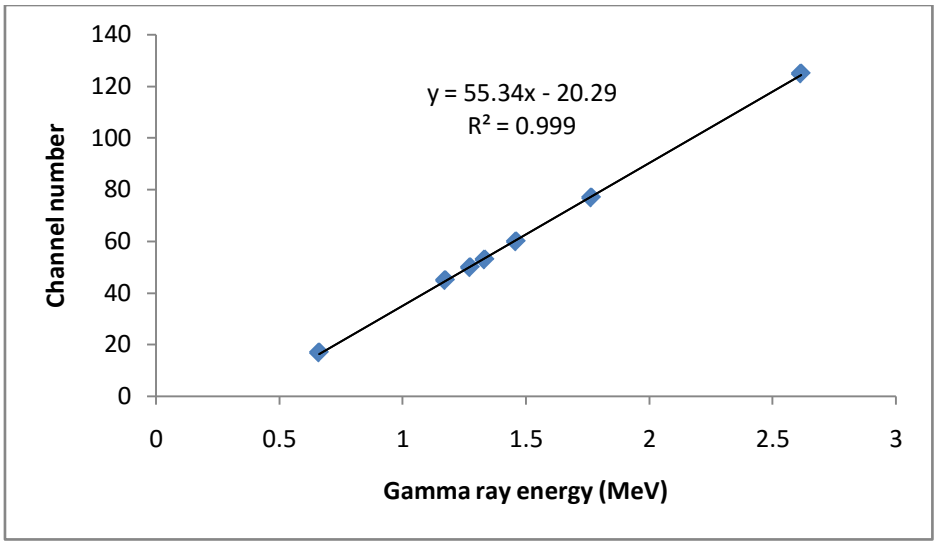


Figure 1: Energy Calibration Line of the Detector Systems

d) Calculation of activity concentration of radionuclide of interest in chemical fertilizers

The activity concentrations of ^{226}Ra in each chemical fertilizer sample was estimated from gamma–ray peak energy of 1.760 MeV associated with the decay of ^{214}Bi, while that of ^{232}Th was determined from gamma–ray peak energy of 2.615 MeV associated with the decay of ^{208}Ti. The activity concentration of ^{40}K was estimated from gamma–ray peak energy of 1.460 MeV from the decay of ^{40}K itself. The net area under the corresponding photopeak in the energy spectrum was calculated by subtracting count due to Compton scattering of the background source from the total (gross) area of the photopeak. The count rate under the photopeak of each of the ^{226}Ra, ^{232}Th, and ^{40}K radionuclides is related to activity concentrations using equation1 (Farai and Isinkaye, 2009; Jibiri and Okeyode, 2012). The mean values were presented in Tables 2 - 5 for the four (4) different chemical fertilizers.

$$C_i(Bq\ kg^{-1}) = KC_n = \frac{C_n}{\varepsilon\ P_\gamma\ M_s} \quad (1)$$

Where C_i is the activity concentration of radionuclide, i in the fertilizer samples measured in $Bq\ kg^{-1}$, C_n is the count rate under the corresponding photopeak which is the net count above the background over the time taken (36,000 seconds), ε is absolute detector efficiency at specific gamma–ray energy, P_γ is the absolute transition or emission probability of the specific gamma–ray, and M_s is the mass of each sample in the container in kg. The detection limit (DL) of a measuring system was needed to provide the minimum detectable activity concentrations in a sample measured in $Bq\ kg^{-1}$calculated for the study using equation 2 (Jibiri *et al.,* 2011).

$$DL\ (Bq\ kg^{-1}) = 4.65\frac{\sqrt{C_b}}{t_b}K \quad (2)$$

Where C_b represents net background count in the corresponding peak, t_b is the background counting time (in seconds), and K is the factor that converts count per seconds (cps) to activity concentration in $Bq\ kg^{-1}$. Detection limits were obtained for each radionuclides^{226}Ra, ^{232}Th and ^{40}K of interest, however, values above the detection limits were recorded in the study.

III. Evaluation of Radiological Hazard Indices

a) Radium equivalent activity Ra_{eq}

Variation in the distribution of radionuclides of ^{226}Ra, ^{232}Th and ^{40}K in phosphate rock deposits and inorganic fertilizer requires that radium equivalent activity is determined in materials. The radium equivalent activity has been defined as single radiological parameters that compare the specific activity of materials containing varying concentrations of ^{226}Ra, ^{232}Th and ^{40}K radionuclides (Berekta and Mathew, 1985). Regarding the radiological health safety assessment, the maximum safety limit of $Ra_{eq} \leq 370\ Bq\ kg^{-1}$ had been set for materials to keep gamma–ray dose below $1.5\ mSv\ y^{-1}$. Equation 3 was used to compute the Ra_{eq} and results presented in Table 6.

$$Ra_{eq} = C_{Ra} + 1.430C_{Th} + 0.077C_K \quad (3)$$

Where C_{Ra}, C_{Th} and, C_K are the concentrations of ^{226}Ra, ^{232}Th and ^{40}K in $Bq\ kg^{-1}$ in the fertilizer samples.

b) Annual gonadal doses equivalent $AGDE$

The annual gonadal dose equivalent ($AGDE$) is a measure of the genetic significance of the yearly dose received by the population reproductive organs (Ravisankar *et al.* 2014). The gonads, bone marrow and the bone surface cell are sensitive to ionizing radiations

© 2018 Global Journals

and are considered as of interest (UNSCEAR, 2000). Increase in $AGDE$ has been reported to affect the bones marrow, causing the destruction of the red blood cells which are then replaced by white blood cells. The $AGDE$ for the different inorganic fertilizers were calculated using equations 4 (Ravisankar *et al.,* 2014) and the results presented in Table 6. Equation 4 was used to compute $AGDE$ in μSvy^{-1}.

$$AGDE\ (\mu Svy^{-1}) = 3.09\ C_{Ra} + 4.18\ C_{Th} + 0.314\ C_K \quad (4)$$

Where C_{Ra}, C_{Th}, and C_K are the concentrations of ^{226}Ra, ^{232}Th and ^{40}K in $Bq\ kg^{-1}$ in the fertilizer samples.

c) Radioactivity hazard Index (I_γ)

Gamma radiation hazards associated with ^{226}Ra, ^{232}Th and ^{40}K radionuclides in the chemical fertilizer brands were assessed using the radioactivity hazard index. According to European Commission guidelines, I_γ should be greater than two (2) but less than 6 ($2< I_\gamma < 6$) for radiation dosed of $1\ mSv\ y^{-1}$ (Khan *et al.,* 1998). Furthermore, the value $I_\gamma \leq 0.5$ corresponds to a dose rate criterion of $0.3\ mSv\ y^{-1}$ whereas $0.5 \leq I_\gamma$corresponds to a criterion of $1\ mSv\ y^{-1}$ (European Commission Report, 1999; Turhan *et al.,* 2008). Equation 5 defines I_γ as

$$I_\gamma = \frac{C_{Ra}}{300} + \frac{C_{Th}}{200} + \frac{C_K}{3000} \quad (5)$$

Where C_{Ra}, C_{Th}, and C_K are the concentrations of ^{226}Ra, ^{232}Th and ^{40}K in $Bq\ kg^{-1}$ in the fertilizer samples.

d) Alpha index (I_α)

Emission of alpha radiation from alpha particles due to the release of radon gas from the samples is called alpha index represented by I_α which was calculated using equation 6 (Khan *et al.,* 1998; Tufail *et al.,* 2007; Hassan *et al.,* 2016).

$$I_\alpha = \frac{C_{Ra}}{200} \quad (6)$$

C_{Ra} represents the concentrations of ^{226}Ra in $Bq\ kg^{-1}$ in the fertilizer samples.

e) Estimation of external gamma doses and internal exposures to radiation doses

Factory workers, marketers or dealers of chemical fertilizers, as well as farmers, are exposed to ionizing radiation doses present in the material through three major pathways: external exposure to gamma–ray during the packing in bags and handling of the materials, internal exposure from inhalation of dust and contaminated air due to the practice and possible internal exposure from any accidental ingestion of the materials. The computed doses due to inhalation and accidental ingestion were summed up to get the total internal doses delivered by ^{226}Ra, ^{232}Th, and ^{40}K radionuclides to the tissues and organs. This was carried out by applying conversion coefficient doses, relevant for this study, supplied by the International Commission on Radiological Protection (ICRP). External exposure to gamma radiation was estimated using equation 7 (Mustapha *et al.,* 2007 Jibiri *et al.,* 2011; Ademola and Oyema, 2014):

$$D_{Ext} = \sum_i A_i\ C_{Ext,\ i}\ T_{ext} \quad (7)$$

Where A_i is the activity concentrations of nuclide, i measured in $(Bq\ kg^{-1})$, $C_{Ext,\ i}$ is the effective dose coefficient for nuclides i as presented in Table 1, T_{ext} is the duration of exposure in a year. For factory workers and markers who work for eight (8) hours per day in twenty (20) working days per month, the duration of exposure per year was calculated as $20 \times 8 \times 12$ which equals 1920 hours per year $(h\ y^{-1})$. Also for this study, we assume that for a farmer working for eight (8) hours per day for three (3) days per a week, which gives a total of twelve (12) days per month. The duration of exposure for such farmer per year was calculated as $12 \times 8 \times 12$ which equals 1152 hours per year $(h\ y^{-1})$ as presented in Table 1.

Internal exposure from inhalation of poultry/manure dust and contaminated air due to the practice was calculated using equation 8 (Mustapha *et al.,* 2007)

$$D_{Inhal} = \sum_i A_i\ C_{Inhal,\ i} \eta_{Inhal} D_f\ T_{ext} \quad (8)$$

where A_i is the activity concentrations of nuclide, i measured in $Bq\ kg^{-1}$, T_{ext} is the duration of exposure in number of years (which for the purpose of this work has been corrected for 1920 for poultry feeds exposure and 1152 for poultry manure exposure), $C_{Inhal,\ i}$ is the dose coefficient for inhalation of nuclide i measured in $Sv\ Bq^{-1}$, η_{Inhal} is the breathing rate measured in m^3/h with coefficient of 1.69 (Mustapha *et al.,* 2007) and D_f is the dust loading factor measured in g/m^{-3} with coefficient of 1.0×10^{-3} $[1.0 \times 10^{-6}\ kg\ m^{-3}]$ (Degrand and Lepicard, 2005).

Internal dose from accidental ingestion of radionuclides was calculated from equation 9 (Kolo *et al.,* 2016)

$$D_{Ingest} = \sum_i A_I C_{Ingest,\ i}\ \eta_{ingest}\ T_{ext} \quad (9)$$

Where A_i is the activity concentrations of nuclide i $(Bq\ kg^{-1})$, $C_{Ingest,\ i}$ is the dose coefficient for ingestion of nuclide, i, measured in $Sv\ Bq^{-1}$, η_{ingest} is the ingestion rate for adults, measured in $kg\ h^{-1}$ whose value is 5.0×10^{-6} (Mustapha *et al.,* 2007) and T_{ext} is the duration of exposure in a year, which for this study was corrected as 1920 for poultry feeds exposure and 1152 for poultry manure exposure.

© 2018 Global Journals

Table 1: Dose coefficient and some risk parameters for radionuclide of interest adopted in this work

Dose coefficient parameters	^{40}K $(Bq\ kg^{-1})$	^{226}Ra $(Bq\ kg^{-1})$	^{232}Th $(Bq\ kg^{-1})$	T_{ext} $(h\ y^{-1})$	References
Effective dose coefficient, C_{ext} $(\eta Sv\ h^{-1}/Bq\ kg^{-1})$	1.175	9.929	0.003		Mustapha *et al.* (2007)
Dose coefficient for inhalation, C_{Inhal} $(Sv\ Bq^{-1})$	3.0 E-09	2.2 E-06	2.9 E-05		1CRP 119 (2012)
Dose coefficient for ingestion C_{Ingest} $(Sv\ Bq^{-1})$	6.2 E-09	2.8 E-07	2.2 E-07		1CRP 119 (2012)
Duration of exposure for marketers/dealers of fertilizer products				1920*	
Duration of exposure for commercial farmers				1152**	

Source: Kolo et al. (2016), except for 1920 and 1152** which were computed for this study.*

IV. Results and Discussion

a) Activity concentration of ^{40}K, ^{226}Ra, and ^{232}Th radionuclides in different fertilizers

Tables 2, 3, 4, and 5 presented the activity concentrations of ^{40}K, ^{226}Ra and ^{232}Th radionuclides for Urea, NPK (15 – 15 – 15), NPK (16 – 16 – 16) and SSP fertilizers used in Ibadan, Nigeria. Observation from Tables 2 to 5 showed that NPK (16 – 16 – 16) recorded the highest mean activity concentration 2929.33±180.47 $Bq\ kg^{-1}$ for ^{40}K while the lowest value 171.70±16.15 $Bq\ kg^{-1}$ was found in Urea. The mean results obtained for NPK (15 – 15 – 15) and NPK (16 – 16 – 16) fertilizer were relatively close and showed exceptional values of concentration among the four fertilizer brands. For ^{226}Ra radionuclides, the highest mean activity concentration 631.17±14.04 $Bq\ kg^{-1}$ was found in SSP fertilizer while the lowest mean activity concentration 9.58±7.08 $Bq\ kg^{-1}$ was found in NPK (15 – 15 – 15) fertilizer samples. While for ^{232}Th radionuclides, it was found that NPK (15 – 15 – 15) fertilizer had the highest mean activity concentration 44.04±6.07 $Bq\ kg^{-1}$ whereas SSP fertilizer had the lowest value 28.53±4.16 $Bq\ kg^{-1}$. The coefficient of variation (CV) calculated in this study show that some data set was relatively high while others were relatively low. Relatively high values of CV indicated that the distributions were widely dispersed (heterogeneous distribution of data set), while relatively lower values of CV indicated closely dispersed distributions (homogenous distribution of data set).

It is interesting to compare the radionuclide activity concentrations of the present study to similar reported study in different countries of the world. The ^{40}K, ^{226}Ra, and ^{232}Th results obtained in SSP fertilizer were higher than the corresponding values for PhF2 (SSP) fertilizers reported in Egypt (Hassan *et al.,* 2016). The ^{226}Ra concentrations obtained for Urea, NPK (15 – 15 – 15) and NPK (16 – 16 – 16) fertilizers were lower than the 571±20 $Bq\ kg^{-1}$, and 325±2 $Bq\ kg^{-1}$ established in Egyptian and Japanese fertilizers (Hassan *et al.,* 2017 b). Furthermore, the mean values of ^{232}Th radionuclides obtained in this study for Urea, NPK (15 – 15 – 15), NPK (16 – 16 – 16) and SSP fertilizers were higher than the results reported for Egyptian and Japanese fertilizers (Hassan *et al.,* 2017). ^{226}Ra and ^{232}Th activity concentrations (except the values obtained for ^{40}K) for both NPK fertilizers of the study were found lower than the corresponding results obtained by Jabbar and Abdul (2014) in Basrah Governorate, Iraq. Variation of the results with literature could be due to chemical compositions of materials used during the manufacturing process.

Except the mean results recorded for Urea, ^{40}K concentrations in NPKs and SSP were found higher than the results reported for Egyptian fertilizers, whereas the entire four fertilizer brands were found lower than the reported results in Japanese fertilizers (Hassan *et al.,* 2017). Moreover, ^{226}Ra concentration in Urea fertilizer of the present study was found lower than the mean value 15.38±2.94 $Bq\ kg^{-1}$ obtained in Urea fertilizer Tarakandi in Jamalpur, Bangladesh (Samad *et al.,* 2011), however, the ^{232}Th concentration was found higher than the mean value 17.16±6.73 $Bq\ kg^{-1}$ in Urea fertilizer Tarakandi in Jamalpur, Bangladesh (Samad *et al.,* 2011).

As observed from **Table 6,** mean value obtained for radium equivalent activity for the four brands of chemical fertilizers, except that of SSP which recorded 706.17 $Bq\ kg^{-1}$, were lower than 613±33 $Bq\ kg^{-1}$ and 454±5 $Bq\ kg^{-1}$ reported in Egyptian and Japanese fertilizers (Hassan *et al.,* 2017). Except for SSP brand, Urea and NPKs recorded Ra_{eq} lower than the recommended worldwide mean value 370 $Bq\ kg^{-1}$, an indication that SSP fertilizer should be handled by marketers and farmers with precautions. All the chemical fertilizer brands investigated, except Urea, had $I_\gamma < 1$ which should be avoided since they will deliver effective dose rate higher than one $(1)\ mSv\ y^{-1}$ to marketers of the products, factory workers, and farmers. The recommended maximum concentration of ^{226}Ra is 200 $Bq\ kg^{-1}$ which represents $I_\alpha = 1$. The values of I_α

© 2018 Global Journals

obtained in Urea, NPKs, except for SSP fertilizers, were less than one ($I_\alpha < 1$) which implied that the Urea and NPKs samples had ^{226}Ra concentrations less than 200 $Bq\,kg^{-1}$ while ^{226}Ra concentrations for SSP fertilizer was three (3) times higher than 200 $Bq\,kg^{-1}$. It, therefore, can be said about SSP fertilizer investigated in this study that possible radon inhalation could be so enormous that the samples warrant restriction. Comparing the activity concentrations of the radionuclides of interest, radium equivalent activity, external and internal doses gamma doses in the brands of chemical fertilizers investigated in this study with the worldwide safety standards for soil samples in $Bq\,kg^{-1}$ would not be necessary since chemical fertilizers are the man–made, manufactured from local industries.

Observation from Table 6 showed that factory workers and marketers of chemical fertilizers investigated in this study would appear to be more exposed to external than internal doses of radiation. This situation was likewise with farmers. Since factory workers and dealers or marketers of the products spend more days than farmers as observed from Table 1, it is expected that the mean values obtained for marketers of the products should be greater than that of farmers who were calculated and recorded in this study. For both marketers and farmers, the highest external exposure to gamma doses of radiation (in $mSv\,y^{-1}$) as observed from Table 6 were found in SSP fertilizers, while the lowest (in $mSv\,y^{-1}$) were found in Urea fertilizers respectively. Likewise, results (in $\mu Sv\,y^{-1}$) were found for internal doses due to accidental ingestion. In general, the most significant exposure to radiation doses was external (in $mSv\,y^{-1}$) followed by inhalation (in $\mu Sv\,y^{-1}$) and then accidental ingestion (in $\mu Sv\,y^{-1}$). Total internal exposure to doses of radiation due to the sum of inhalation and ingestion doses were found lower than that of external exposure doses of radiation. Precaution should be taken by factory workers, marketers of the products and farmers in staying around radiation field from NPKs, and SSP fertilizers to avoid serious radiobiological health challenges.

Table 2: Activity Concentration of Urea Fertilizer Samples

Sample code	^{40}K ($Bq\,kg^{-1}$)	^{226}Ra ($Bq\,kg^{-1}$)	^{232}Th ($Bq\,kg^{-1}$)
Urea 01	168.89±6.63	6.49±5.53	37.12±0.54
Urea 02	155.39±7.95	10.49±4.58	31.45±0.53
Urea 03	172.50±8.81	9.10±4.82	44.53±0.57
Urea 04	168.59±8.46	16.50±3.83	37.59±0.54
Urea 05	165.59±8.46	14.74±3.97	34.45±0.52
Urea 06	187.35±9.56	7.52±5.21	37.12±0.54
Urea 07	154.26±7.87	12.31±4.29	41.91±0.55
Urea 08	206.18±10.51	11.59±4.42	48.61±0.60
Urea 09	166.57±8.51	9.89±4.68	44.26±0.57
Mean±Std. Dev.	**171.70±16.15**	**10.95±3.23**	**39.67±5.49**
CV	0.09	0.19	0.14

Table 3: Activity Concentration of NPK (15 – 15 – 15) Fertilizer Samples

Sample code	^{40}K ($Bq\,kg^{-1}$)	^{226}Ra ($Bq\,kg^{-1}$)	^{232}Th ($Bq\,kg^{-1}$)
NPK1501	3722.56±189.36	4.00±5.25	48.96±0.61
NPK1502	2429.89±123.30	12.19±4.55	38.97±0.56
NPK1503	1587.64±80.76	5.70±6.19	21.78±0.62
NPK1504	2806.73±142.77	6.37±5.78	42.53±0.57
NPK1505	3114.89±158.45	17.20±3.90	51.79±0.63
NPK1506	3410.21±173.47	2.97±2.48	53.11±0.63
NPK1507	2707.09±137.70	22.14±3.47	42.76±0.63
NPK1508	3302.92±168.01	9.04±5.08	49.70±0.61
NPK1509	3029.13±154.09	4.61±6.46	46.76±0.60
Mean±Std. Dev.	2901.23±627.62	9.58±7.08	44.04±9.55
CV	0.22	0.74	0.22

© 2018 Global Journals

Table 4: Activity Concentration of NPK (16 – 16 – 16) Fertilizer Samples

Sample code	^{40}K ($Bq\ kg^{-1}$)	^{226}Ra ($Bq\ kg^{-1}$)	^{232}Th ($Bq\ kg^{-1}$)
NPK1601	2923.94±148.73	14.26±4.10	41.37±0.55
NPK1602	2946.37±149.88	0.49±42.99	37.27±0.54
NPK1603	2694.12±137.04	39.85±2.17	28.19±0.54
NPK1604	3217.68±163.63	23.90±4.71	32.09±0.49
NPK1605	2803.14±142.49	22.93±4.63	43.76±0.57
NPK1606	2696.24±137.15	22.38±4.60	30.33±0.52
NPK1607	2923.19±148.70	19.71±4.59	31.98±0.56
NPK1608	3023.50±153.80	16.99±4.46	29.83±0.53
NPK1609	3135.75±159.51	24.81±4.74	25.89±0.54
Mean±Std. Dev.	2929.33±180.47	20.59±10.40	33.41±6.07
CV	0.06	0.51	0.18

Table 5: Activity Concentration of SSP Fertilizer Samples

Sample code	^{40}K ($Bq\ kg^{-1}$)	^{226}Ra ($Bq\ kg^{-1}$)	^{232}Th ($Bq\ kg^{-1}$)
SSP01	397.21±20.22	492.88±9.02	27.36±0.53
SSP02	496.25±25.25	549.71±9.97	28.19±0.54
SSP03	401.86±20.45	613.76±11.06	32.74±0.60
SSP04	558.68±28.43	923.07±16.37	34.86±0.61
SSP05	416.04±21.17	676.43±12.13	28.22±0.54
SSP06	412.74±21.01	22.38±4.60	30.33±0.52
SSP07	479.67±24.41	743.88±13.28	23.01±0.43
SSP08	342.29±17.43	500.51±9.14	32.48±0.59
SSP09	493.18±25.10	497.30±9.09	23.01±0.43
Mean±Std. Dev.	444.21±66.74	631.17±14.04	28.53±4.16
CV	0.15	0.02	0.15

Table 6: Radiological indices associated with the Chemical Fertilizers

Radiological Indices	Urea fertilizer	NPK(15-15-15)	NPK(16-16-16)	SSP
Ra_{eq} ($Bq\ kg^{-1}$)	80.90	295.95	293.93	706.17
I_γ	0.29	1.22	1.21	2.40
I_α	0.05	0.05	0.10	3.16
D_{Ext} M ($mSv\ y^{-1}$)	0.60	6.73	6.65	13.00
D_{Ext} F ($mSv\ y^{-1}$)	0.35	4.04	3.99	7.80
D_{inhal} M ($\mu Sv\ y^{-1}$)	3.81	4.24	3.31	7.19
D_{inhal} F ($\mu Sv\ y^{-1}$)	2.29	2.60	1.99	4.31
D_{ingest} M ($\mu Sv\ y^{-1}$)	0.12	0.27	0.30	1.78
D_{ingest} F ($\mu Sv\ y^{-1}$)	0.02	0.16	0.18	1.07
$D_{Tot\ inter}$ M ($\mu Sv\ y^{-1}$)	3.93	4.51	3.61	11.50
$D_{Tot\ inter}$ F ($\mu Sv\ y^{-1}$)	2.31	2.76	1.17	5.38

M: Marketers, F: Farmers, $D_{Tot\ inter}$: Total internal exposure to doses of radiation due to the sum of inhalation and ingestion doses

V. Conclusion and Recommendations

Radiological indices due to activity concentrations of ^{40}K, ^{226}Ra and ^{232}Th radionuclides for Urea, NPK (15 – 15 – 15), NPK (16 – 16 – 16), and SSP fertilizers used in Ibadan, Nigeria were determined and recorded to ascertain if marketers and farmers could be exposed to doses of radiation and also to compare their radiological indices. The values of I_γ for NPKs and SSP showed that samples investigated should be avoided if health risk should be minimized. Also, the value of I_α for SSP revealed that health risk should be expected. Findings further showed that total internal exposure to doses of radiation due to the sum of inhalation and ingestion doses were found lower than that of external exposure to radiation doses. Marketers appeared to be more exposed both to external and internal doses of radiation than farmers. Samples of SSP fertilizers investigated had the greatest potentials among the four chemical fertilizer brands to cause radiobiological effects and should be handled with caution. The study did not compare the gamma dose rates/exposures from the radionuclides of ^{40}K, ^{226}Ra and ^{232}Th contained in the chemical fertilizers with their corresponding permissible safety limits for soil and sediment as reported by United Nations Scientific Committee on the Effects of Atomic Radiation (UNSCEAR). Investigation of more samples of chemical fertilizers for an average of ten (10) years in the study area will give a better result, however, preliminary data and information is provided as a prelude to investigations of radiological study of chemical and organic fertilizers in other states in Nigeria and countries

© 2018 Global Journals

of the world. The study recommends monitoring and placing serious restriction to chemical fertilizers rich in ^{40}K, ^{226}Ra and ^{232}Th radionuclides so as to minimize possible health hazards they may pose to users and marketers of the products. It also suggests the need to have local safety radiological standards in Nigeria.

References Références Referencias

1. Ademola, J.A. and Oyema, U.C. (2014). Assessment of natural radionuclides in fly ash produced at Orji River Thermal Power Station, Nigeria and the associated radiological impact. *Natural Science,* 6, 752 – 759.
2. Beretka, J. & Mathew, P.J. (1985).Natural radioactivity of Australian building materials industrial wastes and by–products. *Health physics,* 48(1), 87-95.
3. Degrange, J., Lepicard, S. (2005). Naturally occurring radioactive materials (NORM IV). Proceedings of an International Conference, Szezkyrk, 17 – 21 May, Pp. 230.
4. Elisha, J.J. and Elisha, M.J. (2012). Characterization of selected inorganic fertilizers by atomic absorption spectroscopy: possible carryover of heavy metals from phosphate rock. *International Journal of Science and Research,* 3(5), 94 – 96.
5. European Commission (EC) Report on Radiological Protection Principles concerning the natural radioactivity of building materials. Radiation Protection No. 112. Luxembourg: Directorate – General Environment, Nuclear Safety and Civil Protection; 1999, 6 – 9.
6. Farai, I.P., and Isinkaye, M.O. (2009). Radiological safety assessment of surface – water dam sediments used as building materials in southwestern Nigeria. Journal of Radiological Protection, 29, 85 – 93.
7. Hassan, N.M., Chang Byung – Uck, and Tokonami, S. (2017). Comparison of natural radioactivity of commonly used fertilizer materials in Egypt and Japan. *Journal of Chemistry,* Volume 2017, 8pages, https://doi.org/10.1155/2017/9182768
8. Hassan, N.M., Mansour, N.A., Fayez – Hassan, M., and Sedqy, E. (2016). Assessment of natural radioactivity in fertilizers and phosphate ores in Egypt. *Journal of Taibah Universityfor Science,* 10(2), 296 – 306.
9. Ibeanu, I.G.E., Akpan T.C., Mallam, S.P., Chatta, C. (2009). Evaluation of chemical fertilizer in Nigeria for NORMs Using NAI gamma spectrometry technique. *Nigerian Journal of Physics,* 21(1), 130 – 134.
10. Jabbar, H.J. and Abdul, R.H.S. (2014). Natural radioactivity of some local an d imported fertilizers in Basrah Governorate/Iraq. *Archives of Physics Research,* 5(5): 18 – 22.
11. International Commissinm on Radiological Protection. (2012). ICRP Publication 119: Compendium of dose coefficients based on ICRP Publication 60. Annals of the ICRP41 (Suppl).42(4); e1 – e130.
12. Isinkanye, M.O. and Emelue, H.U. (2015).Natural radioactivity measurements and evaluation of radiological hazards in sediments of Oguta Lake, South East Nigeria. *Journal of Radiation Research and Applied Sciences,* 8(3), 459 – 469.
13. Jibiri, N.N., Alausa, S.K., Owofolaju, A.E. and Adeniran, A.A. (2011).Terrestrial gamma dose rates and physicochemical properties of farm soils from ex – tin mining locations in Jos – Plateau, Nigeria. *African Journal of Environmental Science and Technology,* 5(12), 1039 – 1049.
14. Jibiri, N.N., and Fasae, K.P. (2012).Activity concentrations of ^{226}Ra, ^{232}Th and ^{40}K in brands of fertilizers used in Nigeria. *Radiation Protection Dosimetry,* 148(1), 132 – 137.
15. Jibiri, N.N. and Okeyode, I.C. (2012). Evaluation of radiological hazards in the sediments of Ogun river, South – western Nigeria. *Radiation Physics and Chemistry,* 81, 1829 – 1835.
16. Khan, K., Khan, H.M., Tufail, M. Khatibeh, A.J.A.H., Ahmad, N. (1998). Radiometric analysis of Hazara phosphate rock and fertilizers in Pakistan. *Journal of Environmental Radioactivity,* 38, 77 – 84.
17. Kolo, M.T., Khandarker, M.U., Amin, Y.M., Abdullah, W.H.B. (2016). Quantification and radiological risk estimation due to the presence of natural radionuclides in Maiganga Coal, Nigeria. *Plos ONE,* 11(6): e0158100, doi: 10.1371/journal.pone. 0158100.
18. Mustapha, A., Mbuzukongira, P., Mangala, M. (2007).Occupational radiation exposure of artisans mining columbite – tantalite in Eastern Democratic Republic of Cogo. *Journal of Radiological Protection,* 27(2), 187: PMID: 17664663.
19. Ravisankar, R., Sivakumar, S., Chandrasekaran, A., Prince Prakash Jebakuma, J., Vijayalakshmi, I., Vijayagopal, P. *et al.,* (2014). Spatial distribution of gamma radioactivity levels and radiological hazard indices in the east coast sediment of Tamilnadu, India with statistical approach. *Radiation Physics Chemistry,* 103, 89 – 98.
20. Sahu, S.K., Ajmal, P.Y., Bhaangare, R.C., Tiwari, M., Pandit, G.G. (2014). Natural radioactivity assessment of a phosphate fertilizer plant area. *Journal of Radiological Research and Applied Sciences.* 7(1), 123 – 128.
21. Samad, M.A., Ali, M.I., Paul, D. and Islam, S.M.A. (2011). An environmental impact study of Jamuna Urea Fertilizer Factory at Tarakandi in Jamalpur with radiological indices. *Journal of Environmental Science & Natural Resources,* 4(2), 27 – 33.

© 2018 Global Journals

22. Tufail, M., Akhtar, N., Javied, S., Hamid, T. (2007). Natural radioactivity hazards of building bricks fabricated available from saline soil of two districts of Pakistan. *Journal of Radiological Protection,* 27, 481 – 492.
23. Turhan, S., Baykan, U.N., Sen, K. (2008). Measurement of the natural radioactivity in building materials used in Ankara and assessment of external doses. *Journal of Radiological Protection,* 28, 83 – 91.
24. UNSCEAR, (2000). Sources and effects of ionizing radiation. United Nations Scientific Committee on the Effects of Atomic Radiation Report to the General Assembly with Scientific Annexes, New York.

© 2018 Global Journals

Global Journals Guidelines Handbook 2018

www.GlobalJournals.org

FELLOWS

FELLOW OF ASSOCIATION OF RESEARCH SOCIETY IN SCIENCE (FARSS)

Global Journals Incorporate (USA) is accredited by Open Association of Research Society (OARS), U.S.A and in turn, awards "FARSS" title to individuals. The 'FARSS' title is accorded to a selected professional after the approval of the Editor-in-Chief/Editorial Board Members/Dean.



- The "FARSS" is a dignified title which is accorded to a person's name viz. Dr. John E. Hall, Ph.D., FARSS or William Walldroff, M.S., FARSS.

FARSS accrediting is an honor. It authenticates your research activities. After recognition as FARSB, you can add 'FARSS' title with your name as you use this recognition as additional suffix to your status. This will definitely enhance and add more value and repute to your name. You may use it on your professional Counseling Materials such as CV, Resume, and Visiting Card etc.

The following benefits can be availed by you only for next three years from the date of certification:

FARSS designated members are entitled to avail a 40% discount while publishing their research papers (of a single author) with Global Journals Incorporation (USA), if the same is accepted by Editorial Board/Peer Reviewers. If you are a main author or co-author in case of multiple authors, you will be entitled to avail discount of 10%.

Once FARSB title is accorded, the Fellow is authorized to organize a symposium/seminar/conference on behalf of Global Journal Incorporation (USA). The Fellow can also participate in conference/seminar/symposium organized by another institution as representative of Global Journal. In both the cases, it is mandatory for him to discuss with us and obtain our consent.





You may join as member of the Editorial Board of Global Journals Incorporation (USA) after successful completion of three years as Fellow and as Peer Reviewer. In addition, it is also desirable that you should organize seminar/symposium/conference at least once.

We shall provide you intimation regarding launching of e-version of journal of your stream time to time.This may be utilized in your library for the enrichment of knowledge of your students as well as it can also be helpful for the concerned faculty members.



The FARSS can go through standards of OARS. You can also play vital role if you have any suggestions so that proper amendment can take place to improve the same for the benefit of entire research community.



As FARSS, you will be given a renowned, secure and free professional email address with 100 GB of space e.g. johnhall@globaljournals.org. This will include Webmail, Spam Assassin, Email Forwarders,Auto-Responders, Email Delivery Route tracing, etc.



The FARSS will be eligible for a free application of standardization of their researches. Standardization of research will be subject to acceptability within stipulated norms as the next step after publishing in a journal. We shall depute a team of specialized research professionals who will render their services for elevating your researches to next higher level, which is worldwide open standardization.



The FARSS member can apply for grading and certification of standards of their educational and Institutional Degrees to Open Association of Research, Society U.S.A.
Once you are designated as FARSS, you may send us a scanned copy of all of your credentials. OARS will verify, grade and certify them. This will be based on your academic records, quality of research papers published by you, and some more criteria. After certification of all your credentials by OARS, they will be published on your Fellow Profile link on website https://associationofresearch.org which will be helpful to upgrade the dignity.

The FARSS members can avail the benefits of free research podcasting in Global Research Radio with their research documents. After publishing the work, (including published elsewhere worldwide with proper authorization) you can upload your research paper with your recorded voice or you can utilize chargeable services of our professional RJs to record your paper in their voice on request.



The FARSS member also entitled to get the benefits of free research podcasting of their research documents through video clips. We can also streamline your conference videos and display your slides/ online slides and online research video clips at reasonable charges, on request.



The FARSS is eligible to earn from sales proceeds of his/her researches/reference/review Books or literature, while publishing with Global Journals. The FARSS can decide whether he/she would like to publish his/her research in a closed manner. In this case, whenever readers purchase that individual research paper for reading, maximum 60% of its profit earned as royalty by Global Journals, will be credited to his/her bank account. The entire entitled amount will be credited to his/her bank account exceeding limit of minimum fixed balance. There is no minimum time limit for collection. The FARSS member can decide its price and we can help in making the right decision.

The FARSS member is eligible to join as a paid peer reviewer at Global Journals Incorporation (USA) and can get remuneration of 15% of author fees, taken from the author of a respective paper. After reviewing 5 or more papers you can request to transfer the amount to your bank account.



MEMBER OF ASSOCIATION OF RESEARCH SOCIETY IN SCIENCE (MARSS)

The ' MARSS ' title is accorded to a selected professional after the approval of the Editor-in-Chief / Editorial Board Members/Dean.



The "MARSS" is a dignified ornament which is accorded to a person's name viz. Dr. John E. Hall, Ph.D., MARSS or William Walldroff, M.S., MARSS.

MARSS accrediting is an honor. It authenticates your research activities. After becoming MARSS, you can add 'MARSS' title with your name as you use this recognition as additional suffix to your status. This will definitely enhance and add more value and repute to your name. You may use it on your professional Counseling Materials such as CV, Resume, Visiting Card and Name Plate etc.

The following benefitscan be availed by you only for next three years from the date of certification.



MARSS designated members are entitled to avail a 25% discount while publishing their research papers (of a single author) in Global Journals Inc., if the same is accepted by our Editorial Board and Peer Reviewers. If you are a main author or co-author of a group of authors, you will get discount of 10%.

As MARSS, you will be given a renowned, secure and free professional email address with 30 GB of space e.g. johnhall@globaljournals.org. This will include Webmail, Spam Assassin, Email Forwarders,Auto-Responders, Email Delivery Route tracing, etc.





We shall provide you intimation regarding launching of e-version of journal of your stream time to time.This may be utilized in your library for the enrichment of knowledge of your students as well as it can also be helpful for the concerned faculty members.

The MARSS member can apply for approval, grading and certification of standards of their educational and Institutional Degrees to Open Association of Research, Society U.S.A.





Once you are designated as MARSS, you may send us a scanned copy of all of your credentials. OARS will verify, grade and certify them. This will be based on your academic records, quality of research papers published by you, and some more criteria.

It is mandatory to read all terms and conditions carefully.

AUXILIARY MEMBERSHIPS

Institutional Fellow of Global Journals Incorporation (USA)-OARS (USA)

Global Journals Incorporation (USA) is accredited by Open Association of Research Society, U.S.A (OARS) and in turn, affiliates research institutions as "Institutional Fellow of Open Association of Research Society" (IFOARS).



The "FARSC" is a dignified title which is accorded to a person's name viz. Dr. John E. Hall, Ph.D., FARSC or William Walldroff, M.S., FARSC.

The IFOARS institution is entitled to form a Board comprised of one Chairperson and three to five board members preferably from different streams. The Board will be recognized as "Institutional Board of Open Association of Research Society"-(IBOARS).

The Institute will be entitled to following benefits:

The IBOARS can initially review research papers of their institute and recommend them to publish with respective journal of Global Journals. It can also review the papers of other institutions after obtaining our consent. The second review will be done by peer reviewer of Global Journals Incorporation (USA) The Board is at liberty to appoint a peer reviewer with the approval of chairperson after consulting us.

The author fees of such paper may be waived off up to 40%.

The Global Journals Incorporation (USA) at its discretion can also refer double blind peer reviewed paper at their end to the board for the verification and to get recommendation for final stage of acceptance of publication.





The IBOARS can organize symposium/seminar/conference in their country on behalf of Global Journals Incorporation (USA)-OARS (USA). The terms and conditions can be discussed separately.

The Board can also play vital role by exploring and giving valuable suggestions regarding the Standards of "Open Association of Research Society, U.S.A (OARS)" so that proper amendment can take place for the benefit of entire research community. We shall provide details of particular standard only on receipt of request from the Board.



The board members can also join us as Individual Fellow with 40% discount on total fees applicable to Individual Fellow. They will be entitled to avail all the benefits as declared. Please visit Individual Fellow-sub menu of GlobalJournals.org to have more relevant details.

We shall provide you intimation regarding launching of e-version of journal of your stream time to time. This may be utilized in your library for the enrichment of knowledge of your students as well as it can also be helpful for the concerned faculty members.



After nomination of your institution as "Institutional Fellow" and constantly functioning successfully for one year, we can consider giving recognition to your institute to function as Regional/Zonal office on our behalf.
The board can also take up the additional allied activities for betterment after our consultation.

The following entitlements are applicable to individual Fellows:



Open Association of Research Society, U.S.A (OARS) By-laws states that an individual Fellow may use the designations as applicable, or the corresponding initials. The Credentials of individual Fellow and Associate designations signify that the individual has gained knowledge of the fundamental concepts. One is magnanimous and proficient in an expertise course covering the professional code of conduct, and follows recognized standards of practice.

Open Association of Research Society (US)/ Global Journals Incorporation (USA), as described in Corporate Statements, are educational, research publishing and professional membership organizations. Achieving our individual Fellow or Associate status is based mainly on meeting stated educational research requirements.



Disbursement of 40% Royalty earned through Global Journals : Researcher = 50%, Peer Reviewer = 37.50%, Institution = 12.50% E.g. Out of 40%, the 20% benefit should be passed on to researcher, 15 % benefit towards remuneration should be given to a reviewer and remaining 5% is to be retained by the institution.

We shall provide print version of 12 issues of any three journals [as per your requirement] out of our 38 journals worth $ 2376 USD.

Other:

The individual Fellow and Associate designations accredited by Open Association of Research Society (US) credentials signify guarantees following achievements:

- The professional accredited with Fellow honor, is entitled to various benefits viz. name, fame, honor, regular flow of income, secured bright future, social status etc.

- In addition to above, if one is single author, then entitled to 40% discount on publishing research paper and can get 10%discount if one is co-author or main author among group of authors.
- The Fellow can organize symposium/seminar/conference on behalf of Global Journals Incorporation (USA) and he/she can also attend the same organized by other institutes on behalf of Global Journals.
- The Fellow can become member of Editorial Board Member after completing 3yrs.
- The Fellow can earn 60% of sales proceeds from the sale of reference/review books/literature/publishing of research paper.
- Fellow can also join as paid peer reviewer and earn 15% remuneration of author charges and can also get an opportunity to join as member of the Editorial Board of Global Journals Incorporation (USA)
- • This individual has learned the basic methods of applying those concepts and techniques to common challenging situations. This individual has further demonstrated an in–depth understanding of the application of suitable techniques to a particular area of research practice.

Note :

"

- In future, if the board feels the necessity to change any board member, the same can be done with the consent of the chairperson along with anyone board member without our approval.
- In case, the chairperson needs to be replaced then consent of 2/3rd board members are required and they are also required to jointly pass the resolution copy of which should be sent to us. In such case, it will be compulsory to obtain our approval before replacement.
- In case of "Difference of Opinion [if any]" among the Board members, our decision will be final and binding to everyone.

"

Preferred Author Guidelines

We accept the manuscript submissions in any standard (generic) format.

We typeset manuscripts using advanced typesetting tools like Adobe In Design, CorelDraw, TeXnicCenter, and TeXStudio. We usually recommend authors submit their research using any standard format they are comfortable with, and let Global Journals do the rest.

Alternatively, you can download our basic template from https://globaljournals.org/Template.zip

Authors should submit their complete paper/article, including text illustrations, graphics, conclusions, artwork, and tables. Authors who are not able to submit manuscript using the form above can email the manuscript department at submit@globaljournals.org or get in touch with chiefeditor@globaljournals.org if they wish to send the abstract before submission.

Before and during Submission

Authors must ensure the information provided during the submission of a paper is authentic. Please go through the following checklist before submitting:

1. Authors must go through the complete author guideline and understand and *agree to Global Journals' ethics and code of conduct,* along with author responsibilities.
2. Authors must accept the privacy policy, terms, and conditions of Global Journals.
3. Ensure corresponding author's email address and postal address are accurate and reachable.
4. Manuscript to be submitted must include keywords, an abstract, a paper title, co-author(s') names and details (email address, name, phone number, and institution), figures and illustrations in vector format including appropriate captions, tables, including titles and footnotes, a conclusion, results, acknowledgments and references.
5. Authors should submit paper in a ZIP archive if any supplementary files are required along with the paper.
6. Proper permissions must be acquired for the use of any copyrighted material.
7. Manuscript submitted *must not have been submitted or published elsewhere* and all authors must be aware of the submission.

Declaration of Conflicts of Interest

It is required for authors to declare all financial, institutional, and personal relationships with other individuals and organizations that could influence (bias) their research.

Policy on Plagiarism

Plagiarism is not acceptable in Global Journals submissions at all.

Plagiarized content will not be considered for publication. We reserve the right to inform authors' institutions about plagiarism detected either before or after publication. If plagiarism is identified, we will follow COPE guidelines:

Authors are solely responsible for all the plagiarism that is found. The author must not fabricate, falsify or plagiarize existing research data. The following, if copied, will be considered plagiarism:

- Words (language)
- Ideas
- Findings
- Writings
- Diagrams
- Graphs
- Illustrations
- Lectures

- Printed material
- Graphic representations
- Computer programs
- Electronic material
- Any other original work

Authorship Policies

Global Journals follows the definition of authorship set up by the Open Association of Research Society, USA. According to its guidelines, authorship criteria must be based on:

1. Substantial contributions to the conception and acquisition of data, analysis, and interpretation of findings.
2. Drafting the paper and revising it critically regarding important academic content.
3. Final approval of the version of the paper to be published.

Changes in Authorship

The corresponding author should mention the name and complete details of all co-authors during submission and in manuscript. We support addition, rearrangement, manipulation, and deletions in authors list till the early view publication of the journal. We expect that corresponding author will notify all co-authors of submission. We follow COPE guidelines for changes in authorship.

Copyright

During submission of the manuscript, the author is confirming an exclusive license agreement with Global Journals which gives Global Journals the authority to reproduce, reuse, and republish authors' research. We also believe in flexible copyright terms where copyright may remain with authors/employers/institutions as well. Contact your editor after acceptance to choose your copyright policy. You may follow this form for copyright transfers.

Appealing Decisions

Unless specified in the notification, the Editorial Board's decision on publication of the paper is final and cannot be appealed before making the major change in the manuscript.

Acknowledgments

Contributors to the research other than authors credited should be mentioned in Acknowledgments. The source of funding for the research can be included. Suppliers of resources may be mentioned along with their addresses.

Declaration of funding sources

Global Journals is in partnership with various universities, laboratories, and other institutions worldwide in the research domain. Authors are requested to disclose their source of funding during every stage of their research, such as making analysis, performing laboratory operations, computing data, and using institutional resources, from writing an article to its submission. This will also help authors to get reimbursements by requesting an open access publication letter from Global Journals and submitting to the respective funding source.

Preparing your Manuscript

Authors can submit papers and articles in an acceptable file format: MS Word (doc, docx), LaTeX (.tex, .zip or .rar including all of your files), Adobe PDF (.pdf), rich text format (.rtf), simple text document (.txt), Open Document Text (.odt), and Apple Pages (.pages). Our professional layout editors will format the entire paper according to our official guidelines. This is one of the highlights of publishing with Global Journals—authors should not be concerned about the formatting of their paper. Global Journals accepts articles and manuscripts in every major language, be it Spanish, Chinese, Japanese, Portuguese, Russian, French, German, Dutch, Italian, Greek, or any other national language, but the title, subtitle, and abstract should be in English. This will facilitate indexing and the pre-peer review process.

The following is the official style and template developed for publication of a research paper. Authors are not required to follow this style during the submission of the paper. It is just for reference purposes.

Manuscript Style Instruction (Optional)

- Microsoft Word Document Setting Instructions.
- Font type of all text should be Swis721 Lt BT.
- Page size: 8.27" x 11'", left margin: 0.65, right margin: 0.65, bottom margin: 0.75.
- Paper title should be in one column of font size 24.
- Author name in font size of 11 in one column.
- Abstract: font size 9 with the word "Abstract" in bold italics.
- Main text: font size 10 with two justified columns.
- Two columns with equal column width of 3.38 and spacing of 0.2.
- First character must be three lines drop-capped.
- The paragraph before spacing of 1 pt and after of 0 pt.
- Line spacing of 1 pt.
- Large images must be in one column.
- The names of first main headings (Heading 1) must be in Roman font, capital letters, and font size of 10.
- The names of second main headings (Heading 2) must not include numbers and must be in italics with a font size of 10.

Structure and Format of Manuscript

The recommended size of an original research paper is under 15,000 words and review papers under 7,000 words. Research articles should be less than 10,000 words. Research papers are usually longer than review papers. Review papers are reports of significant research (typically less than 7,000 words, including tables, figures, and references)

A research paper must include:

a) A title which should be relevant to the theme of the paper.
b) A summary, known as an abstract (less than 150 words), containing the major results and conclusions.
c) Up to 10 keywords that precisely identify the paper's subject, purpose, and focus.
d) An introduction, giving fundamental background objectives.
e) Resources and techniques with sufficient complete experimental details (wherever possible by reference) to permit repetition, sources of information must be given, and numerical methods must be specified by reference.
f) Results which should be presented concisely by well-designed tables and figures.
g) Suitable statistical data should also be given.
h) All data must have been gathered with attention to numerical detail in the planning stage.

Design has been recognized to be essential to experiments for a considerable time, and the editor has decided that any paper that appears not to have adequate numerical treatments of the data will be returned unrefereed.

i) Discussion should cover implications and consequences and not just recapitulate the results; conclusions should also be summarized.
j) There should be brief acknowledgments.
k) There ought to be references in the conventional format. Global Journals recommends APA format.

Authors should carefully consider the preparation of papers to ensure that they communicate effectively. Papers are much more likely to be accepted if they are carefully designed and laid out, contain few or no errors, are summarizing, and follow instructions. They will also be published with much fewer delays than those that require much technical and editorial correction.

The Editorial Board reserves the right to make literary corrections and suggestions to improve brevity.



Format Structure

It is necessary that authors take care in submitting a manuscript that is written in simple language and adheres to published guidelines.

All manuscripts submitted to Global Journals should include:

Title

The title page must carry an informative title that reflects the content, a running title (less than 45 characters together with spaces), names of the authors and co-authors, and the place(s) where the work was carried out.

Author details

The full postal address of any related author(s) must be specified.

Abstract

The abstract is the foundation of the research paper. It should be clear and concise and must contain the objective of the paper and inferences drawn. It is advised to not include big mathematical equations or complicated jargon.

Many researchers searching for information online will use search engines such as Google, Yahoo or others. By optimizing your paper for search engines, you will amplify the chance of someone finding it. In turn, this will make it more likely to be viewed and cited in further works. Global Journals has compiled these guidelines to facilitate you to maximize the web-friendliness of the most public part of your paper.

Keywords

A major lynchpin of research work for the writing of research papers is the keyword search, which one will employ to find both library and internet resources. Up to eleven keywords or very brief phrases have to be given to help data retrieval, mining, and indexing.

One must be persistent and creative in using keywords. An effective keyword search requires a strategy: planning of a list of possible keywords and phrases to try.

Choice of the main keywords is the first tool of writing a research paper. Research paper writing is an art. Keyword search should be as strategic as possible.

One should start brainstorming lists of potential keywords before even beginning searching. Think about the most important concepts related to research work. Ask, “What words would a source have to include to be truly valuable in a research paper?” Then consider synonyms for the important words.

It may take the discovery of only one important paper to steer in the right keyword direction because, in most databases, the keywords under which a research paper is abstracted are listed with the paper.

Numerical Methods

Numerical methods used should be transparent and, where appropriate, supported by references.

Abbreviations

Authors must list all the abbreviations used in the paper at the end of the paper or in a separate table before using them.

Formulas and equations

Authors are advised to submit any mathematical equation using either MathJax, KaTeX, or LaTeX, or in a very high-quality image.

Tables, Figures, and Figure Legends

Tables: Tables should be cautiously designed, uncrowned, and include only essential data. Each must have an Arabic number, e.g., Table 4, a self-explanatory caption, and be on a separate sheet. Authors must submit tables in an editable format and not as images. References to these tables (if any) must be mentioned accurately.

Figures

Figures are supposed to be submitted as separate files. Always include a citation in the text for each figure using Arabic numbers, e.g., Fig. 4. Artwork must be submitted online in vector electronic form or by emailing it.

Preparation of Eletronic Figures for Publication

Although low-quality images are sufficient for review purposes, print publication requires high-quality images to prevent the final product being blurred or fuzzy. Submit (possibly by e-mail) EPS (line art) or TIFF (halftone/ photographs) files only. MS PowerPoint and Word Graphics are unsuitable for printed pictures. Avoid using pixel-oriented software. Scans (TIFF only) should have a resolution of at least 350 dpi (halftone) or 700 to 1100 dpi (line drawings). Please give the data for figures in black and white or submit a Color Work Agreement form. EPS files must be saved with fonts embedded (and with a TIFF preview, if possible).

For scanned images, the scanning resolution at final image size ought to be as follows to ensure good reproduction: line art: >650 dpi; halftones (including gel photographs): >350 dpi; figures containing both halftone and line images: >650 dpi.

Color charges: Authors are advised to pay the full cost for the reproduction of their color artwork. Hence, please note that if there is color artwork in your manuscript when it is accepted for publication, we would require you to complete and return a Color Work Agreement form before your paper can be published. Also, you can email your editor to remove the color fee after acceptance of the paper.

Tips for Writing a Good Quality Science Frontier Research Paper

Techniques for writing a good quality Science Frontier Research paper:

1. Choosing the topic: In most cases, the topic is selected by the interests of the author, but it can also be suggested by the guides. You can have several topics, and then judge which you are most comfortable with. This may be done by asking several questions of yourself, like "Will I be able to carry out a search in this area? Will I find all necessary resources to accomplish the search? Will I be able to find all information in this field area?" If the answer to this type of question is "yes," then you ought to choose that topic. In most cases, you may have to conduct surveys and visit several places. Also, you might have to do a lot of work to find all the rises and falls of the various data on that subject. Sometimes, detailed information plays a vital role, instead of short information. Evaluators are human: The first thing to remember is that evaluators are also human beings. They are not only meant for rejecting a paper. They are here to evaluate your paper. So present your best aspect.

2. Think like evaluators: If you are in confusion or getting demotivated because your paper may not be accepted by the evaluators, then think, and try to evaluate your paper like an evaluator. Try to understand what an evaluator wants in your research paper, and you will automatically have your answer. Make blueprints of paper: The outline is the plan or framework that will help you to arrange your thoughts. It will make your paper logical. But remember that all points of your outline must be related to the topic you have chosen.

3. Ask your guides: If you are having any difficulty with your research, then do not hesitate to share your difficulty with your guide (if you have one). They will surely help you out and resolve your doubts. If you can't clarify what exactly you require for your work, then ask your supervisor to help you with an alternative. He or she might also provide you with a list of essential readings.

4. Use of computer is recommended: As you are doing research in the field of science frontier then this point is quite obvious. Use right software: Always use good quality software packages. If you are not capable of judging good software, then you can lose the quality of your paper unknowingly. There are various programs available to help you which you can get through the internet.

5. Use the internet for help: An excellent start for your paper is using Google. It is a wondrous search engine, where you can have your doubts resolved. You may also read some answers for the frequent question of how to write your research paper or find a model research paper. You can download books from the internet. If you have all the required books, place importance on reading, selecting, and analyzing the specified information. Then sketch out your research paper. Use big pictures: You may use encyclopedias like Wikipedia to get pictures with the best resolution. At Global Journals, you should strictly follow here.



6. Bookmarks are useful: When you read any book or magazine, you generally use bookmarks, right? It is a good habit which helps to not lose your continuity. You should always use bookmarks while searching on the internet also, which will make your search easier.

7. Revise what you wrote: When you write anything, always read it, summarize it, and then finalize it.

8. Make every effort: Make every effort to mention what you are going to write in your paper. That means always have a good start. Try to mention everything in the introduction—what is the need for a particular research paper. Polish your work with good writing skills and always give an evaluator what he wants. Make backups: When you are going to do any important thing like making a research paper, you should always have backup copies of it either on your computer or on paper. This protects you from losing any portion of your important data.

9. Produce good diagrams of your own: Always try to include good charts or diagrams in your paper to improve quality. Using several unnecessary diagrams will degrade the quality of your paper by creating a hodgepodge. So always try to include diagrams which were made by you to improve the readability of your paper. Use of direct quotes: When you do research relevant to literature, history, or current affairs, then use of quotes becomes essential, but if the study is relevant to science, use of quotes is not preferable.

10. Use proper verb tense: Use proper verb tenses in your paper. Use past tense to present those events that have happened. Use present tense to indicate events that are going on. Use future tense to indicate events that will happen in the future. Use of wrong tenses will confuse the evaluator. Avoid sentences that are incomplete.

11. Pick a good study spot: Always try to pick a spot for your research which is quiet. Not every spot is good for studying.

12. Know what you know: Always try to know what you know by making objectives, otherwise you will be confused and unable to achieve your target.

13. Use good grammar: Always use good grammar and words that will have a positive impact on the evaluator; use of good vocabulary does not mean using tough words which the evaluator has to find in a dictionary. Do not fragment sentences. Eliminate one-word sentences. Do not ever use a big word when a smaller one would suffice.

Verbs have to be in agreement with their subjects. In a research paper, do not start sentences with conjunctions or finish them with prepositions. When writing formally, it is advisable to never split an infinitive because someone will (wrongly) complain. Avoid clichés like a disease. Always shun irritating alliteration. Use language which is simple and straightforward. Put together a neat summary.

14. Arrangement of information: Each section of the main body should start with an opening sentence, and there should be a changeover at the end of the section. Give only valid and powerful arguments for your topic. You may also maintain your arguments with records.

15. Never start at the last minute: Always allow enough time for research work. Leaving everything to the last minute will degrade your paper and spoil your work.

16. Multitasking in research is not good: Doing several things at the same time is a bad habit in the case of research activity. Research is an area where everything has a particular time slot. Divide your research work into parts, and do a particular part in a particular time slot.

17. Never copy others' work: Never copy others' work and give it your name because if the evaluator has seen it anywhere, you will be in trouble. Take proper rest and food: No matter how many hours you spend on your research activity, if you are not taking care of your health, then all your efforts will have been in vain. For quality research, take proper rest and food.

18. Go to seminars: Attend seminars if the topic is relevant to your research area. Utilize all your resources.

19. Refresh your mind after intervals: Try to give your mind a rest by listening to soft music or sleeping in intervals. This will also improve your memory. Acquire colleagues: Always try to acquire colleagues. No matter how sharp you are, if you acquire colleagues, they can give you ideas which will be helpful to your research.

20. Think technically: Always think technically. If anything happens, search for its reasons, benefits, and demerits. Think and then print: When you go to print your paper, check that tables are not split, headings are not detached from their descriptions, and page sequence is maintained.

21. Adding unnecessary information: Do not add unnecessary information like "I have used MS Excel to draw graphs." Irrelevant and inappropriate material is superfluous. Foreign terminology and phrases are not apropos. One should never take a broad view. Analogy is like feathers on a snake. Use words properly, regardless of how others use them. Remove quotations. Puns are for kids, not grunt readers. Never oversimplify: When adding material to your research paper, never go for oversimplification; this will definitely irritate the evaluator. Be specific. Never use rhythmic redundancies. Contractions shouldn't be used in a research paper. Comparisons are as terrible as clichés. Give up ampersands, abbreviations, and so on. Remove commas that are not necessary. Parenthetical words should be between brackets or commas. Understatement is always the best way to put forward earth-shaking thoughts. Give a detailed literary review.

22. Report concluded results: Use concluded results. From raw data, filter the results, and then conclude your studies based on measurements and observations taken. An appropriate number of decimal places should be used. Parenthetical remarks are prohibited here. Proofread carefully at the final stage. At the end, give an outline to your arguments. Spot perspectives of further study of the subject. Justify your conclusion at the bottom sufficiently, which will probably include examples.

23. Upon conclusion: Once you have concluded your research, the next most important step is to present your findings. Presentation is extremely important as it is the definite medium though which your research is going to be in print for the rest of the crowd. Care should be taken to categorize your thoughts well and present them in a logical and neat manner. A good quality research paper format is essential because it serves to highlight your research paper and bring to light all necessary aspects of your research.

Informal Guidelines of Research Paper Writing

Key points to remember:

- Submit all work in its final form.
- Write your paper in the form which is presented in the guidelines using the template.
- Please note the criteria peer reviewers will use for grading the final paper.

Final points:

One purpose of organizing a research paper is to let people interpret your efforts selectively. The journal requires the following sections, submitted in the order listed, with each section starting on a new page:

The introduction: This will be compiled from reference matter and reflect the design processes or outline of basis that directed you to make a study. As you carry out the process of study, the method and process section will be constructed like that. The results segment will show related statistics in nearly sequential order and direct reviewers to similar intellectual paths throughout the data that you gathered to carry out your study.

The discussion section:

This will provide understanding of the data and projections as to the implications of the results. The use of good quality references throughout the paper will give the effort trustworthiness by representing an alertness to prior workings.

Writing a research paper is not an easy job, no matter how trouble-free the actual research or concept. Practice, excellent preparation, and controlled record-keeping are the only means to make straightforward progression.

General style:

Specific editorial column necessities for compliance of a manuscript will always take over from directions in these general guidelines.

To make a paper clear: Adhere to recommended page limits.



© Copyright by Global Journals | Guidelines Handbook

Mistakes to avoid:

- Insertion of a title at the foot of a page with subsequent text on the next page.
- Separating a table, chart, or figure—confine each to a single page.
- Submitting a manuscript with pages out of sequence.
- In every section of your document, use standard writing style, including articles ("a" and "the").
- Keep paying attention to the topic of the paper.
- Use paragraphs to split each significant point (excluding the abstract).
- Align the primary line of each section.
- Present your points in sound order.
- Use present tense to report well-accepted matters.
- Use past tense to describe specific results.
- Do not use familiar wording; don't address the reviewer directly. Don't use slang or superlatives.
- Avoid use of extra pictures—include only those figures essential to presenting results.

Title page:

Choose a revealing title. It should be short and include the name(s) and address(es) of all authors. It should not have acronyms or abbreviations or exceed two printed lines.

Abstract: This summary should be two hundred words or less. It should clearly and briefly explain the key findings reported in the manuscript and must have precise statistics. It should not have acronyms or abbreviations. It should be logical in itself. Do not cite references at this point.

An abstract is a brief, distinct paragraph summary of finished work or work in development. In a minute or less, a reviewer can be taught the foundation behind the study, common approaches to the problem, relevant results, and significant conclusions or new questions.

Write your summary when your paper is completed because how can you write the summary of anything which is not yet written? Wealth of terminology is very essential in abstract. Use comprehensive sentences, and do not sacrifice readability for brevity; you can maintain it succinctly by phrasing sentences so that they provide more than a lone rationale. The author can at this moment go straight to shortening the outcome. Sum up the study with the subsequent elements in any summary. Try to limit the initial two items to no more than one line each.

Reason for writing the article—theory, overall issue, purpose.

- Fundamental goal.
- To-the-point depiction of the research.
- Consequences, including definite statistics—if the consequences are quantitative in nature, account for this; results of any numerical analysis should be reported. Significant conclusions or questions that emerge from the research.

Approach:

- Single section and succinct.
- An outline of the job done is always written in past tense.
- Concentrate on shortening results—limit background information to a verdict or two.
- Exact spelling, clarity of sentences and phrases, and appropriate reporting of quantities (proper units, important statistics) are just as significant in an abstract as they are anywhere else.

Introduction:

The introduction should "introduce" the manuscript. The reviewer should be presented with sufficient background information to be capable of comprehending and calculating the purpose of your study without having to refer to other works. The basis for the study should be offered. Give the most important references, but avoid making a comprehensive appraisal of the topic. Describe the problem visibly. If the problem is not acknowledged in a logical, reasonable way, the reviewer will give no attention to your results. Speak in common terms about techniques used to explain the problem, if needed, but do not present any particulars about the protocols here.

The following approach can create a valuable beginning:

- Explain the value (significance) of the study.
- Defend the model—why did you employ this particular system or method? What is its compensation? Remark upon its appropriateness from an abstract point of view as well as pointing out sensible reasons for using it.
- Present a justification. State your particular theory(-ies) or aim(s), and describe the logic that led you to choose them.
- Briefly explain the study's tentative purpose and how it meets the declared objectives.

Approach:

Use past tense except for when referring to recognized facts. After all, the manuscript will be submitted after the entire job is done. Sort out your thoughts; manufacture one key point for every section. If you make the four points listed above, you will need at least four paragraphs. Present surrounding information only when it is necessary to support a situation. The reviewer does not desire to read everything you know about a topic. Shape the theory specifically—do not take a broad view.

As always, give awareness to spelling, simplicity, and correctness of sentences and phrases.

Procedures (methods and materials):

This part is supposed to be the easiest to carve if you have good skills. A soundly written procedures segment allows a capable scientist to replicate your results. Present precise information about your supplies. The suppliers and clarity of reagents can be helpful bits of information. Present methods in sequential order, but linked methodologies can be grouped as a segment. Be concise when relating the protocols. Attempt to give the least amount of information that would permit another capable scientist to replicate your outcome, but be cautious that vital information is integrated. The use of subheadings is suggested and ought to be synchronized with the results section.

When a technique is used that has been well-described in another section, mention the specific item describing the way, but draw the basic principle while stating the situation. The purpose is to show all particular resources and broad procedures so that another person may use some or all of the methods in one more study or referee the scientific value of your work. It is not to be a step-by-step report of the whole thing you did, nor is a methods section a set of orders.

Materials:

Materials may be reported in part of a section or else they may be recognized along with your measures.

Methods:

- Report the method and not the particulars of each process that engaged the same methodology.
- Describe the method entirely.
- To be succinct, present methods under headings dedicated to specific dealings or groups of measures.
- Simplify—detail how procedures were completed, not how they were performed on a particular day.
- If well-known procedures were used, account for the procedure by name, possibly with a reference, and that's all.

Approach:

It is embarrassing to use vigorous voice when documenting methods without using first person, which would focus the reviewer's interest on the researcher rather than the job. As a result, when writing up the methods, most authors use third person passive voice.

Use standard style in this and every other part of the paper—avoid familiar lists, and use full sentences.

What to keep away from:

- Resources and methods are not a set of information.
- Skip all descriptive information and surroundings—save it for the argument.
- Leave out information that is immaterial to a third party.



© Copyright by Global Journals | Guidelines Handbook

Results:

The principle of a results segment is to present and demonstrate your conclusion. Create this part as entirely objective details of the outcome, and save all understanding for the discussion.

The page length of this segment is set by the sum and types of data to be reported. Use statistics and tables, if suitable, to present consequences most efficiently.

You must clearly differentiate material which would usually be incorporated in a study editorial from any unprocessed data or additional appendix matter that would not be available. In fact, such matters should not be submitted at all except if requested by the instructor.

Content:

- Sum up your conclusions in text and demonstrate them, if suitable, with figures and tables.
- In the manuscript, explain each of your consequences, and point the reader to remarks that are most appropriate.
- Present a background, such as by describing the question that was addressed by creation of an exacting study.
- Explain results of control experiments and give remarks that are not accessible in a prescribed figure or table, if appropriate.
- Examine your data, then prepare the analyzed (transformed) data in the form of a figure (graph), table, or manuscript.

What to stay away from:

- Do not discuss or infer your outcome, report surrounding information, or try to explain anything.
- Do not include raw data or intermediate calculations in a research manuscript.
- Do not present similar data more than once.
- A manuscript should complement any figures or tables, not duplicate information.
- Never confuse figures with tables—there is a difference.

Approach:

As always, use past tense when you submit your results, and put the whole thing in a reasonable order.

Put figures and tables, appropriately numbered, in order at the end of the report.

If you desire, you may place your figures and tables properly within the text of your results section.

Figures and tables:

If you put figures and tables at the end of some details, make certain that they are visibly distinguished from any attached appendix materials, such as raw facts. Whatever the position, each table must be titled, numbered one after the other, and include a heading. All figures and tables must be divided from the text.

Discussion:

The discussion is expected to be the trickiest segment to write. A lot of papers submitted to the journal are discarded based on problems with the discussion. There is no rule for how long an argument should be.

Position your understanding of the outcome visibly to lead the reviewer through your conclusions, and then finish the paper with a summing up of the implications of the study. The purpose here is to offer an understanding of your results and support all of your conclusions, using facts from your research and generally accepted information, if suitable. The implication of results should be fully described.

Infer your data in the conversation in suitable depth. This means that when you clarify an observable fact, you must explain mechanisms that may account for the observation. If your results vary from your prospect, make clear why that may have happened. If your results agree, then explain the theory that the proof supported. It is never suitable to just state that the data approved the prospect, and let it drop at that. Make a decision as to whether each premise is supported or discarded or if you cannot make a conclusion with assurance. Do not just dismiss a study or part of a study as "uncertain."

Research papers are not acknowledged if the work is imperfect. Draw what conclusions you can based upon the results that you have, and take care of the study as a finished work.

- You may propose future guidelines, such as how an experiment might be personalized to accomplish a new idea.
- Give details of all of your remarks as much as possible, focusing on mechanisms.
- Make a decision as to whether the tentative design sufficiently addressed the theory and whether or not it was correctly restricted. Try to present substitute explanations if they are sensible alternatives.
- One piece of research will not counter an overall question, so maintain the large picture in mind. Where do you go next? The best studies unlock new avenues of study. What questions remain?
- Recommendations for detailed papers will offer supplementary suggestions.

Approach:

When you refer to information, differentiate data generated by your own studies from other available information. Present work done by specific persons (including you) in past tense.

Describe generally acknowledged facts and main beliefs in present tense.

The Administration Rules

Administration Rules to Be Strictly Followed before Submitting Your Research Paper to Global Journals Inc.

Please read the following rules and regulations carefully before submitting your research paper to Global Journals Inc. to avoid rejection.

Segment draft and final research paper: You have to strictly follow the template of a research paper, failing which your paper may get rejected. You are expected to write each part of the paper wholly on your own. The peer reviewers need to identify your own perspective of the concepts in your own terms. Please do not extract straight from any other source, and do not rephrase someone else's analysis. Do not allow anyone else to proofread your manuscript.

Written material: You may discuss this with your guides and key sources. Do not copy anyone else's paper, even if this is only imitation, otherwise it will be rejected on the grounds of plagiarism, which is illegal. Various methods to avoid plagiarism are strictly applied by us to every paper, and, if found guilty, you may be blacklisted, which could affect your career adversely. To guard yourself and others from possible illegal use, please do not permit anyone to use or even read your paper and file.

Criterion for Grading a Research Paper (Compilation) by Global Journals

Please note that following table is only a Grading of "Paper Compilation" and not on "Performed/Stated Research" whose grading solely depends on Individual Assigned Peer Reviewer and Editorial Board Member. These can be available only on request and after decision of Paper. This report will be the property of Global Journals.

Topics	Grades		
	A-B	**C-D**	**E-F**
Abstract	Clear and concise with appropriate content, Correct format. 200 words or below	Unclear summary and no specific data, Incorrect form Above 200 words	No specific data with ambiguous information Above 250 words
Introduction	Containing all background details with clear goal and appropriate details, flow specification, no grammar and spelling mistake, well organized sentence and paragraph, reference cited	Unclear and confusing data, appropriate format, grammar and spelling errors with unorganized matter	Out of place depth and content, hazy format
Methods and Procedures	Clear and to the point with well arranged paragraph, precision and accuracy of facts and figures, well organized subheads	Difficult to comprehend with embarrassed text, too much explanation but completed	Incorrect and unorganized structure with hazy meaning
Result	Well organized, Clear and specific, Correct units with precision, correct data, well structuring of paragraph, no grammar and spelling mistake	Complete and embarrassed text, difficult to comprehend	Irregular format with wrong facts and figures
Discussion	Well organized, meaningful specification, sound conclusion, logical and concise explanation, highly structured paragraph reference cited	Wordy, unclear conclusion, spurious	Conclusion is not cited, unorganized, difficult to comprehend
References	Complete and correct format, well organized	Beside the point, Incomplete	Wrong format and structuring

Index

A

Antifermion · 25, 30
Attenuation · 44

B

Boukhenfouf · 50, 63

C

Coaxially · 37, 39

E

Emelue · 52, 63, 74, 75, 80
Emphasize · 9

H

Helmholtz's · 22

I

Ibeanu · 50, 51, 61, 63, 74, 80
Incomprehension · 9

L

Lagrangian · 24, 25, 27, 29, 30, 31

O

Okedeye · 51, 63

P

Penetrates · 38
Planckian · 2

S

Schwarzschild · 2, 3
Skewness · 61

T

Turbidity · 46

U

Unambiguous · 26, 27



Global Journal of Science Frontier Research

Visit us on the Web at www.GlobalJournals.org | www.JournalofScience.org
or email us at helpdesk@globaljournals.org

ISSN 9755896



© Global Journals